



**Adaptation of the Light-Sheet-Fluorescence-Microscope Z.1  
System to Enable *in-vivo* Odour Exposure Experiments for 3D  
Calcium Imaging in Insects**

Bachelor Thesis

Submitted in Partial Fulfilment of the Requirements for the Degree of  
Bachelor of Science

Ernst-Abbe-Hochschule, Jena

Department of Business Administration and Engineering  
Bachelor Business Administration and Engineering (Industry)

Presented by:	Eckard Esteban Schumann
Date of birth:	15.08.1993
Student Number:	637611
Reviewer:	Prof. Dr.-Ing. habil. Frank Engelmann
Institute:	Max Planck Institute for Chemical Ecology Hans-Knoell-Strasse 8 D-07745 Jena
Supervisor:	Dr. Jürgen Rybak
Day of submission:	November 29, 2018

## Acknowledgements

I want to thank Dr. Jürgen Rybak for introducing me to neurobiology in the first place and supporting my work on every level. I would also like to thank Prof. Dr. Bill S. Hansson for giving me the opportunity to undertake my thesis at the Max-Planck-Institute for Chemical Ecology.

I also want to mention the indispensable help I got from Fabio Miazzi, Martin Niebergall, Daniel Veit, Ana Depetris-Chauvin, Ian Keeseey, Veit Grabe, Lydia Gruber and Rodolfo Ferber. Your answers to my questions, as well as your suggestions offered me clarity in navigating through the complexity of biological systems. Last but not least, a big thank you goes to all the members of the Evolutionary Neuroethology Department for providing a welcoming environment for an engineering student.

Finally I thank my parents, family and friends for their support at all times during my thesis.

Gracias a todos!

Eckard Schumann

## Declaration of Authorship

I, Eckard Schumann, hereby declare that this thesis and the work presented in it are my own and have been generated by me as the result of my own original research. All direct and indirect source of information used are cited in the text and acknowledged as references in the bibliography.

---

Date and Signature

## Abstract

Brain function has always attracted great interest, but how neuronal information is encoded into neuronal circuits still remains an open question. Nowadays new technologies allow to research brain areas that were previously inaccessible, such as the olfactory system. In order to understand how odour information is encoded in the brain we plan to use genetically expressed fluorescence labels in the peripheral, olfactory organs (sensilla of the funiculus/palpus) to indicate odour-induced neuronal activity in the vinegar fly *Drosophila melanogaster*.

Light-Sheet-Fluorescence-Microscopy (LSFM) is a technology that allows rapid recording of whole brain images of animal probes at cellular and sub-cellular resolution. Due to its high speed performance, the phototoxicity and the photobleaching of biological probes remains significantly low, in comparison to other fluorescence microscopy techniques. This imaging method is therefore, suited to track developmental and neuronal processes in an intact brain preparation.

The closed condition of the optical chamber of the Z.1 LSFM microscope offers a convenient environment to control experimental conditions, such as temperature and air composition in order to prolong the life of the animal as long as possible. This is important for our odour exposure experiments that require certain amount of time in order to record neural activity. Therefore, the main system was subdivided in 3 sub systems: the Ringer solution flow sub system, the odour flow system and the extraction sub system

In my thesis, I designed an odour delivery device for the Z.1 microscope. In addition, the odour exposure was simulated using the Computational Fluid Dynamics program from Autodesk. A digital model of the optical chamber was generated and adapted for surface rendering as well as a model of the odour distributor model that was designed specifically for the Z.1 microscope.

The simulations include: odour in- and out-flux for seven different outlets combinations, 21 Ringer solution in- and out flux from the optical chamber, in all, that accounted to 21 possible inlets and outlets combinations. Out of these only three options were suitable to optimally rinse the optical chamber. Afterwards these three outlets possibilities were combined with the odour delivery using the odour distributor model as the inlet for the diluted odour. Thereof certain numerical values were obtained such as the Reynolds number, average velocity and residence time within the optical chamber along with visual characteristics of the odour and Ringer solution flow, from which the optimal combination was chosen with the aid of a scoring method.

In summary the goal of this thesis was to adapt the Z.1 microscope optical chamber, in order to be able to perform *in-vivo* odour exposure experiments while still exploiting the advantages of the microscope in the visualization of brain structures involved in odour processing. This goal was achieved in a digital environment but further live test should be conducted to test the conclusion resulting from these simulations.

## Zusammenfassung

Die Gehirnfunktion hat schon immer großes Interesse auf sich gezogen. Wie neuronale Informationen in neuronalen Schaltkreisen kodiert werden, bleibt jedoch eine offene Frage. Heutzutage ermöglichen neue Technologien die Erforschung von Gehirnbereichen, die bisher nicht zugänglich waren, beispielsweise im Riechsystem. Um zu verstehen, wie die Geruchsinformation im Gehirn kodiert wird, planen wir, genetisch exprimierte Fluoreszenzmarkierungen in den peripheren, olfaktorischen Organen (Sensillen des Funiculus / Palpus) zu verwenden, um die geruchsinduzierte neuronale Aktivität in der Essigfliege *Drosophila melanogaster* anzuzeigen.

Die Light-Sheet-Fluoreszenz-Mikroskopie (LSFM) ist eine Technologie, die eine schnelle Aufnahme ganzer Gehirnbilder von Tierproben mit zellulärer und subzellulärer Auflösung ermöglicht. Aufgrund ihrer Hochgeschwindigkeitsleistung bleiben die Phototoxizität und das Photobleaching von biologischen Sonden im Vergleich zu anderen Fluoreszenzmikroskopietechniken deutlich niedrig. Dieses bildgebende Verfahren ist daher geeignet, Entwicklungsprozesse und neuronale Prozesse in einem intakten Gehirnpräparat zu verfolgen.

Der geschlossene Zustand der optischen Kammer des Z.1-LSFM-Mikroskops bietet eine günstige Umgebung zur Kontrolle der experimentellen Bedingungen wie Temperatur und Luftzusammensetzung, um die Lebensdauer des Tieres so lange wie möglich zu verlängern. Dies ist wichtig für unsere Geruchsexpositionsexperimente, die eine gewisse Zeit benötigen, um die neuronale Aktivität aufzuzeichnen. Daher wurde das Hauptsystem in 3 Subsysteme unterteilt: das Ringer-Lösungsfluss-Subsystem, das Geruchsflusssystem und das Extraktions-Subsystem

In meiner Diplomarbeit habe ich ein Geruchsverteilermodell für das Z.1-Mikroskop entworfen. Darüber hinaus wurde die Geruchsgabe mit dem Programm Computational Fluid Dynamics von Autodesk simuliert. Zu diesem Zweck wurde ein digitales Modell der optischen Kammer und des Geruchsverteilermodells erstellt und angepasst, letzteres wurde speziell für das Z.1-Mikroskop entwickelt.

Die Simulationen umfassen: Duft im Flussmittel mit 7 verschiedenen Auslasskombinationen, die Ringer-Lösung in- und aus Auslass des Flussmittels in der optischen Kammer, die insgesamt 21 mögliche Einlass- und Auslasskombinationen ausmachten. Von den 21 möglichen Kombinationen waren nur drei Optionen zum Spülen der optischen Kammer optimal geeignet. Anschließend wurden diese drei

Auslassmöglichkeiten mit der Geruchsgabe kombiniert, wobei das Geruchsverteilermodell als Einlass für den verdünnten Geruch verwendet wurde. Hieraus wurden bestimmte Zahlenwerte wie Reynolds-Zahl, durchschnittliche Geschwindigkeit und Verweildauer des Duftes und des Ringers in der optischen Kammer zusammen mit den visuellen Eigenschaften der Duftverteilung und des Ringerlösungsflusses erhalten, aus denen die optimale Kombination mit Hilfe eines Bewertungsverfahrens ausgewählt wurde.

Zusammenfassend bestand das Ziel dieser Arbeit darin, die optische Kammer des Z.1-Mikroskops anzupassen, um *in-vivo* Geruchsexpositionsexperimente durchführen zu können und gleichzeitig die Vorteile des Mikroskops bei der Visualisierung von an der Geruchsverarbeitung beteiligten Gehirnstrukturen zu nutzen. Dieses Ziel wurde in einer digitalen Umgebung erreicht. Es sollten jedoch ein weitere *in-vivo*-Experimentes durchgeführt werden, um die Schlussfolgerung aus diesen Simulationen zu testen.



Acknowledgements .....	I
Declaration of Authorship .....	II
Abstract .....	III
Zusammenfassung .....	V
Table of Figures .....	IX
Table of Tables .....	XII
Table of Equations .....	XII
1 Thematic Overview .....	1
1.1 Goal .....	2
1.2 Method .....	2
2 Light Microscopy and Fluorescence Microscopy .....	5
3 Light-Sheet-Fluorescence-Microscopy .....	8
3.1 Illumination .....	8
3.2 The Set-up of the Z.1 LSM .....	9
3.3 Mounting .....	10
3.4 Beam Path .....	12
4 Olfaction .....	15
4.1 The Sensory Organs .....	15
4.2 Basic Information on Insects .....	16
4.2.1 <i>Drosophila melanogaster</i> .....	16
4.2.2 Comparable Organism for the Olfactory System .....	16
4.3 <i>In vivo</i> Experiments on Antennal Olfactory Neurons .....	17
4.4 Calcium Imaging Experiments .....	18
4.4.1 In-vivo preparations .....	18
4.4.2 <i>Ex-vivo</i> Preparations .....	19
5 The Need of New Imaging Methods .....	21
5.1 Light-Sheet-Fluorescence-Microscope Z.1 for <i>in-vivo</i> odour exposure experiments ..	21
5.2 Description of the function .....	22
5.3 Requirement List .....	23
6 Derivation the Function of the Product .....	25
6.1 Optical Chamber of the Light-Sheet-Fluorescence-Microscope .....	25
6.2 Defining the Structure of the Function .....	26
6.2.1 Main Function .....	26
6.2.2 Sub Functions .....	27

6.3	Solutions conception to enable odour exposure experiment inside the optical chamber of the Z.1 microscope.....	30
6.3.1	Storage.....	30
6.3.2	Pumps.....	30
6.3.3	Fluid Dynamics.....	34
6.3.4	Odour Distributor model.....	36
6.3.5	Computational Fluid Dynamics.....	39
6.3.6	Simulation within the Odour Distributor Model.....	42
6.4	Development of Possible Active Structures.....	51
6.4.1	Morphological Box and Defining Active Structures.....	51
6.4.2	Morphological Box of the Ringer Solution Flow.....	52
6.4.3	Morphological Box of the Odour Flow.....	53
6.4.4	Active structures.....	55
6.5	Scoring Method for the Optimal Modular Structure.....	57
6.5.1	Requirements for the Scores.....	58
6.5.2	Results of the Scoring Method.....	60
7	Conclusion.....	61
	References.....	XII
	Appendix.....	XIII

## Table of Figures

Figure 1 Structure for the systematic development of prototypes. It show the flow that the development of a porduct should go through. Going from defining the goals and the scope until the end product: Adapted from the VDI 2221[4].....	3
Figure 2 Comparison between light microscopy and fluorecence microscopy A) the basic design of a light microscope. Source:[7] B) The basic structure of a fluorecence microscope where the excitation and the emission share the same path from the light source through the objective. In contrast to the lighr microscope only the fluorecent emission light is detected (visuailized) [8]. ....	5
Figure 3 Example of photobleaching A) Two glomeruli of the antennal lobe of Drosophila melanogaster labelled with GFP during the first exposure to the excitation laser. B) The antennal lobes fluorecence loses intensity due to the exposure time and the intensity of the laser of the confocal microscope after prolonged scanning time. ....	6
Figure 4 Imaging sectioning A) Example of imaging sectioning, where a Z-stack is generated with various images with defined focus panels with a given depth difference B) A 3-D model reconstructed out of the Z-stack Source: [12].....	7
Figure 5 Different types of illumination for fluorecence microscopes. A) An example of epi-illumination used by normal fluorecence microscopes, such as the confocal and the apotome. It is clear that the beam of light is illuminating the whole probe even though only one section of it is being detected by the lens. B) The Light-Sheet-Fluorecence-Microscope only illuminates a small portion of the sample while detecting simultaneously only on the focal overlap. after:[16]. ....	8
Figure 6 Set-up of the Light-Sheet-Fluorecence-Microscope Z.1 manufactured by Zeiss with an example of an imaged zebra fish on the monitor[20]. ....	9
Figure 7 Illumination path for the Z.1 microscope A) This figure shows how the light beam, the probe, and the objective path interact on one specific position with the optical chamber surrounding the system. Source:[16] B). The illumination path and the objective path converge on one place where the probe is placed to enable the imaging process. There is an orthogonal relation between the two paths [9]. ....	10
Figure 8 Mounting of the sample Different options to mount the sample with the illumination path Source: [16].....	11
Figure 9 Core the Light-Sheet-Fluorecence-Microscope Z.1 Source: [16]. A: external view on the optical chamber, with a: probe column, b: optical chamber, c: frontal camera, and d: direction of laser beam. B: Laser beam path in the LSFM.....	12
Figure 10 Sheet of the light path in the Z.1 [16].....	13
Figure 11 Drosophila melanogaster olfactory system. Modified from [28] .....	15
Figure 12 Image of a Drosophila melanogaster. Modified from [31] .....	16
Figure 13 Single sensillum of the third antenna of Drosophila melanogaster with two olfactory receptor neurons (ORN). Modified from [35] .....	17

Figure 14 Set-up of an in-vivo odour exposure experiment A) Frontal view of the mounting of the fly B) Frontal view of the mounted fly C) Image taken with an epi-fluorescence microscope of the funiculi and the glomeruli of <i>Drosophila melanogaster</i> expressing of Ca <sup>2+</sup> reporter GCaMP. D) Head of the <i>Drosophila melanogaster</i> with the antennae and palps emitting Source:[42, 43] .....	19
Figure 15 Example of an in-vivo odour exposure experiment A) A cut of the third segment of the antenna (funiculus) of the <i>Drosophila melanogaster</i> reveals neuronal cell bodies before (B) and after (C) odor exposure. Modified from [44] .....	20
Figure 16 Scans made with the Z.1 microscope A) The antenna of the genetically modified <i>Drosophila melanogaster</i> show a response of the olfactory sensory neurons but the cuticle prevents the laser of deep penetrating and therefore the internal structures remained partly obscured. B) The palp of the leaf beetle is cleared enough to show internal structures without damaging the cuticle. This is possible due to the genetically modified and cleared cuticle [45] .....	21
Figure 17 A) 3-D Model of the optical chamber of the Z.1 LSM, upper right side B) Photograph of the optical chamber of the Z.1 LSM, upper left side. ....	25
Figure 18 Black Box visualization of the main system .....	26
Figure 19 Main function diagram with the sub-functions and the side function after [47] .....	29
Figure 20 Principle of the peristaltic pumps [51] .....	31
Figure 21 Example of a solenoid pump[54] .....	32
Figure 22 Fusion 4000 syringe pump [55] .....	33
Figure 23 Optical chamber of the Z.1 microscope. The area where the probe will be submerged is marked in grey. ....	34
Figure 24 Example of the Osborne Reynolds experiment to determine the differential factors of laminar and turbulent flows [63] .....	36
Figure 25 A) Odour distributor model B) Odour distributor model mounted on the optical chamber of the Z.1 LSM C) Back view of the optical chamber of the Z.1 LSM with the odour distributor mounted D) Front view of the optical chamber of the Z.1 LSM with the odour distributor mounted.....	37
Figure 26 Blueprint of the odour distributor model.....	38
Figure 27 A) Original optical chamber of the LSM Z.1 B) Digital modified optical chamber of the LSM Z.1. : removal of external physical properties (arrow). 40	
Figure 28 A) Optical chamber of the Z.1 LSM with the odour distributor model mounted. B) Example of the surface wrapping rendering the digital 3D shape. ....	41
Figure 29 A) Back view of the odour distributor model B) Front view of the odour distributor model.....	42
Figure 30 Fluid dynamics simulation within the odour distributor model.....	42
Figure 31 The inlets and outlets of the optical chamber of the Z.1 A) Left side of the optical chamber. It shows the inlet A and the outlet 1. B) The right side shows the inlet B and the outlets 2 and 3.....	43

Figure 32 Simulation of ringer solution flow using Inlet B and Outlets 1, 2 and 3..44

Figure 33 Example of one Ringer solution flow simulation utilizing the inlets A and B, and the outlet 1 .....45

Figure 34 3 Possible combinations for the Ringer solution distribution system utilizing two inlets. A) Outlets 1 and 2 allow the flow to the whole chamber. B) The combination of the outlets 1 and 3 cause a similar effect that the combination 1 and 2. The flow spreads along the whole volume inside the optical chamber C) Utilizing the outlets 1, 2 and 3 allows the flow to reach the whole chamber while having a lower out volume flow in comparison with the other possibilities.....46

Figure 35 3 Possible combinations for the odour distribution. A) Outlets 1 and 2 allow the flow to the whole chamber. B) The outlets 1 and 3 cause a similar effect that the combination 1 and 2. C) Utilizing the three outlets allow the flow to reach all the chamber while having a lower out volume flow in comparison with the other possibilities .....49

## Table of Tables

Table 1 List of requirements for odour exposure experiments on the Z.1 microscope.....	24
Table 2 Material comparison for storage units.....	30
Table 3 Simulation results utilizing the inlets A and B and the outlets 1 and 2 .....	47
Table 4 Simulation results utilizing the inlets A and B and the outlets 1 and 3 .....	47
Table 5 Simulation results utilizing the inlets A and B and the outlets 1, 2 and 3 ..	47
Table 6 Odour simulation result utilizing the outlets 1 and 2 .....	50
Table 7 Odour simulation result utilizing the outlets 1 and 3 .....	50
Table 8 Odour simulation result utilizing the outlets 1, 2 and 3 .....	50
Table 9 Morphological box of the Ringer solution flow sub function .....	52
Table 10 Morphological box of the odour flow sub function.....	53
Table 11 Active structures displaying different alternatives to solve the main issue .....	54
Table 12 Table of requirements for the values .....	58
Table 13 Scoring table. Evaluation of combinations of system characteristics (modular structures) depicted in a cross diagram. ....	60

## Table of Equations

Equation 1 Reynolds number equation [63].....	36
---	----

# 1 Thematic Overview

Industrial engineering focuses on the improvement and optimization of existing systems and processes with a focus on business administration and engineering, while having a broad interdisciplinary understanding of various themes. This extensive knowledge facilitates an engineer to adapt and combine remote disciplines, e.g. neurobiology, machine engineering, and fluid dynamics. This interdisciplinary knowledge can thus be employed to analyse, simplify, and solve complicate tasks, such as the designing setups for biological experiments.

Finding new combinations for known microscopy systems and biological experiments can open the possibility for more accurate studies. Therefore, an adaptation of a Light-Sheet-Fluorescence-Microscope Z.1 to enable odour exposure experiments constitutes a good example of a science-based assignment for an industrial engineer.

Brain function has always attracted great interest, but how neuronal information is encoded in neuronal circuits remains an open question. New technologies allow scientist to investigate brain areas that were previously inaccessible. Studies on the vinegar fly, *Drosophila melanogaster*, as a model organism seek to gain knowledge on how external stimuli are processed within the different regions of the brain. In order to understand how odour information is encoded in the brain genetically expressed fluorescence labels are used, to indicate odour induced neuronal activity in the peripheral, olfactory organs in the vinegar fly. Different experiments focus on the antennae or the glomeruli in the brain have revealed crucial information about the internal neuronal connectivity, while exposing the fly to abnormally invasive conditions with high toxicity levels thus inflicting irreversible damage to the animal.

The Light-Sheet-Fluorescence-Microscope Z.1 (Z.1-LSFM) from Zeiss is based on a 100 year old method, where the sample is illuminated horizontally with a sheet of light [1]. While gaining high-resolution images, it also reduces the amount of light exposure to the biological probe, or specimen, thus increasing its life sustainability. The optical chamber of the Z.1 system offers a closed system flooded with water, or physiological Ringer solution where the probe can be introduced from above, a convenient environment to control experimental conditions such as temperature, position, and oxygen/CO<sub>2</sub> levels in order to prolong the life of the animal as long as possible. The mobility of the probe enables the possibility to generate fast and automatic 3D-image data sets, thus allowing optimal positioning of the sample.[2]

## 1.1 Goal

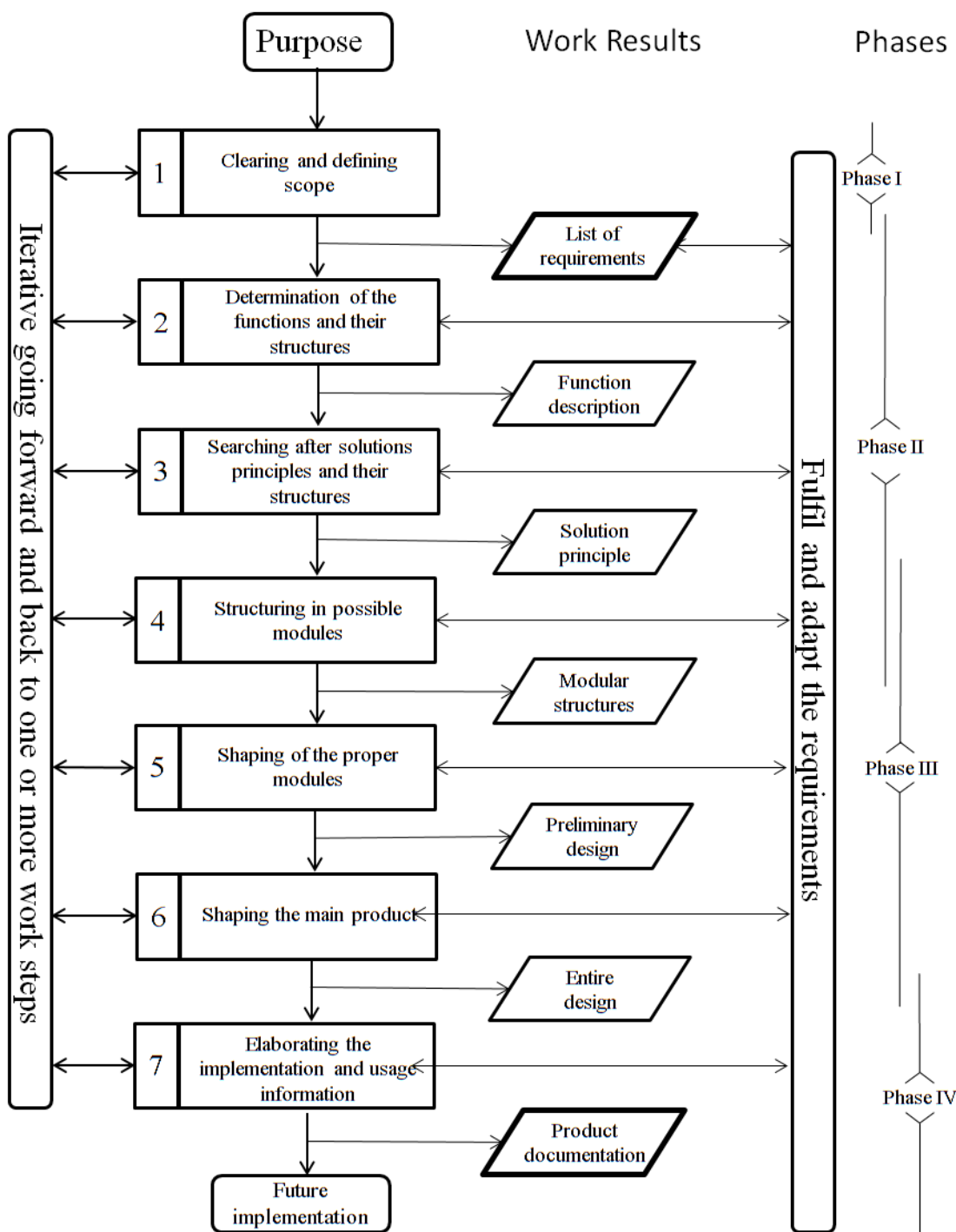
To examine living specimen it is ideal to keep the integrity of the organism intact and, thus gaining information about developmental and internal live processes with a high level of reliability. The Z.1 contains the probe in its optical chamber where the survival of the animal is guaranteed for extended periods of time. This support allows experimental protocols, where the influence of different stimuli applied on the animal can be tested[2].

The conventional setup of the Z.1 microscope is currently not capable of controlling the in- and out-flux of odorous chemicals. Therefore, the goal of this thesis is the modification of a Light-Sheet-Fluorescence-Microscope optical chamber, to enable reliable odour exposure experiments on an *in-vivo* vinegar fly and subsequently visualizing the external and internal odour processes in the brain. These odour exposure experiments require a certain exposure of time and a complete control the odour in- and out flux in order to get valid results.

## 1.2 Method

The development and design of the modified optical chamber relies on the systematic approach according to the guidelines of the VDI 2221 "*Methodik zum Entwickeln und Konstruieren technische Systeme und Produkte*". This guideline gives a general method to approach any development and design of new products [3, 4]. (**Figure 1**)





**Figure 1 Structure for the systematic development of prototypes.** It shows the flow that the development of a product should go through. Going from defining the goals and the scope until the end product: Adapted from the VDI 2221[4]

Developing and adapting the existing Z.1 optical chamber requires deep knowledge on how the microscope works. Basic information on the olfactory system of *Drosophila*

*melanogaster* combined with protocols of odour exposure experiments should provide the technical information needed to define the requirements of the new odour exposure system.

The guideline requires defining the function and the structure of the whole system in subordinate simpler sub functions and then finding individual solutions for each sub function. The designing and development of the framework conditions are structured according to the requirements of two different processes, these being:

- requirements for the odour exposure experiment such as duration of the exposure, quantity of the exposure, type of reaction, location of the reaction, control of the odour flux, odour addition and odour extraction system
- Technical aspects and requirements of the Z.1, such as volume of the chamber, laser positioning, imaging process

Afterwards a scoring method is used to evaluate the different possibilities to solve the main function. The outcome of the evaluation delivers the optimal solution for the adaptation of the Light-Sheet-Fluorescence-Microscope optical chamber to enable odour exposure experiments.

## 2 Light Microscopy and Fluorescence Microscopy

Light microscopy is a well know method used to magnify and help in the visualisation of small objects which cannot be seen by the naked human eye. The system consists of a light source and a set of lenses that resolve properties of the object (**Figure 2 A**). This has been the most used instrument to investigate microorganisms for at last 400 years [5].

Fluorescence microscopy uses the principle of excitation, and emission of fluorophores in addition to the basic design of a light microscope[6]. The wavelength used to excite by the illuminated probe is shorter than the emission wavelength (Stoke-shift). A specific set of dichroic filters is used to control excitation and the emission wavelengths so that the detector (human eye or camera) is able to detect the emission wavelength (**Figure 2 B**). This detection technique allows a high contrast of the fluorescent probe against a dark background.

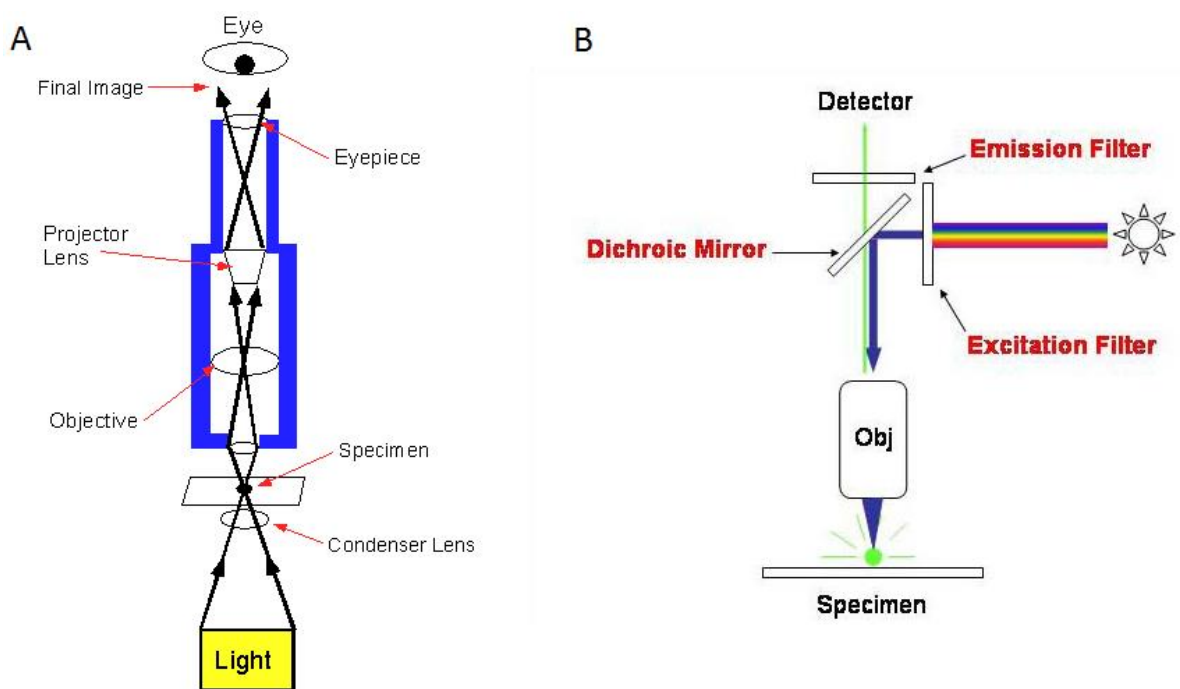
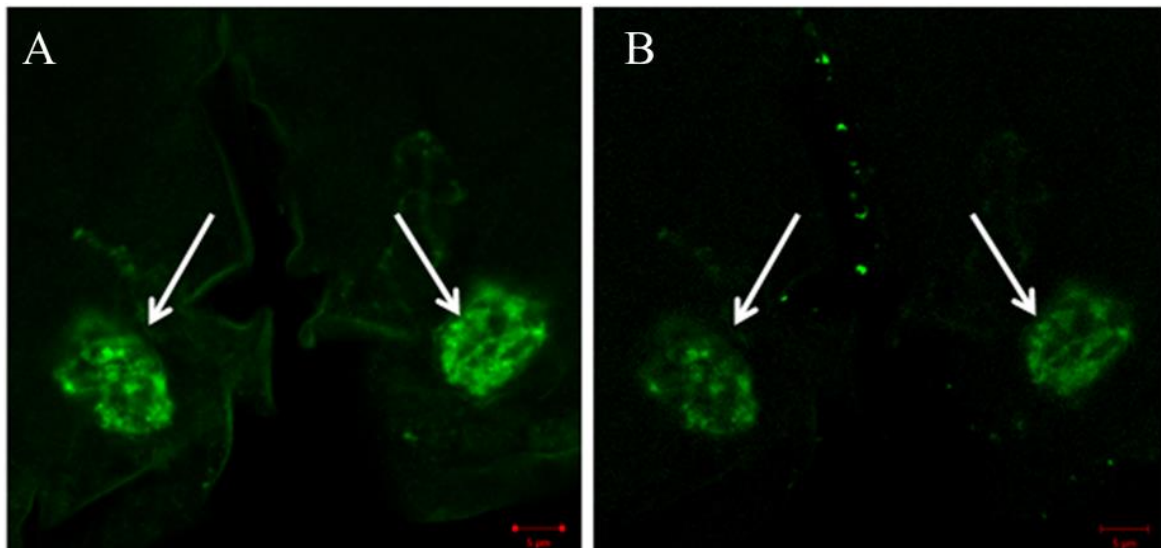


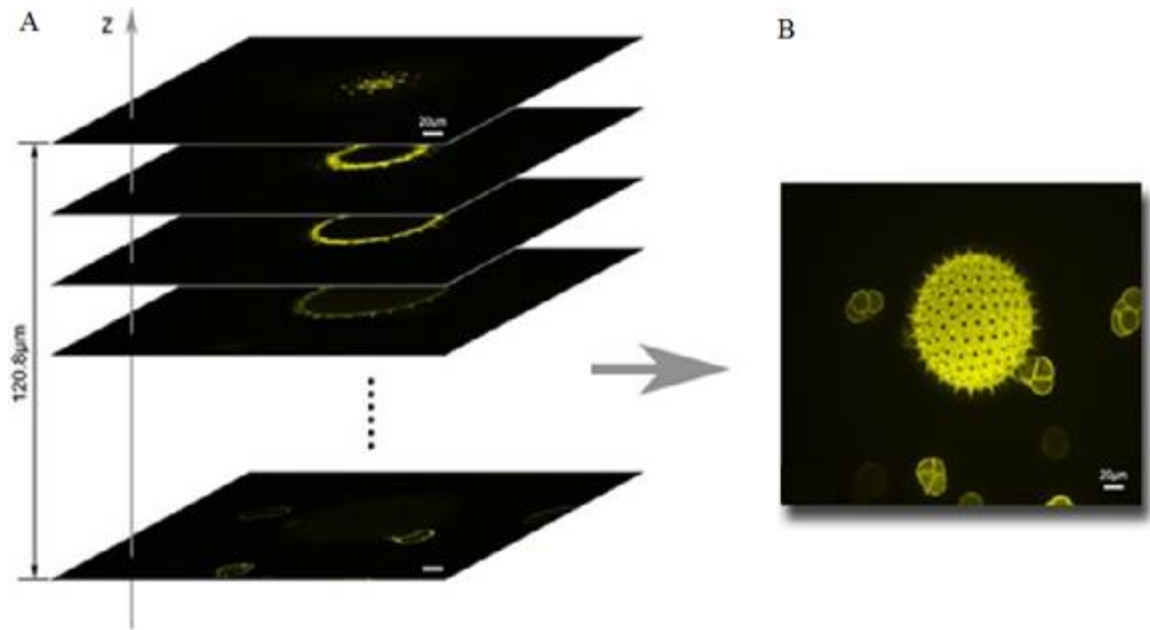
Figure 2 Comparison between light microscopy and fluorescence microscopy A) the basic design of a light microscope. Source:[7] B) The basic structure of a fluorescence microscope where the excitation and the emission share the same path from the light source through the objective. In contrast to the light microscope only the fluorescent emission light is detected (visualized) [8].

Nowadays, this technology is needed in the biological research. In microscopy the confocal microscope has been developed, and technology has been improved with researchers are now able to stain specific structures with fluorophores to recognize certain biological structures. Classic fluorescence microscopy illuminates the whole probe. Therefore, chemical damage (photobleaching) is inflicted, even if the region is not being scanned [9]. Photobleaching or fading represents one of the major adversities of fluorescence microscopy. It occurs when irreversible damage is cause to the fluorophore due to long exposure times. The photobleachings time varies according to the type of the fluorophore, the exposure time, and the intensity of the energy coming from the excitation source[2] (**Figure 3**).



**Figure 3** Example of photobleaching A) Two glomeruli of the antennal lobe of *Drosophila melanogaster* labelled with GFP during the first exposure to the excitation laser. B) The antennal lobes fluorescence loses intensity due to the exposure time and the intensity of the laser of the confocal microscope after prolonged scanning time.

Modern fluorescence microscopes, such as the confocal microscope or the Light-Sheet-Fluorescence-Microscope (LSFM), can be designed to generate image stacks at of different foci with a given depth within the sample (**Figure 3**). This technique is called optical sectioning and is used to reconstruct 3-D models from the images taken [10]. This avoids the need of physically sectioning the specimen and [9, 11] (**Figure 4**).



**Figure 4 Imaging sectioning A) Example of imaging sectioning, where a Z-stack is generated with various images with defined focus panels with a given depth difference B) A 3-D model reconstructed out of the Z-stack Source: [12]**

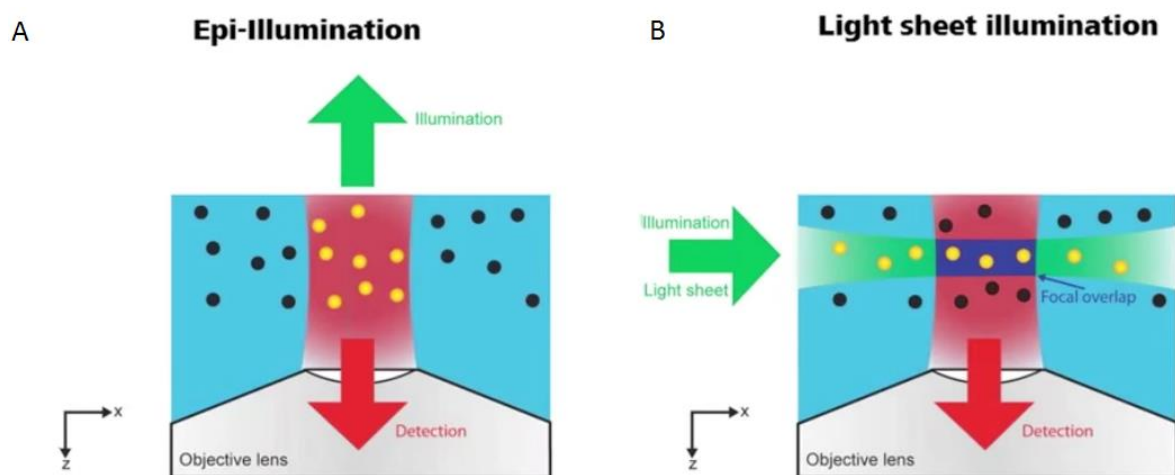
### 3 Light-Sheet-Fluorescence-Microscopy

#### 3.1 Illumination

Common fluorescence microscopes work according to the epifluorescence principle, where only one objective constitutes the light path for excitation the emission [13].

In addition, in confocal microscopy the pin-hole principle is used to remove the out of focus background fluorescence[14]. The background blur occurs because all the planes are being illuminated and therefore, being excited during scanning. The confocal microscope achieves high-resolution images, but still creates a high grade of photobleaching[14] (**Figure 5A**).

An advantage of the Light-Sheet-Fluorescence-Microscope is that the probe is illuminated from the side with a thin sheet of light (**Figure 5 B**) [15]. Thus, the detected fluorescence is only on the overlap of the focal volume and the excitation beam. This means that, in comparison with the confocal, there is almost no out of focus light. This reduces significantly the light exposure on the sample.



**Figure 5 Different types of illumination for fluorescence microscopes.** A) An example of epi-illumination used by normal fluorescence microscopes, such as the confocal and the apotome. It is clear that the beam of light is illuminating the whole probe even though only one section of it is being detected by the lens. B) The Light-Sheet-Fluorescence-Microscope only illuminates a small portion of the sample while detecting simultaneously only on the focal overlap. after:[16].

Therefore, the Zeiss Light sheet microscope, named Z.1 (LSFM), enables the imaging of optical sections of large living samples by producing almost no phototoxicity or

photobleaching, while gaining crucial information about the internal structures and the development of living probes, by providing high resolution images

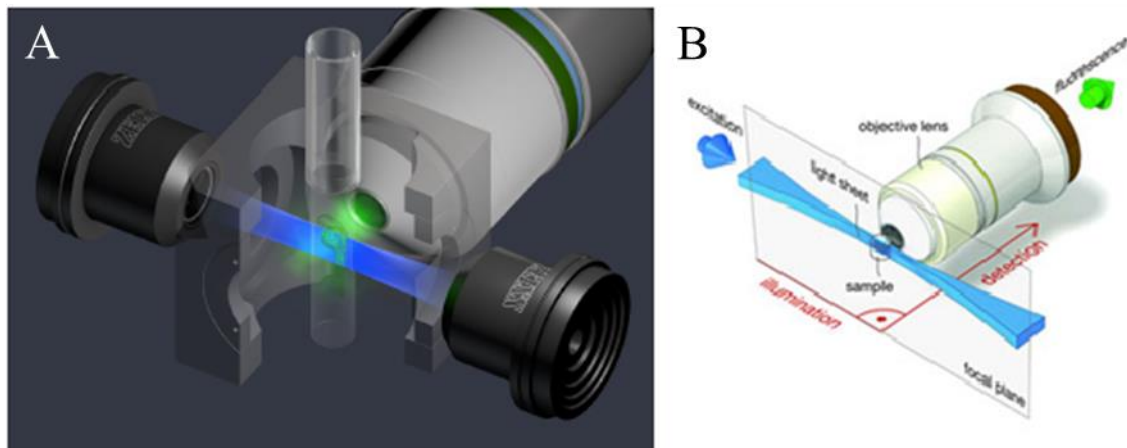
### 3.2 The Set-up of the Z.1 LSM

This type of microscopy has been available for more than 100 years[17], but it was not until 1993 that Voe et al. combined this old technology with fluorescence labelling to image the intact internal structure of a cleared guinea pig cochlea[18]. Only after 2004 when Huisken et al. introduced a version of Light-Sheet-Fluorescence-Microscopy with a technique called Selective-Plane-Illumination-Microscopy which has the capacity to image living probes during extended periods of time with reduced phototoxicity by keeping photobleaching at certain minimum levels[19]. Zeiss then started the commercialization of this type of microscopy with the introduction of the first Light-Sheet-Fluorescence-Microscopy (Z.1) in 2012(**Figure 6**)[20].



**Figure 6 Set-up of the Light-Sheet-Fluorescence-Microscope Z.1 manufactured by Zeiss with an example of an imaged zebra fish on the monitor[20].**

The principle behind this different type of microscopy is simple and shows some clear advantages when compared to other microscope techniques, such as confocal microscopy. The first major difference is that it has two orthogonally arranged light paths. In other words, one path comes from the excitation source with a 90 degrees angle relative to the detection path. Secondly, the light beam coming from the excitation source comes in the form of a sheet (blue: in **Figure 7 A**). Any light emitted by the probe due to its fluorescence properties is then detected by the objective lens (green: in **Figure 7**). This is the basic principle of Light-Sheet-Fluorescence-Microscopy. (**Figure 7 B**)



**Figure 7** Illumination path for the Z.1 microscope A) This figure shows how the light beam, the probe, and the objective path interact on one specific position with the optical chamber surrounding the system. Source:[16] B). The illumination path and the objective path converge on one place where the probe is placed to enable the imaging process. There is an orthogonal relation between the two paths [9].

Light-Sheet-Fluorescence-Microscopy enables a more accurate illumination of the probe, this being crucial to avoid phototoxicity and photobleaching. While other technologies illuminate the whole probe and only concentrate the focus on one plane. Another important aspect to mention is that in confocal microscopy, as shown in Figure 5, both excitation and emission light is passed through the same objective[19]. In addition, this type of microscope has a laser scanning process, where it has to excite the probe, point by point, and then collect the emission for each focus point. This causes long scanning times and therefore, long exposure times. The Z.1 LSFM parallelize this process by using a camera that collects all the light of the large illuminated panel at the same time, which reduces significantly the time it takes to image the probe[20].

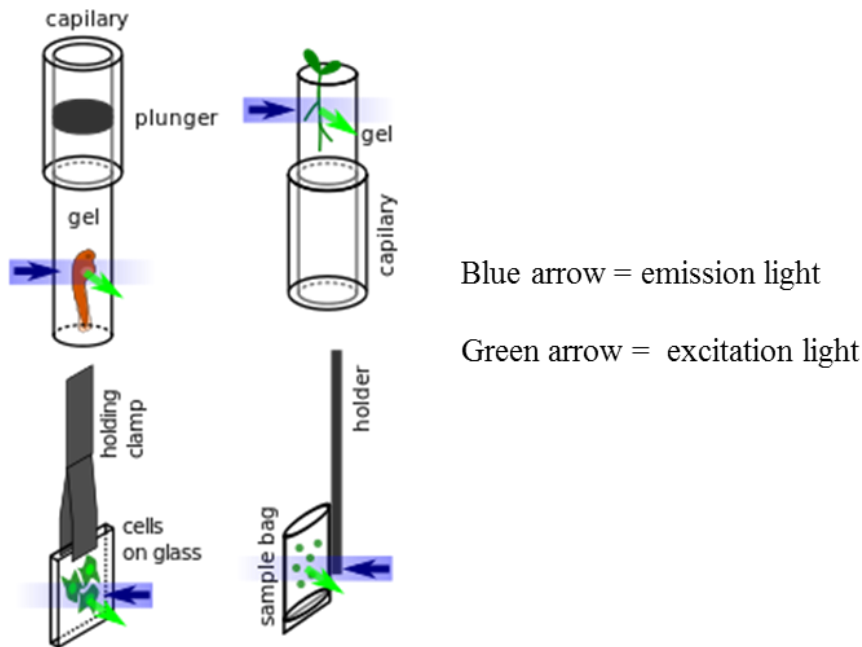
### 3.3 Mounting

Mounting the sample as it is the case of the Z.1 optical chamber offers some exceptional advantages not provided by other microscopes. It opens the possibility to vary the size of the probes, and it also favours the rotation of the prepared sample. The stage where the sample is mounted has the ability to rotate 360 degrees move in the, x-axis, y-axis z-axis almost freely. This allows scans of the sample from multiple angles and the search for the optimal position to image the biological structure of interest[21].

Normal microscopes need the sample to be mounted on a cover slip. This requires the samples to be accommodated in a way that biological structures to examine are reachable for scanning, due to the flatness of the slip. The Z.1, on the other hand, has the sample



hanging, embedded or enclosed in a medium, such as Agar, positioned from above (Figure 8). This opens the possibility to focus on different areas of the sample without having to adjust the latter manually[16].



**Figure 8 Mounting of the sample Different options to mount the sample with the illumination path Source: [16]**

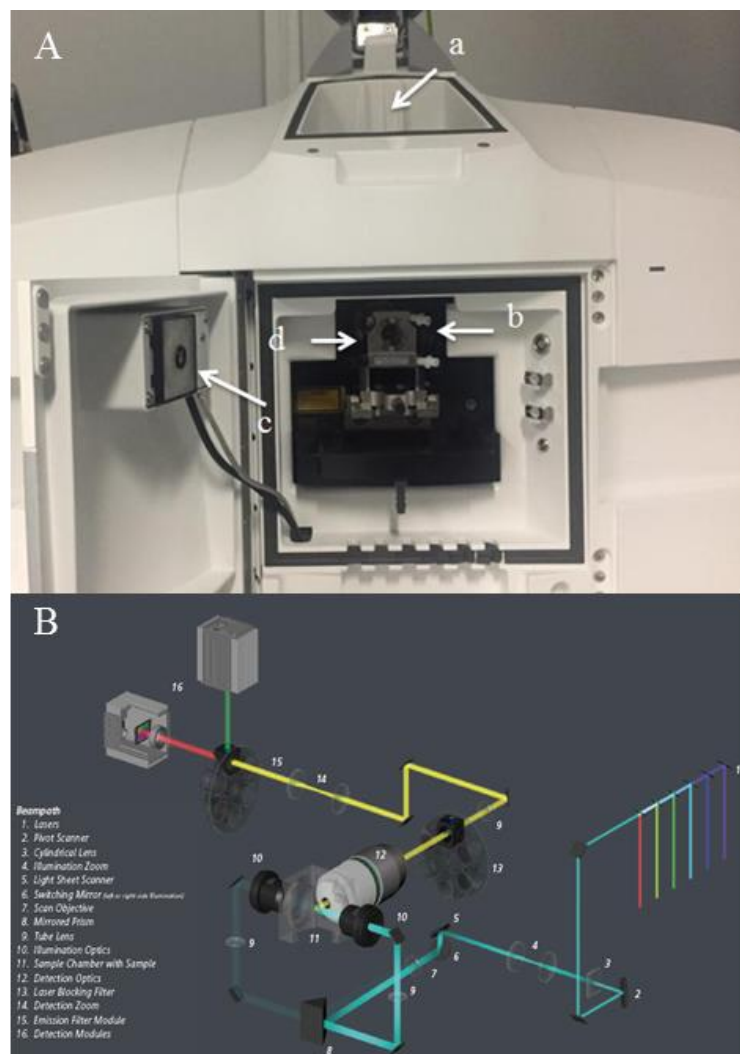
The Z.1 works with a chamber that is flooded with a medium such as a physiological water solution with a known refractive index (RI: 1.33 for water) according to the RI of the detection objective in use[21]. This offers some significant advantages, e. g. to maintain the physiological conditions to keep the sample alive and to record over long periods of time.

The Z.1 microscope is built around the sample (Figure 9). The latter is located in the centre of the chamber. For imaging, the probe is illuminated from the side of the chamber, where the probe is suspended. A set of mirrors is used to direct the sheet of light to any specific structures.

Locating the sample using only the laser fluorescence is difficult, because the laser only illuminates one plane of the whole sample. A frontal camera located on the opposite side of the detection objective helps detecting the sample and adjusting its position to the focus point before the fluorescent imaging starts.

### 3.4 Beam Path

The beam path of the microscope has a pivot scanner to eliminate the shadows casted by the structures while illuminating with the laser. A cylindrical lens is responsible of creating the sheet of light. The illumination zoom helps to control the thickness of the light beam. A scanner moves the sheet of light across the sample inside the chamber. The light is then directed to the detection chamber, where it meets the detection path coming from the objective. A revolver selects the filter to eliminate the scatter light from the emission source.

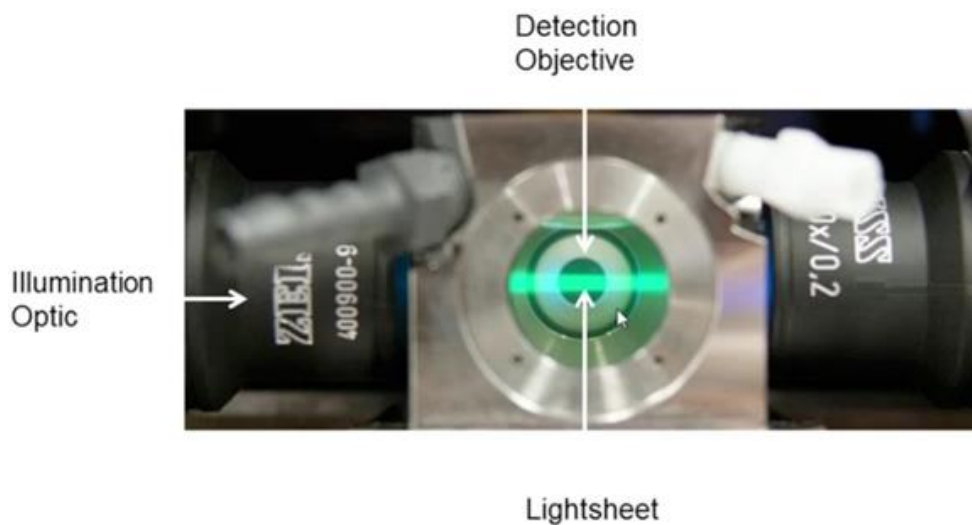


**Figure 9 Core of the Light-Sheet-Fluorescence-Microscope Z.1 Source: [16]. A: external view on the optical chamber, with a: probe column, b: optical chamber, c: frontal camera, and d: direction of laser beam. B: Laser beam path in the LSM.**

The Z.1 works with a 20x objective submerged in an aqueous environment. A zoom mechanism helps to zoom in and zoom out the sample. The emission filter module divides

the light to create and record two different channels with different wavelengths, or in other words different lasers, simultaneously[20].

The frontal view of the chamber gives a better understanding on how the system works and how and where the illumination and the detection paths converge (**Figure 10**). During the imaging process the laser moves up and down to create a homogeneous illumination. This occurs during the acquisition mode, which lasts around 15 ms per image taken, when the system is averaging out the exposure, and therefore, the emission. This helps to create a very consistent image.



**Figure 10** Sheet of the light path in the Z.1 [16]

The strength of the sheet of light and the quality of the image depend on the time that the light needs to travel through the sample, and the optical density of the probe. To solve this problem several scans are taken from different angles thus getting information that would otherwise get lost. A further disadvantage is that shadows are casted by objects or artefacts within the probe. This creates stripes behind these objects. To correct the shadowing the Z.1 does some small adjustments with an operation mode called the pivot scan. The pivot scan adjusts the angle of the light sheet lower and higher than the original position it is then possible to illuminate behind the object that casts the shadow. An average of the images is then done thus reducing the shadows casted and improving the quality of the image[20].

The rotation of the also opens the possibility to create 3-D models without having to reconstruct manually from the images taken. Different stacks from different angles are taken and fused together to generate a figure within seconds.

To control all the available parameters a software design by Zeiss is used. It allows it users to control with precision the position of the probe, the intensity of the lasers, the thickness of the light sheet, to change the filters when needed, to locate the sample, and to program scans for experiments over long periods of time[20].

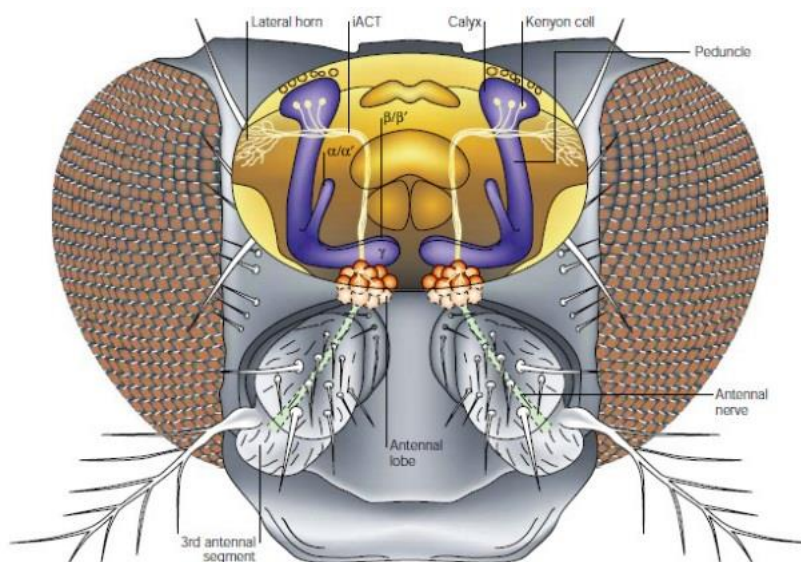
## 4 Olfaction

The need to interact and react to changing environmental conditions has marked the evolution of life as we know it for millions of years.[22, 23]. Tactility, vision, and chemoreception are a few mechanisms used by different organism to survive and behave within the environment surrounding them.[24] The ability to detect chemicals has helped life forms survive since the beginning of their existence. Olfaction and gustation constitute the main, and the oldest of this interaction. [22]

### 4.1 The Sensory Organs

The olfactory system is essential to recognise the quantity and the nature of chemical properties that are crucial for the survival, breeding, and feeding of the animal [25, 26]. Although olfactory organs vary among different species, the primary sensory structure, e.g. olfactory receptor bearing cells (OSN) where the transduction of the odour molecules into electric impulses occurs, remains the same. In case of *Drosophila* the respective olfactory organs are the antennae and the maxillary palps (**Figure 11**).

Olfactory receptors project to the antennal lobe in the insects and the olfactory bulb in vertebrate share to similar structures called glomeruli. These are small bundles of different type of neurons that are interacting with one another. These clusters of neurons are odorant specific and receive, process, and transfer crucial information to the brain[27].



**Figure 11** *Drosophila melanogaster* olfactory system. Modified from [28]

## 4.2 Basic Information on Insects

### 4.2.1 *Drosophila melanogaster*

The study of *Drosophila melanogaster* (DM) (**Figure 12**), commonly known as the vinegar fly, has been the foundation of genetically research for the last 100 years due to the fact that its whole genome was the first to be defined [29]. It has also been used as a base for understanding other species. This is due to its short life span, simple diet, fast reproduction, and the fact that its behaviour and development is similar to the one of other life forms[30]. This allows scientists to conduct and repeat experiments along several generations in a much simpler organism, while gaining basic knowledge about other species.



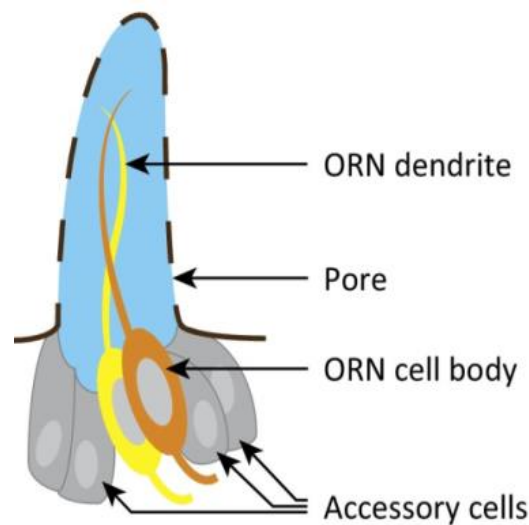
**Figure 12** Image of a *Drosophila melanogaster*. Modified from [31]

### 4.2.2 Comparable Organism for the Olfactory System

The basic structure of the olfactory system of DM is similar compared to vertebrates and other species of invertebrates. This simplifies the task of figuring out the complexity of odour recognition and processing [27, 32].

The olfactory chemoreception in the *Drosophila melanogaster* takes place in the third antennal segment called funiculus and in the maxillary palps bearing -small hair-like structures called sensilla (**Figure 13**) [33]. Each of them is responsible for detecting specific odorants, or pheromones[34]. In some cases, as much as 4 olfactory sensory neurons are housed in one sensillum [24]. They transduce the olfactory sensation into

electric impulses, and thus, pass on information about quality and quantity of odour to the antennal lobe where further processing occurs.



**Figure 13** Single sensillum of the third antenna of *Drosophila melanogaster* with two olfactory receptor neurons (ORN). Modified from [35]

### 4.3 *In vivo* Experiments on Antennal Olfactory Neurons

Given the fact that signal transmission occurs via electrical impulses the idea of measuring the voltage in extracellularly in odour response experiments or electroantennograms (EAG) materialized (Schneider 1963), EAG on the intact fly have been conducted for the least 50 years. Two glass pipettes filled with a conductive fluid are positioned: one at the tip of the antenna and the other one at the base, the odorant are then blown to the antenna while the electrodes record any voltage difference caused by the neurons. The main goal is to determine if there is any odour perception at all. [36]

Knowing which odorants are perceived raises the question: Where on the antennae does the perception of each one take place? Single sensillum recognition (SSR) is a more selective type of electrophysiology that enables to record each sensillum individually, while giving more information regarding the sensitivity, selectivity one of olfactory receptor neurons. Within SSR the electrode is inserted into one sensillum to enable recordings of individual receptor cells. With the help of SSR sensilla maps of the antenna have been made helping scientist to classify different olfactory sensory neurons. [36]

## 4.4 Calcium Imaging Experiments

Even though SSR opened the possibility for more accurate and specific recordings; it also opens up questions about how internal brain processing of odours occurs.

The importance of  $\text{Ca}^{2+}$  became known during 1880 after Sydney Ringer solution discovered that “lime salt” was necessary for the frog’s heart contractions[37]. This discovery brought scientists to notice that  $\text{Ca}^{2+}$  is also involved in many cellular functions such as signal transmission, segregation, and muscle contraction[38]. Scientists were left with the clear message: it is imperative to know how, where, and when  $\text{Ca}^{2+}$  operates in order to understand the physiology of organisms, in particular for the nervous system.

Calcium imaging is a technique that has been developed over the last two decades. It takes advantage of calcium indicators detected by fluorescence microscopy. Calcium indicators are fluorophores that change their fluorescence characteristics when they bind to  $\text{Ca}^{2+}$  ions. In other words, the fluorophores emit light of a certain wavelength after they are bound to calcium ions. There are two types of calcium indicators: chemical indicators [39] and genetic indicators[40]. Chemical indicators are molecules that bind selectively to calcium ions changing their fluorescence properties. These indicators can be loaded to the cells via micropipette or bath solutions. Genetically encoded calcium indicators, such as GCaMP, are derivatives of the green fluorescent protein (GFP), whose genes can be transferred into living cells. They are not injected into the cells but are expressed Trans genetically in specific cells or in intra cellular structures. [41]. Confocal and two-photon microscopes are usually employed in viewing and resolving the respective fluorescence signals upon activity within the tissue.[38]

Currently, scientists are working with two types (*ex-vivo* and *in-vivo*) of experiments to analyse the cellular structures of the antennae in *Drosophila melanogaster*.

### 4.4.1 In-vivo preparations

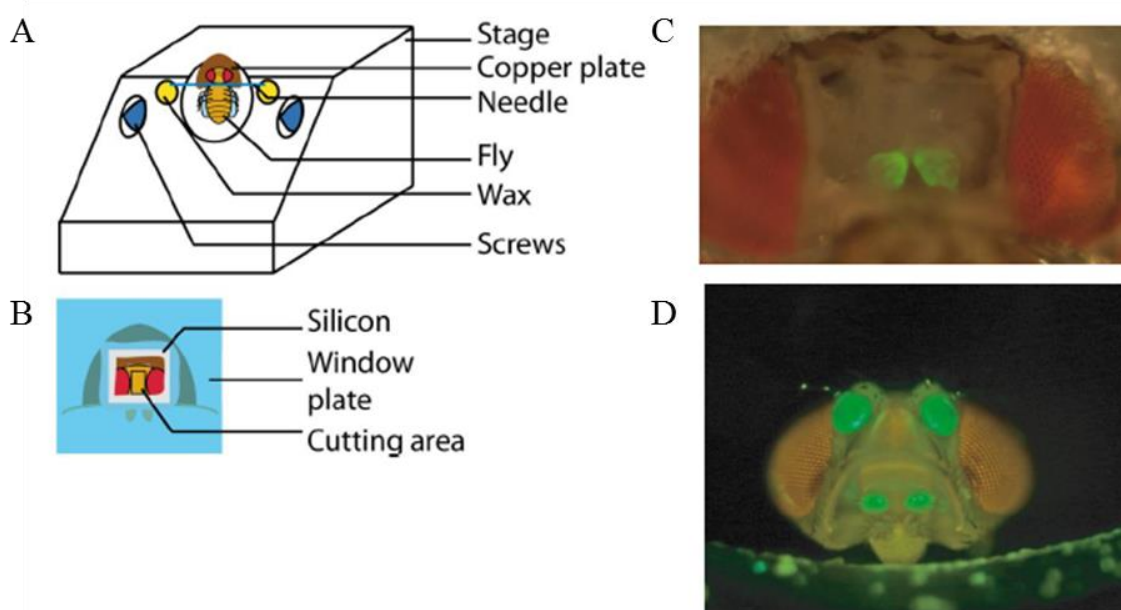
In-vivo preparations require a special set up (**Figure 14**) to hold the fly while leaving the antennae and the head free. Due to the thickness of the cuticle, an invasive method has to be used. Cutting a small window in the head of the fly facilitates the screening of the primary olfactory neuropil: the antennal lobe. The fly is fixed on a custom- made holder leaving the antennae exposed. The stability of the fly is of extreme importance, because every movement could take the imaged structure out of focus. Therefore, the head is fixed using a minutia needle, wax to glue it to the holder, and resin to hold the back of the head.



The odour is then delivered via air using a pump and valves system to control the amount and the duration of the odour exposure e.g. [42, 43].

These precautions are important to keep the fly alive for the duration of the experiment. The major disadvantages are:

- 1) The phototoxicity and the photobleaching of laser light during the experiment
- 2) It is a very invasive method that does not represent a sustainable environment of the fly over prolonged periods (days).
- 3) Movement artefacts

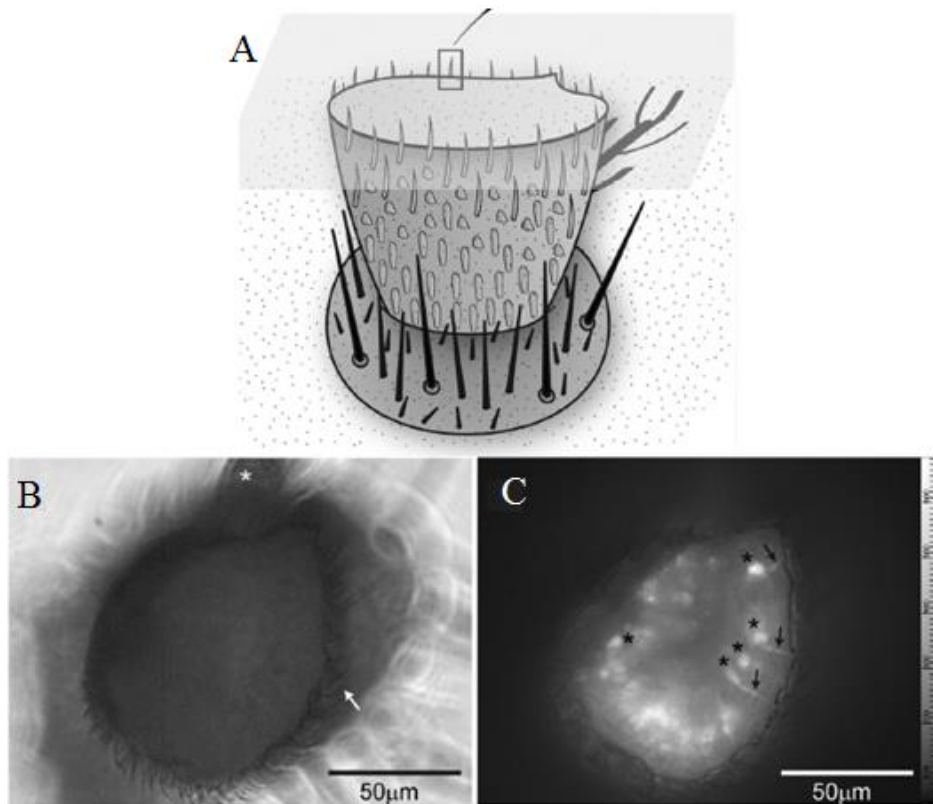


**Figure 14** Set-up of an in-vivo odour exposure experiment A) Frontal view of the mounting of the fly B) Frontal view of the mounted fly C) Image taken with an epifluorescence microscope of the funiculi and the glomeruli of *Drosophila melanogaster* expressing of Ca<sup>2+</sup> reporter GCamP. D) Head of the *Drosophila melanogaster* with the antennae and palps emitting Source:[42, 43]

#### 4.4.2 Ex-vivo Preparations

Ex-vivo experiments differ in the experimental set-up. This technic intends to gain information about cellular processes at the antenna sensilla. Here, only the antenna is dissected and mounted inside a small chamber on a coverslip with a Ringer solution bath to keep humidity thus prolonging the life of the cells. The third segment (funiculus) is then cut open in order to expose different olfactory sensory neurons (**Figure 15**). In the experiment the odour is added via a Ringer solution flow solution. A system with pumps and valves control the Ringer solution flux and the dosage of the odour. Using the map-

recording from the SSR experiments it is possible to test neurons that are known to react to specific odours and expose the internal interaction of the neuron[44].

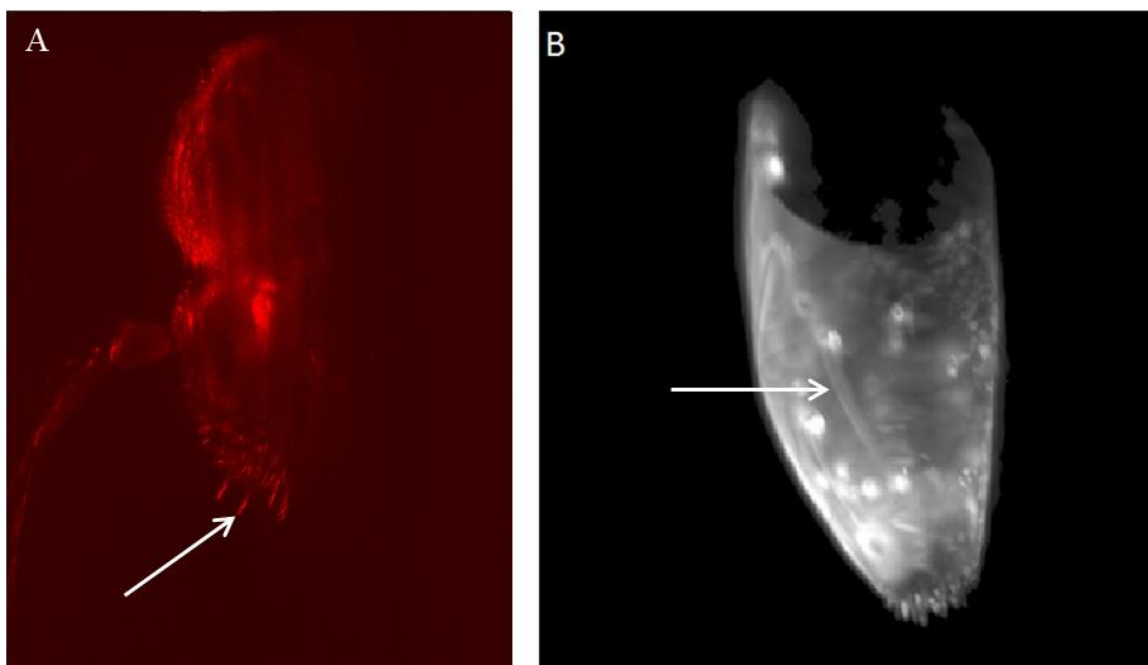


**Figure 15** Example of an in-vivo odour exposure experiment A) A cut of the third segment of the antenna (funiculus) of the *Drosophila melanogaster* reveals neuronal cell bodies before (B) and after (C) odor exposure. Modified from [44]

## 5 The Need of New Imaging Methods

The Zeiss Light sheet Microscope Z.1 (LSFM) opened the path for more complete and fast imaging. Previous experiments have proven the feasibility of optical imaging of internal structures in the olfactory system of the *Drosophila melanogaster*. After opening the cuticle the activity olfactory receptors and olfactory sensory neurons are recordable (see, above).

In order to record nervous active in a more invasive manner, cuticle clearing methods have to be applied. In the black beetle combined with Z.1 fluorescence imaging have shown that after clearing a dark cuticle using genetic methods [45] the visualization of the internal structures such as the muscles are feasible (**Figure 16A**).



**Figure 16** Scans made with the Z.1 microscope A) The antenna of the genetically modified *Drosophila melanogaster* show a response of the olfactory sensory neurons but the cuticle prevents the laser of deep penetrating and therefore the internal structures remained partly obscured. B) The palp of the leaf beetle is cleared enough to show internal structures without damaging the cuticle. This is possible due to the genetically modified and cleared cuticle [45]

### 5.1 Light-Sheet-Fluorescence-Microscope Z.1 for *in-vivo* odour exposure experiments

The optical chamber of the Z.1 provides a static environment ideal for imaging but odour exposure experiments are not feasible although the optical chamber possess two inlets and 3 outlets ideal to adapt the system to different needs. To gain more information of the internal structure olfactory system of an intact *Drosophila melanogaster* an adaptation of the

optical chamber of the Z.1 microscope to enable odour in- and out flux image the fly during odour exposure is proposed.

## 5.2 Description of the function

Light-Sheet-Fluorescence-Microscopes such as the Zeiss Z.1 use a focused beam path that creates a sheet of light, thus keeping light exposure to the probe at a minimum. This minimizes the phototoxicity and photobleaching of the fluorophores. The optical chamber provides a stable environment ideal for long exposure experiments, where the probe can remain alive for extended periods[15]. The imaging process varies from other fluorescence microscopes, such as confocal in speed and 3D quality of the recorded image stacks.

The set-up of the odour exposure experiment may vary depending on the type of transport medium for the odour. Since the Z.1 optical chamber where the probe is placed is filled with an aqueous substance an adaptation should work using parameters similar to experiments with a liquid medium for the odour [44]. Airborne odour would interfere with the imaging process of the Z.1 microscope causing undesired turbulence, and forcing the light sheet to cross water and air before illuminating the sample. Since air and water have different refractive indexes ( $n_{\text{air}} = 1.0$  and  $n_{\text{water}} = 1.33$ , respectively) and therefore, diminishing optical resolution[46].

Liquid borne odour exposure experiments require a dynamic environment, where the probe can be exposed to different odorants, and the system is able to clear up any residual odour traces. The time point and quantity of odours (concentration) exposed to the sensilla on the antennae needs to be reliably controllable during recordings. The setup needs a specific pH value of 7.3 to ensure the survival of the exposed cells [44].

The experimental procedure has different phases. First, the antenna or the whole fly with exposed antennae has been fixed and placed in a Ringer solution. Second, the odour with a desired concentration and quantity has to be added. The odour presentation and the imaging recording process take place simultaneously. This enables the scientist to visualize any difference in the fluorescence when calcium ions activate the genetically modified fluorophores in the fly. After the experiment, a washing process starts to remove the odour from the Z.1 chamber. The washing continues until the fluorescence signal disappears. Afterwards, it is possible to expose the fly again to the odour. This allows investigations on neuronal processing. The Zeiss ZEN software that is used to control the

microscope and the imaging process can also be programmed to image certain area of the fly and create simultaneous to the exposure a series of image stacks.

Thus, the goal is to adapt the existing Z.1 optical chamber to allow calcium recordings during odour exposure experiments. This adaptation should support all aqueous solutions where odour molecules can be transported. This variation of the Z.1 microscope will allow scientists to gain more information on the internal nervous processing of neurons, after odour presentation without having to dissect and fixing the antennae, that is: in a non-invasive way.

Since the experiments are to be conducted using the optical chamber of the Z.1 a control and a reliable forecast of the odour flow are required to properly conduct the odour exposure. A desired design would not involve an alteration of the chamber itself but an addition to the latter given the fact that the chamber is not of mass production product and the costs of such an alteration for commercial use would be out of scope. The image operation of the Light-Sheet-Fluorescence-Microscope to perform should not be affected by the addition of the odour exposure design to the system.

## 5.3 Requirement List

As the basis of every construction and product development of the topic creation this area and the requirements of the experiments created. The requirement list is a working basis that accompanies the entire development process, which is constantly updated through the exchange of information with the scientists

The understanding the biological process behind the calcium imaging protocols for odour exposure combined with the technical knowledge of the Light-Sheet-Fluorescence-Microscope Z.1 is necessary and vital to create a list of the requirements and need of both systems for them to collaborate. There are no norms or legal safety requirements to consider.

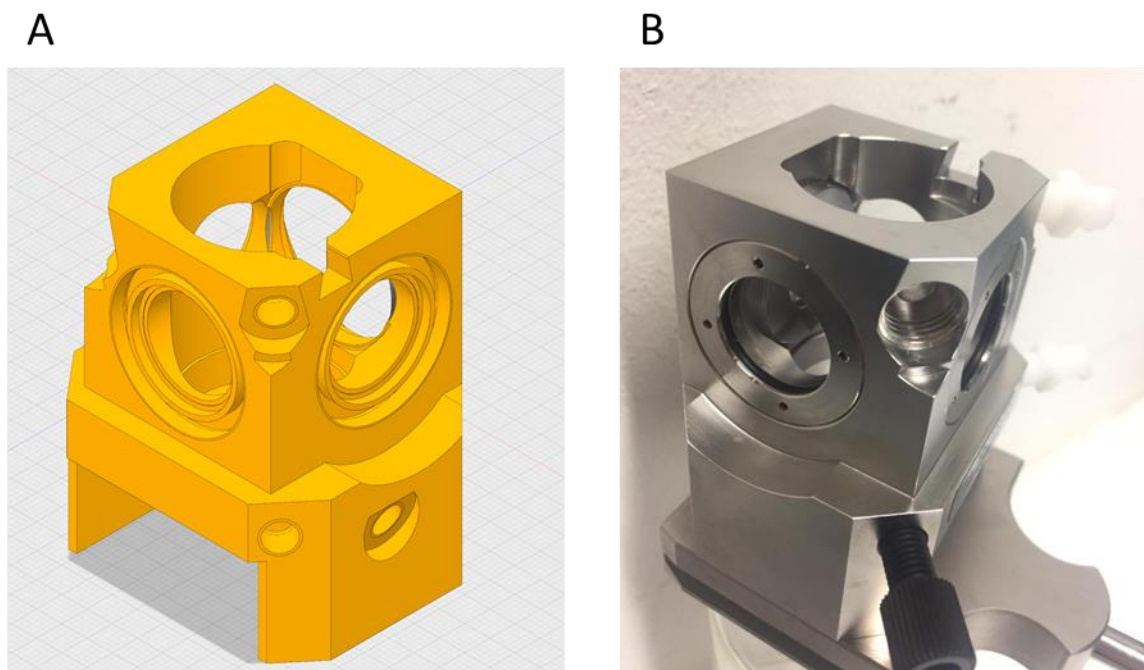
**Table 1 List of requirements for odour exposure experiments on the Z.1 microscope**

Modified: 12/07/2018 Version: 05		An odour chamber for in-vivo 3D calcium imaging in insect brains for the use on the Light-Sheet-Fluorescence-Microscope Z.1			Reviser: Eckard Schumann	
<b>Product and Performance Requirements</b>						
Nr.	Mandatory/ Optional	Detail Specifications	Value		Source	
			Minimal Fulfilment	Ideal Fulfilment		
<b>1 Light-Sheet-Fluorescence-Microscope</b>						
1.1	M	Aqueous Environment			System	
1.2	M	Free Movement of the Probe (collision)			System	
1.3	O	Simple Cleaning of the System	Autoclave		System	
1.4	M	Beam Path	No interference		System	
1.5	O	Sample Positioning (imaging)	Sample		System	
1.6	R				System	
<b>2 Calcium Imaging Experiment</b>						
2.1	M	Odour Residence Time	100	300s	Experiment	
2.2	M	Single odour contact of receptors			Experiment	
2.3	M	Acid or Base solutions (ph 7.3)			Experiment	
2.4	M	Reproducibility			Experiment	
2.5	O	Odour Storage	1 odour	Several odours	Experiment	
2.6	M	Odour Flow Foreseeability			Experiment	
2.7	M	Complete Extraction			Experiment	
2.8	M	Odour flow rate	5 mL/min	30mL/min	Experiment	
2.9	M	Ringer solution flow rate	10mL/s	30mL/s	Experiment	
<b>3 Odour distributor properties</b>						
3.1	M	Flow rate	5 mL/min	30mL/min	E. S.	
3.2	M	Velocity of the Flow			E. S.	
3.3	O	Low Attrition			E. S.	
3.4	M	Inert and odourless Material			Experiment	
3.5	M	Simple Mounting			E. S.	

## 6 Derivation the Function of the Product

### 6.1 Optical Chamber of the Light-Sheet-Fluorescence-Microscope

The optical chamber of the Z.1 LSFM is the base of any desired adaptation. Therefore, understanding its dimensions, properties and capabilities is crucial to develop any modifications to extend or improve its performance potentials.



**Figure 17 A) 3-D Model of the optical chamber of the Z.1 LSFM, upper right side B) Photograph of the optical chamber of the Z.1 LSFM, upper left side.**

The blue print of the optical chamber shows the possibilities available to adapt the current system for the desired experiments. (Appendix Blueprint). The Z.1 chamber possesses two inlets on the upper part and three outlets on the underpart all of them equipped with threads connectors suitable for the connection to external tubes systems. According to the developers of the chamber the material should not interact or be affected in any way on contact to acidic or basic substances or during the cleaning process in the autoclave.

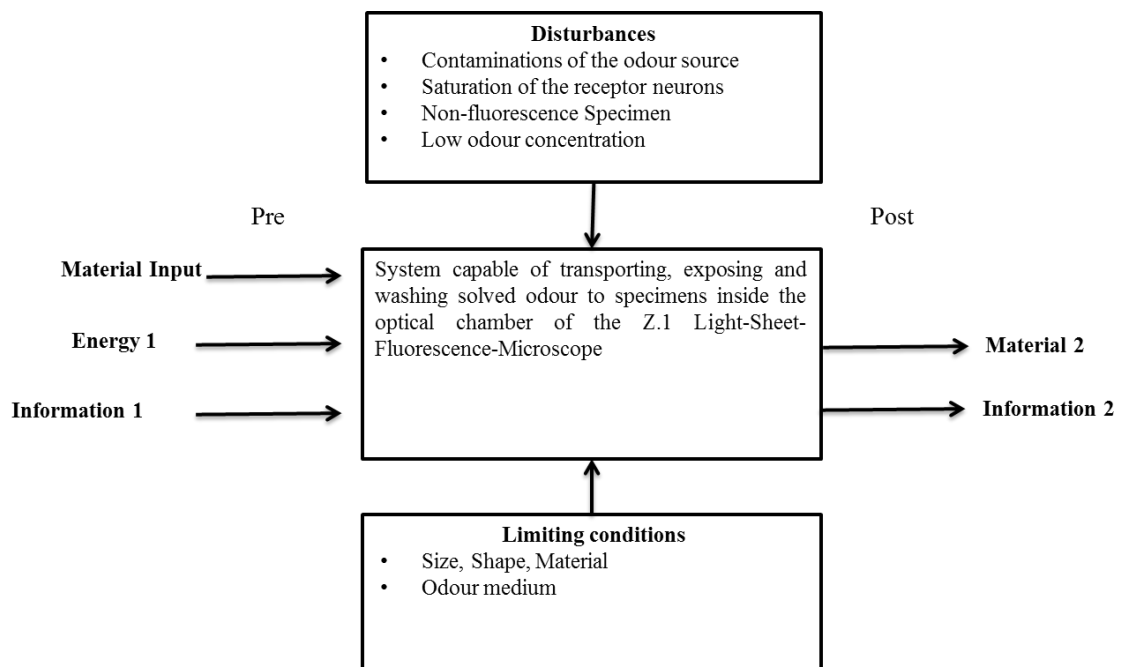
The whole system of the Light-Sheet-Fluorescence-Microscope is closed in order to contain watery solution within the chamber during operation. (**Figure 18**) This assures the safety of the system and the operator as the risk of contact of the skin with dangerous chemicals and the laser with the eyes is minimal.

## 6.2 Defining the Structure of the Function

The guidelines of the norm VDI 2221 help to structure the search for an optimal solution. The entire function represents the complete problem and subdivides it in partial functions. These partial functions describe only one certain aspect of the whole system.

### 6.2.1 Main Function

A methodical approach is needed for any optimisation or construction of the required solutions. The first step should simplify the entire function as an abstract issue, before the partial functions are defined. Here fore, the “Black Box” is used. The “Black Box” is created out of the requirements and the desires of the main function and the end product.



Material 1: Ringer solution, Dissolved odour in Ringer solution, Fluorescent probe (*Drosophila melanogaster*)

Energy 1: Mechanical forces, Electrical energy, Excitation Laser beam

Information 1: Amount of odour, Type of odour, Probe positioning

Material 2: Solution waste, Specimen

Energy 2: Emission, thermic Energy

Information 2: Fluorescent changes, Image stacks

**Figure 18 Black Box visualization of the main system**

The Black Box visualization of the main system, as shown in Figure 18, helps to understand how the system in an abstract way. It shows how certain input changes in the system delivering the desired output. The broad explanation of the changes of the input such as material, energy, and information is influenced by limiting conditions. Taking the disturbances into account helps to comprehend the complexity of the system.



The adaptation of the Z.1 optical chamber should enable the odour exposure to the specimen being image utilizing in the given set up. It should not affect the performance of the microscope thus represent an addition to the current system.

The odour and the Ringer solution represent two different systems that join within the optical chamber. The storage of these substances takes place outside the microscope and has to be pumped in. Therefore, a set of pumps is needed to control the influx and out flux. Since the position of the probe may vary depending on which part on the fly is imaged, the distribution of the odour has to be targeted to specific locations of the specimen. This represents an area of 15 mm long and 5 mm width in the middle of the chamber relative to the detecting objective. The mobility of the probe is an aspect of major relevancy since any collision with the odour distribution device must be avoided.

## 6.2.2 Sub Functions

To effectively search for the optimal solution the division of the main function in sub-functions is essential. It helps not only to understand better the main problem thus providing a better representation of each individual system as an independent function but also reveals their relation to other sub-function. The purpose of the scheme (as shown in **Figure 19**) is to handle each sub function by itself and then combine their solutions to solve the main problem.

The main function of a system able to transport, expose and wash odour presented to the specimens inside the optical chamber the without affecting the imaging performance of the LSM. This main function is subdivided into two sub-functions that converge within the optical chamber of the Z.1 microscope side function. First sub-function: the odour function consists of the side functions storage, transport, distribution and direction. Second: the Ringer solution sub function consists of the side functions storage, transport and the distribution. Those two sub systems join in the optical chamber of the Z.1 microscope and work simultaneously during the imaging process.

A third sub-function consists of extracting the odour waste out of the optical chamber after it made contact with the specimen and storing it. The complete and fast extraction of the odour in a washing step is crucial to guarantee the reproducibility of subsequent odour exposure regimes.

As shown on the diagram Figure 19, the odour and Ringer solution system are additions to the existing Z.1. The Ringer solution has to be stored in a bottle ensuring the

cleanliness of the liquid. The solution has to be transported via a pump to assure a constant flow and distribution in the Z.1 utilizing one or two of existing inlets.

The odour flow function starts also with storage where the odour cannot interact with other substances. It then has to be sent with a small but constant flow to an odour distribution system. The odour distribution sub function has to guarantee that the odour reaches the specimen within the optical chamber to ensure a spatially and timely defined exposure. The odour extracting system has to extract the waste in the same amount of liquid entering the chamber. This waste is then transported to storage for its removal.

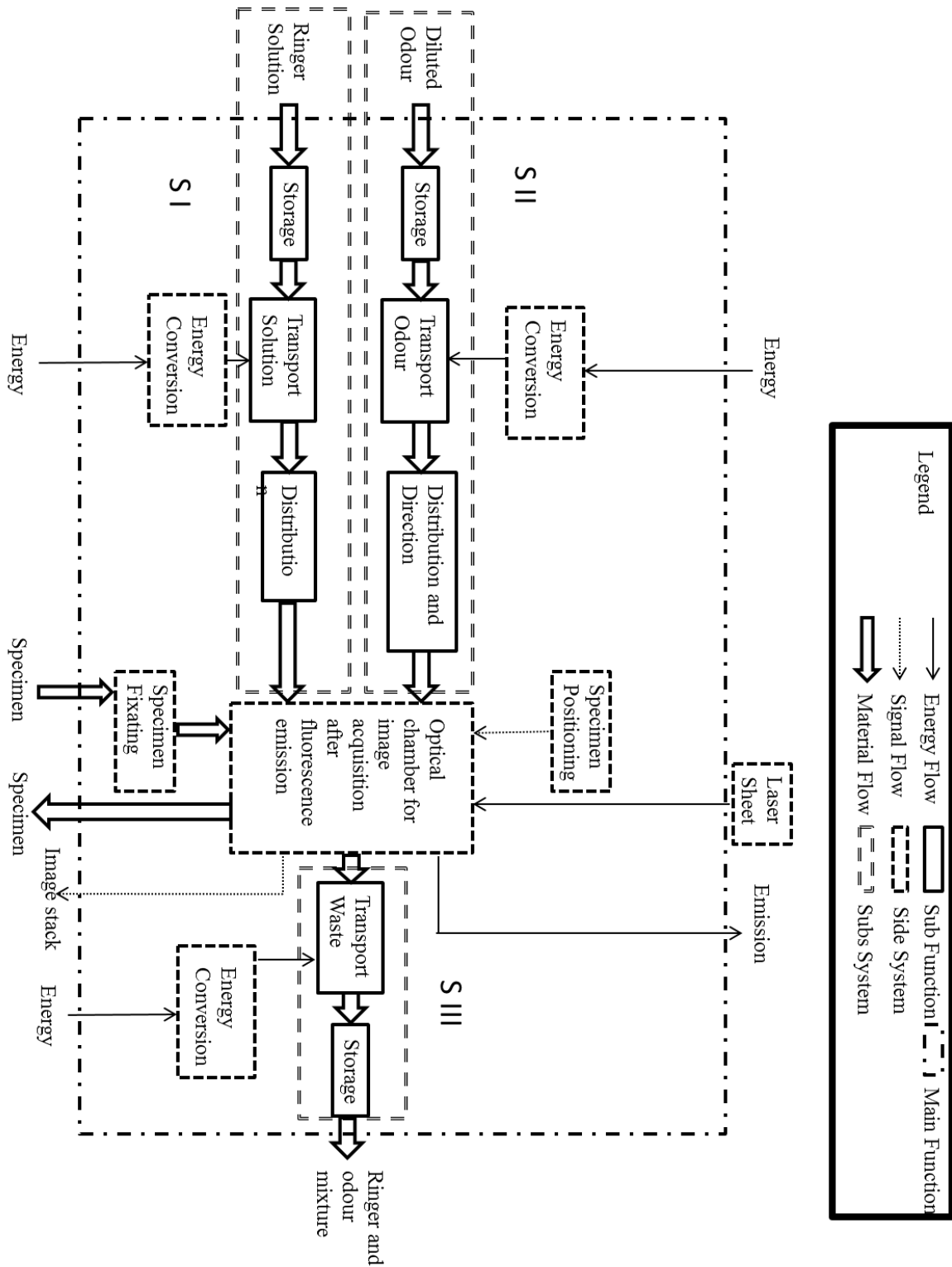


Figure 19 Main function diagram with the sub-functions and the side function after [47]

### 6.3 Solutions conception to enable odour exposure experiment inside the optical chamber of the Z.1 microscope

#### 6.3.1 Storage

For the storage of liquids it is important that the liquid does not react or is affected by the container it is being kept in. Therefore, the storage container has to remain intact and has to be cleanable or in this case autoclavable. Since the amount of odour used for these experiments is small, the volume of the storage units should be around 250 mL.

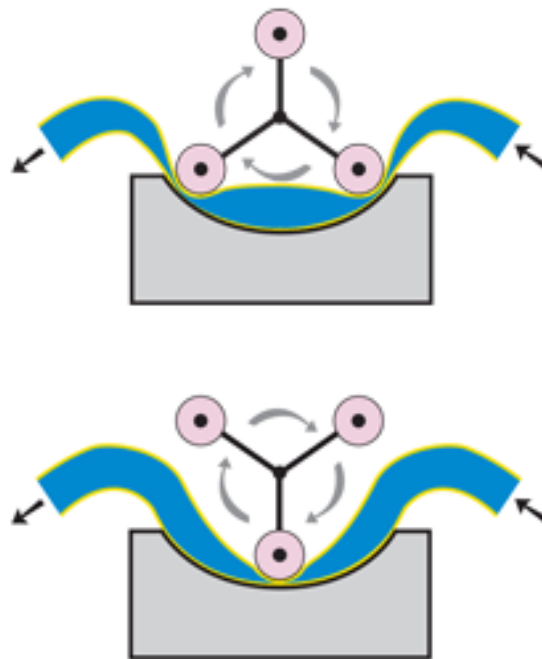
**Table 2 Material comparison for storage units**

Material	Polypropylene [48]	Glass [49]	Fluoropolymer[50]
Characteristics	Inert against required chemicals	Inert against required chemicals	Inert against required chemicals
Colour	White Translucent	Transparent	White Translucent
Size	250 mL	250 mL	125 mL
Temperature	-40 °C-121 °C	121°C	-270°C to 250°C
Cleaning Method	Autoclavable	Autoclavable	Autoclavable

#### 6.3.2 Pumps

##### 6.3.2.1 Peristaltic Pump:

The peristaltic pump works with a set of rollers attached to a circular rotor and a flexi tube that is located inside the round cover surrounding the rotor. The pump creates the positive displacement after the rollers compress and close the tube on one end and the rotors turns forcing the liquid inside the tube to move through the pipe. This pumps work with one or more rollers, which trap and mobilize the liquid along the tube.



**Figure 20 Principle of the peristaltic pumps [51]**

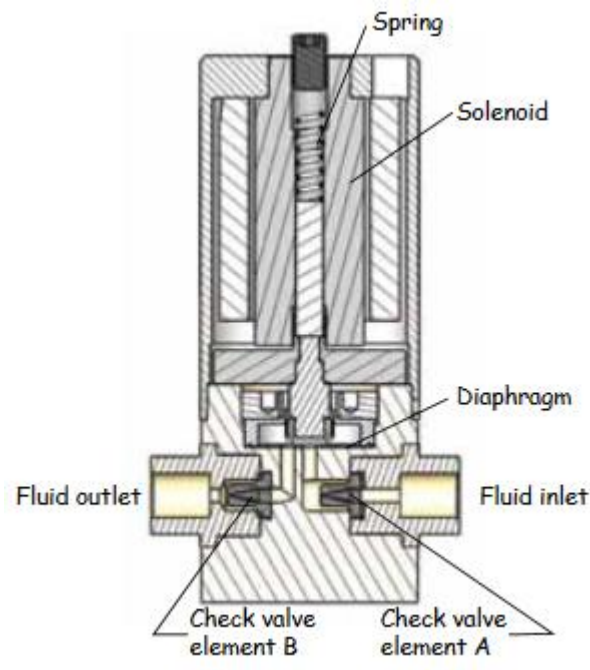
The peristaltic pumps are suitable for any processes that require sterile or highly reactive fluids, because its components do not come in contact with the fluid being pumped. The rollers affect the continuity of the flow, because it gets interrupted due to the rollers. The pulsation created by the rollers is affected by the flow rate, the length of the tube, the revolutions per minute, and the density of the fluid. To reduce this pulsation more rollers can be added to the rotor. This would decrease the amplitude of the pulsation. [52]

A four roller Reglo quick pump can manage flow rates up to 230 mL/min working with tubes with a 3.2 mm diameter and wall thickness of 1.6 mm for a flow rate between 2.1 and 103 mL/min. [53]

#### 6.3.2.2 Solenoid Pump

A solenoid micro pump is a machine which is designed to control, duplicate and supply low volume flows. The current of the flow remains out of contact with the pump mechanism by diaphragm. The action mechanism is controlled by the solenoid located on the upper part of the pump. When the solenoid is charged the diaphragm retracts and creates a vacuum within the casing of the pump. This vacuum sucks the liquid from the inlet and at the same time closes the outlet valve. Then the solenoid is discharged and the

spring pushed the diaphragm back to its initial position. This closes the inlet valve, while the liquid is pushed through the outlet valve.



**Figure 21 Example of a solenoid pump from Bio Chem[54]**

This mechanism creates a small pulsation due to the cyclical movement of the membrane. The discharge volume can vary from 20 to 250 microliters per cycle or a max flow rate between 2.4 and 7.2 mL/min with a repeatability of +/- 5%. The pump is programmed to work at 2 Hz, but the rate can be changed adjusting the “down” time, which is the time in between pulsations. [54]

### 6.3.2.3 Syringe Pump

Research syringe pumps are used for tasks that require small fluid volume flux. A motor moves a plate that pushes the syringe discharging the liquid. These pumps can hold several syringes at the same time ideal for experiments with different fluids, while managing to operate very low flow rates with high precision. The flow rates vary from micro, nano, and picolitre per minute. Some of the parameters the system is able to control are, for example, the pressure which enables the flow of liquids with high viscosity, and the temperature.

The Fusion 4000 syringe pump provides the system with 2 different independent regulated channels. The system can hold syringes with 0.5 microliter until 60 millilitre and controls

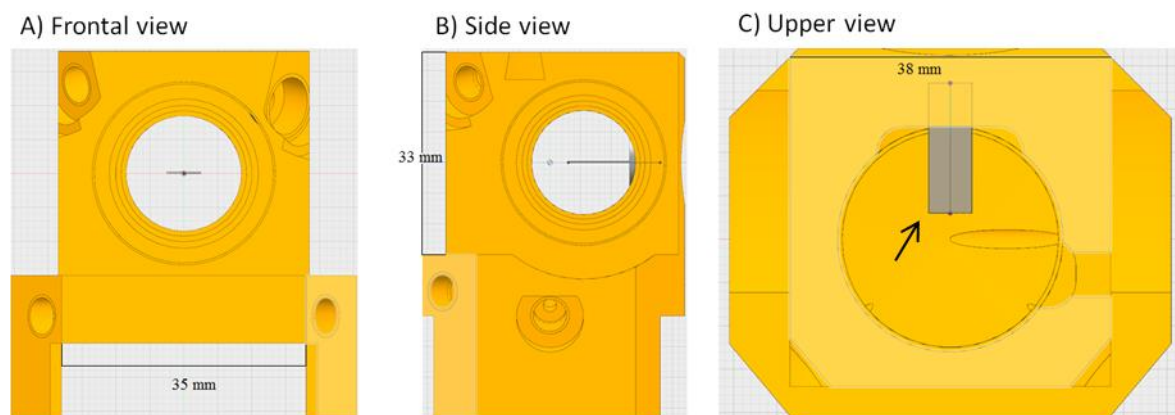
flow rates from 1.6 pL/min to 102 mL/min. The interface allows the researcher to program the system beforehand accordingly to necessities of the different experiments [55].



**Figure 22 Fusion 4000 syringe pump [55]**

### 6.3.3 Fluid Dynamics

Odour exposure experiment requires that the antenna has a direct contact with the odour molecules. The Z.1 optical chamber free mobility of the probe represents a major challenge for the exposure experiments. A direct exposure on the antenna is therefore not possible due to the collision risk. The focus point of the objective in the Z.1 microscope is in the back part of the optical chamber. (**Figure 23**) Thus, the probe has to be located in that area for imaging. The area has to be 5 mm width and 15 mm length and in a certain distance from the objective at the centre of the chamber (**Figure 23**). This area are has to be reached by odour to ensure the exposure of the probe. Therefore a model has to be created to ensure that the odour reaches this specific are without affecting the functionality of the microscope.



**Figure 23 Optical chamber of the Z.1 microscope. The area where the probe will be submerged is marked in grey.**

Understanding the dynamics of the odour mixture molecules entering the Ringer solution inside the optical chamber is of extreme importance to guarantee the effectiveness of the system.

The study of forces affecting liquids in motion and is part of the fluid dynamics, which focus on mechanic and forces on fluids, gases. The study of fluids is a tool used by engineers to calculate forces, defining mass flow rates within certain compartments, thus predicting flow patterns. These calculations are defined by defined properties of fluids such as flow velocity, compressibility, density, temperature and pressure in a specific time and space. The foundation of the fluid dynamics relies on mechanics. The conservation laws such as the conservation of mass, Newton's second law of motion[56] and the first law of thermodynamics [57]. Fluids are a group of molecules that collide with one another and with the environment surrounding them [58]. This provokes that on each given point



the basic characteristics such as the temperature, pressure, density and velocity vary from one point to another. There are two way to calculate the physical properties of an aqueous flow: The Eulerian method and the Lagrangian method.

The Eulerian method focuses on how the changes of velocity and pressure in specific spatial locations in  $x$ ,  $y$ , and  $z$ . In this method the characteristics, such as velocity, acceleration and location, of singular particles are not relevant. Instead it focuses on any possible position within the selected field.

The Langragian method focuses on singular particles and calculates the properties of every single of them. Therefore, it is more demanding to calculate than the Eulerian method.

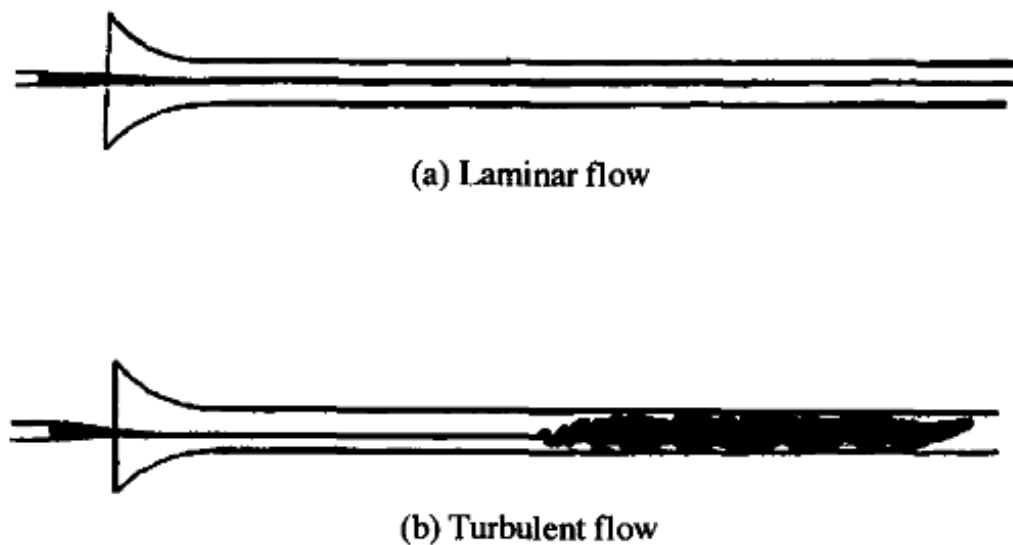
The most used and effective method to study and predict how the movement of the flow is going to behave is the Eulerian method instead of the Lagrangian method due to the computational demand of the later [58-61].

### 6.3.3.1 Steady Flow and Unsteady Flow

A flow in which its defined properties do not change over time it is called a steady flow. A flow in which its conditions change over time it is called unsteady flow[62]. It is clear that any changing processes are unsteady such as all the starting operations, but become stable after a certain time.

### 6.3.3.2 Laminar Flow and Turbulent Flow

There are two types of flows described by Osborne Reynold utilizing a coloured liquid that enters a tube filled with water [62, 63].Using this setup showed that the laminar or sheet-like flow enters the other liquid and does not mix with the latter (**Figure 24**). It is not until the entering liquid reaches a certain speed value, that the flow becomes turbulent and mixes with the surrounding water.



**Figure 24 Example of the Osborne Reynolds experiment to determine the differential factors of laminar and turbulent flows [63]**

After conducting several experiments utilizing glass tubes with different diameters and changing the water temperatures he defined the critical point when a flow turns turbulent depending on the fluid viscosity, fluid density, average velocity and the tube diameter.

**Equation 1 Reynolds number equation [63]**

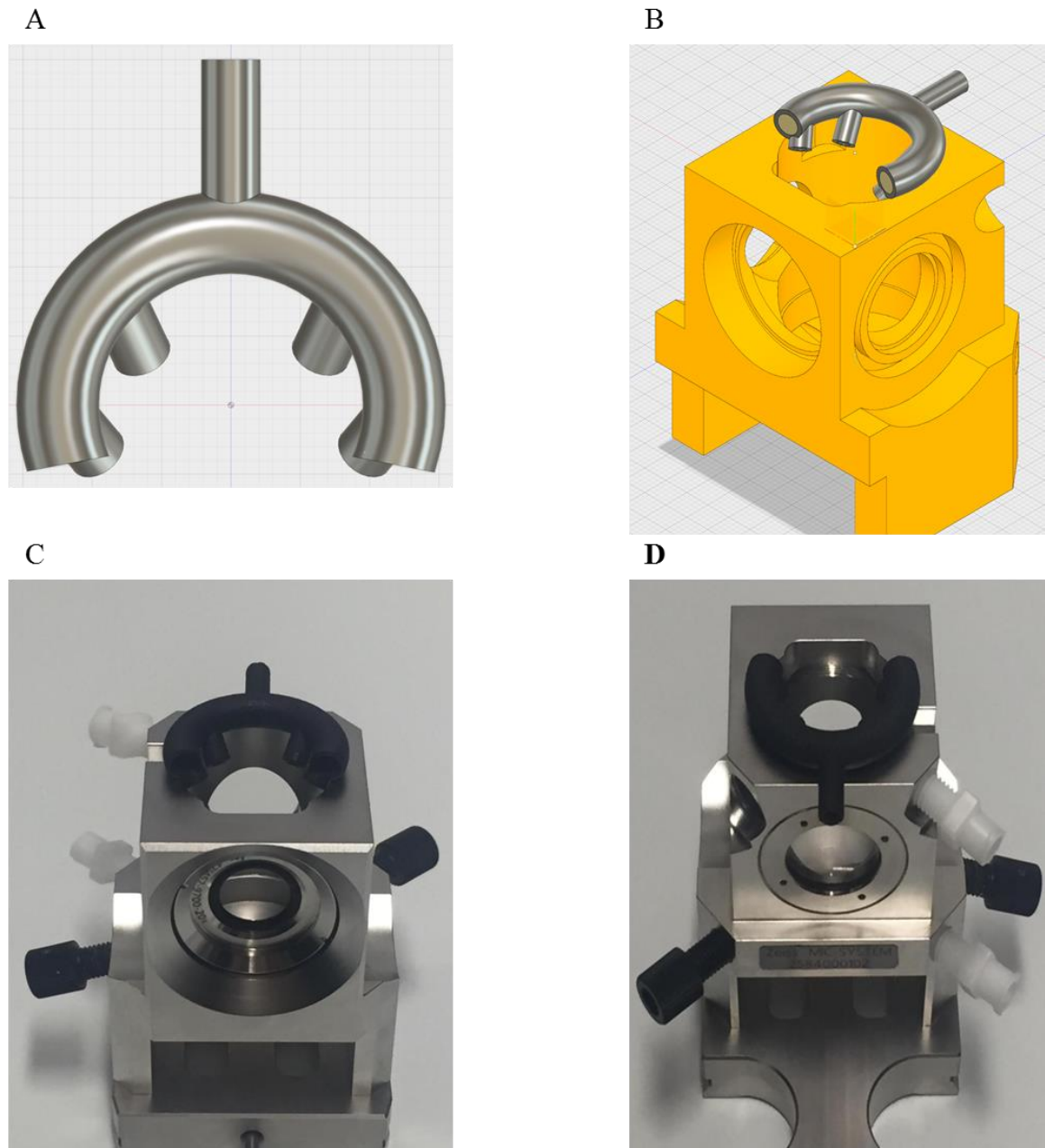
$$Re = \frac{\rho v d}{\mu}$$

Considering these principles after odour distributor model Figure 26 A was to be built. To create a laminar flow that reaches the area of interest (**Figure 24 B**) without mixing with the fluid surrounding it.

### 6.3.4 Odour Distributor model

The odour distribution prototype tube controls and distributes the flow in such a manner that the area where the probe is located in the Z.1 chamber (see above) is going to come in contact with the odour. Thus the chambers inner shape and curved geometry needs to be considered. To distribute the odour to the area of exposure different outlets are needed with different angles so that the outlets are directed properly. The ideal position to avoid any collisions with the probe is on the frontal side of the chamber because it is outside the

range of movement of the probe. The curved tube splits into four outlets, 2 on the left side and 2 on the right side. This will allow the odour to flow from two sides.



**Figure 25 A) Odour distributor model B) Odour distributor model mounted on the optical chamber of the Z.1 LSFM C) Back view of the optical chamber of the Z.1 LSFM with the odour distributor mounted D) Front view of the optical chamber of the Z.1 LSFM with the odour distributor mounted**

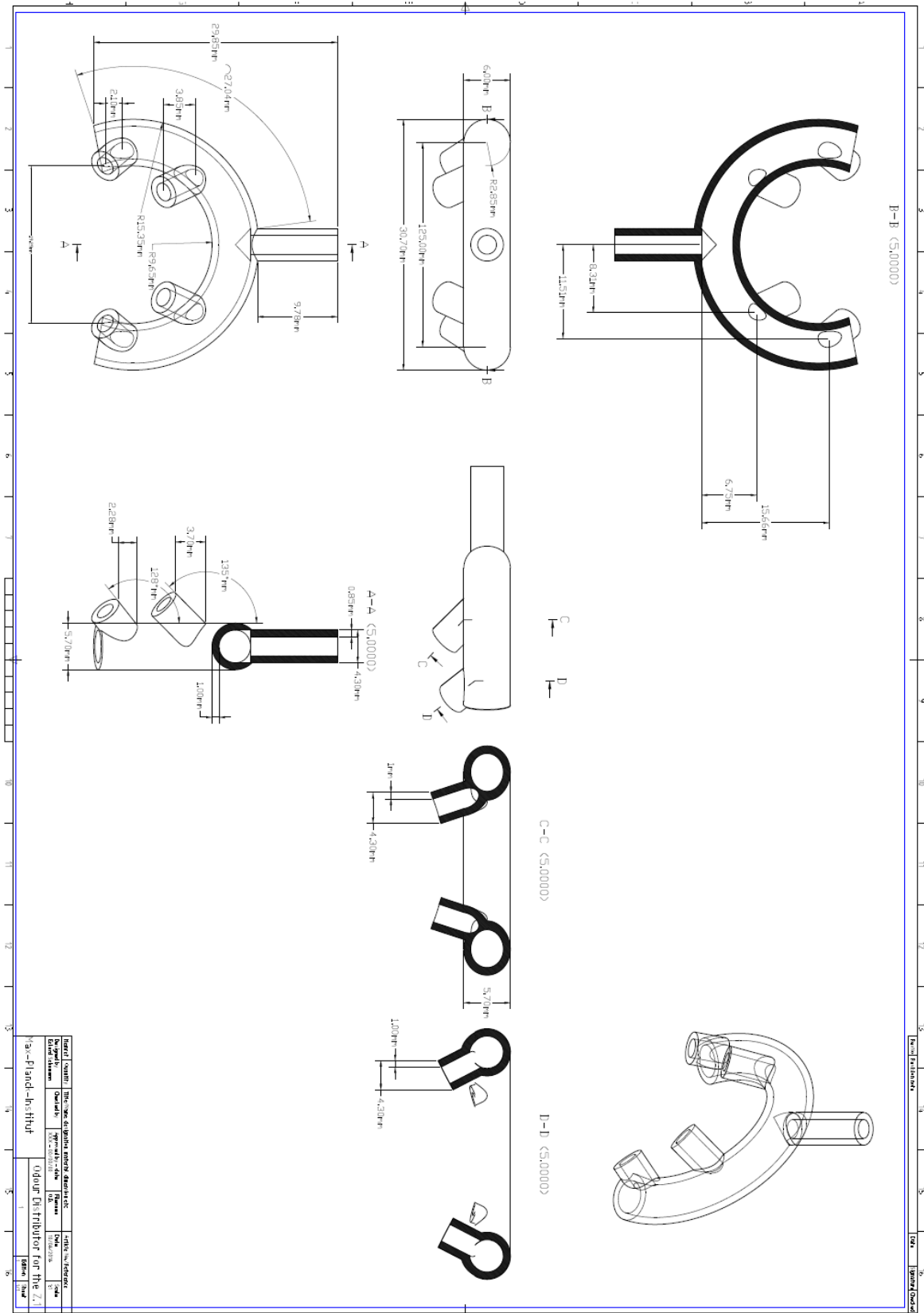


Figure 26 Blueprint of the odour distributor model

In order to avoid any extra costs of producing prototypes and recreating conditions to emulate the experiments a Computational Fluid Dynamics simulations program is used to gain the needed to have a better visualisation and understanding of the whole experimental set-up system.

## 6.3.5 Computational Fluid Dynamics

Mathematical approaches try to help and simplify the design process of any product. Autodesk Inc. created a Computational Fluid Dynamics (CFD) program to analyse, and help solving issues utilizing a numerical approach [64]. A computer with a high work capacity as well as fast processor is needed to process these simulations and designs given the amount of information it processes to calculate the interaction between gases or fluids.

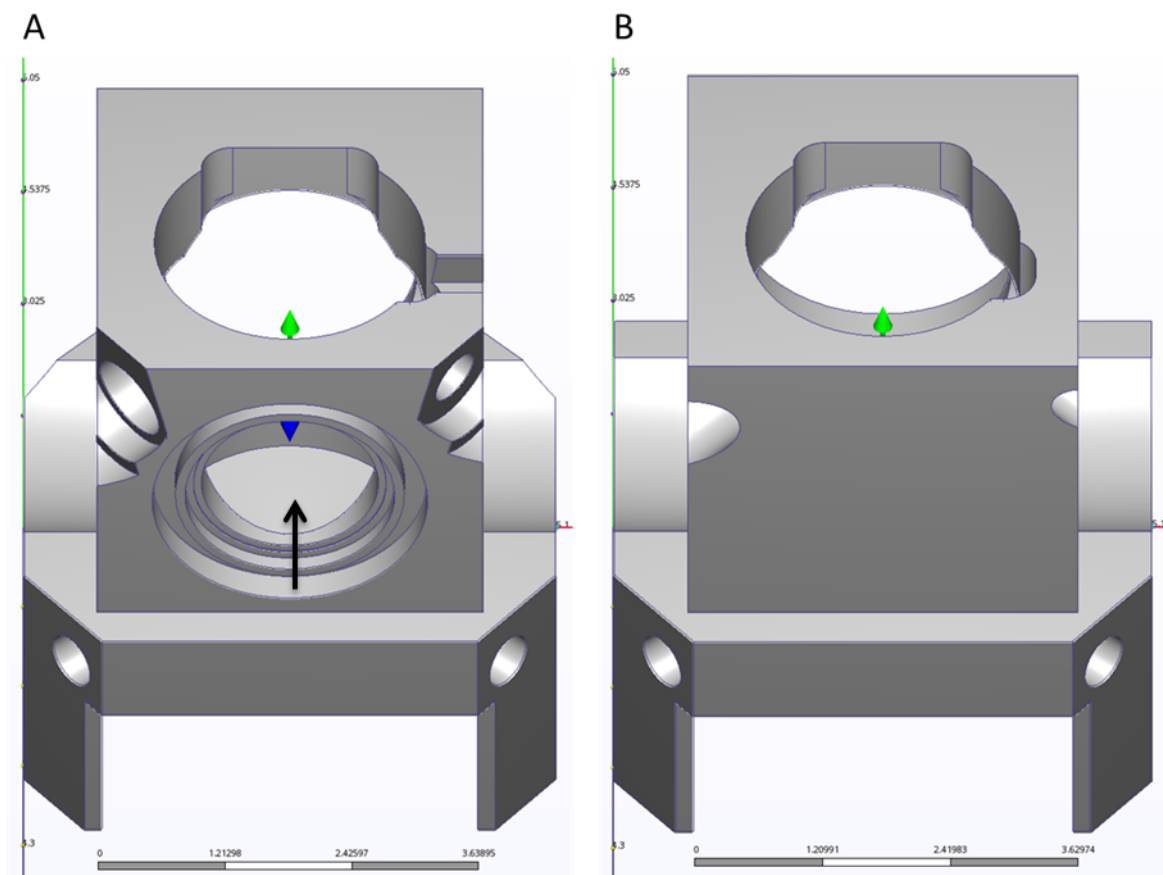
The main purpose of simulation programs is to simplify and aid developers to create functional prototypes thus minimizing risks and efforts while optimizing time and resources. The software is also able to gain information of internal interactions between fluids or gases within the desired system. Being able to adapt products to needs and requirements and tests those before the production takes place give the developers the ability to test more variations and optimize them using a computer.

Several studies have been conducted to prove if the predictions of such simulations anticipate correctly the real outcome [58, 65]. For a computer program to be able to simulate certain situations and to obtain reliable information about the functionality, internal pressures, speed and particle movement the boundary values of the situation have to be defined. The boundary conditions determine the restrictions of the system, the most common being intake, symmetry, physically, cyclic, pressure, and exit conditions [57, 66, 67].

Knowing how the particles behave inside the chamber is crucial to develop any kind of prototypes able to supply the current system with odour. Therefore simulation of the dynamics of the fluids required for the experiments is necessary to recreate the situation to prove if the designed prototype is suitable for the desired application.

### 6.3.5.1 Surface Wrapping

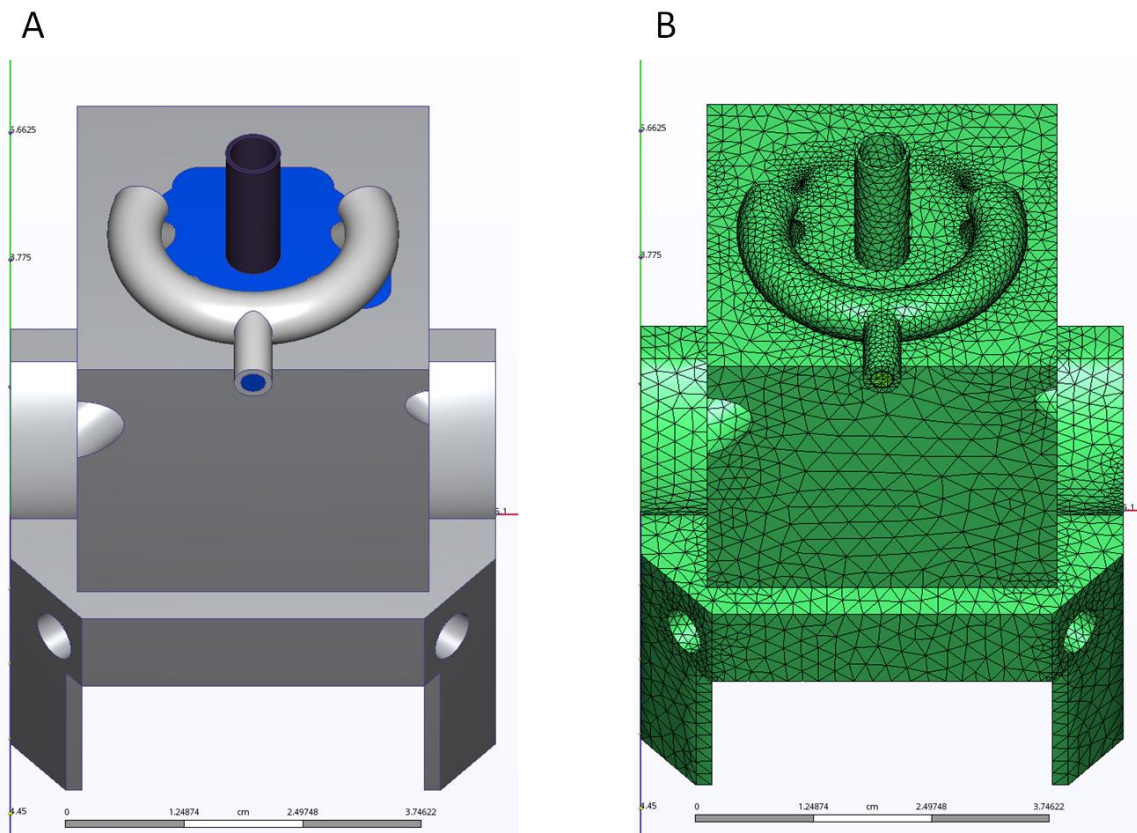
For the simulation to take place a meshing step is needed[68]. The meshing of the model is the splitting of the existing volumes into subdomains that in the case of CFD are triangle shaped (**Figure 28**). These subdomains help the program solve the equations needed on each one of the domains. The combination of the results of each subdomain gives the overall result of the simulation. Having complex geometries makes the task of creating the subdomains a challenging task for a computer. Therefore I simplified the original geometry of the optical chamber to create the mesh, while keeping the key characteristics intact. External characteristics are missing from the original model of the Z.1 optical chamber as shown in figure 27. Since the interactions to be analysed are given by the internal geometry of the chamber, changing the outside characteristics does not affect the future simulations.



**Figure 27 A) Original optical chamber of the LSFM Z.1 B) Digital modified optical chamber of the LSFM Z.1. : removal of external physical properties (arrow).**

6.3.5.2 Surface wrapping of the optical chamber

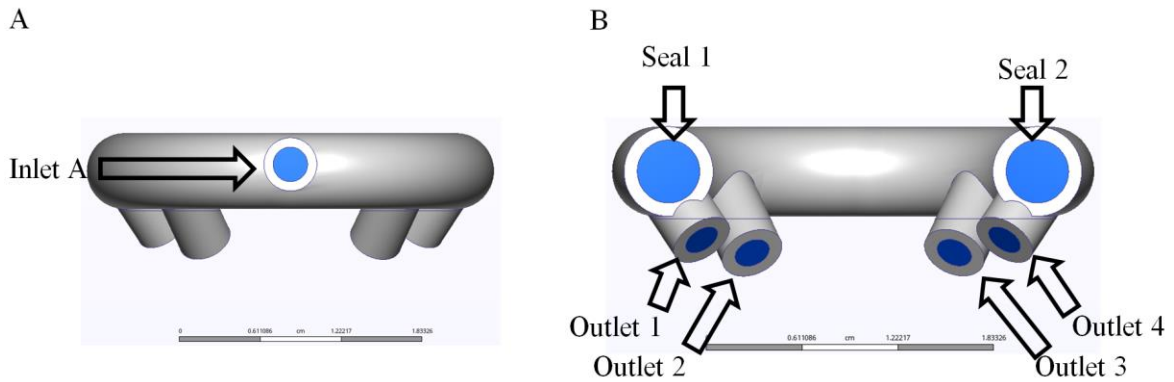
Upper frontal View



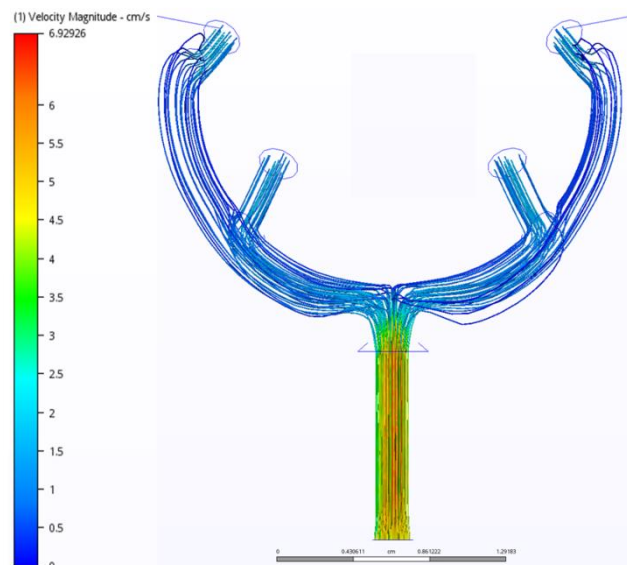
**Figure 28 A) Optical chamber of the Z.1 LSMF with the odour distributor model mounted. B) Example of the surface wrapping rendering the digital 3D shape.**

### 6.3.6 Simulation within the Odour Distributor Model

The odour distributor works with one inlet and four outlets that spread the odour through the chamber (**Figure 29**). The simulation also shows how the liquid is spread evenly inside the distributor pipes, although it loses speed by reaching the outlets. (**Figure 30**)



**Figure 29 A) Back view of the odour distributor model B) Front view of the odour distributor model**

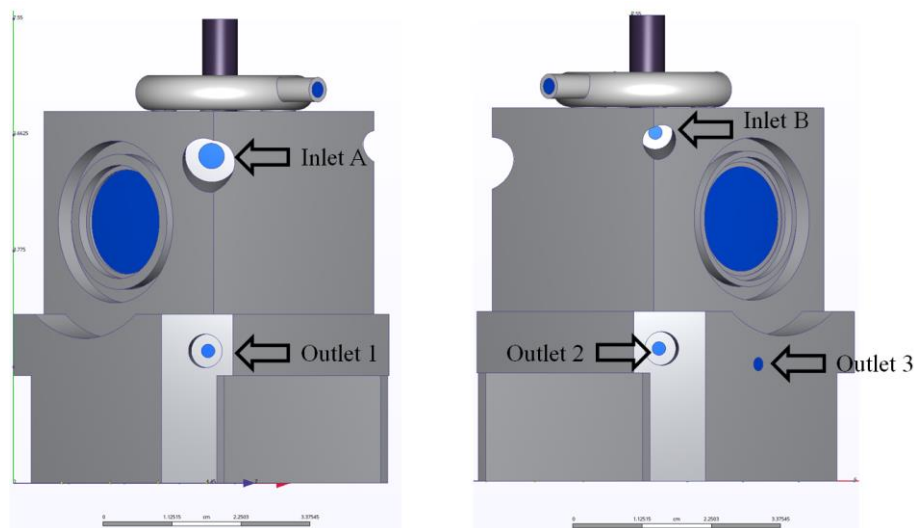


**Figure 30 Fluid dynamics simulation within the odour distributor model**



### 6.3.6.1 Simulation of the Ringer Solution Flow within the Z.1 Optical Chamber

The optical chamber of the Z.1 possesses two inlets and three outlets (**Figure 31**) which can be used for the Ringer solution flow sub function. This is considering that the system will have a downstream inside the chamber. The distribution of the Ringer solution into the chamber has to be in a controlled manner maintaining a laminar flow while having a flow rate of 10 cm<sup>3</sup>/s and is used to transport the remaining odour (the 'waste') to the Z.1 outlets. The Z.1 chamber inlets are located on the frontal upper part of the chamber, one on the left side and the other on the right part. They also have different diameters as shown on the blueprint on the appendix for Blue Prints from Carl ZEISS. The outlets are positioned on the frontal under part of the chamber. This allows the flow to stream downwards. The outlets are distributed on the left frontal side, the right frontal side with another one on the right side which connects to the centre of the chamber. This provides the system with 21 possible combinations to create the Ringer solution flow.



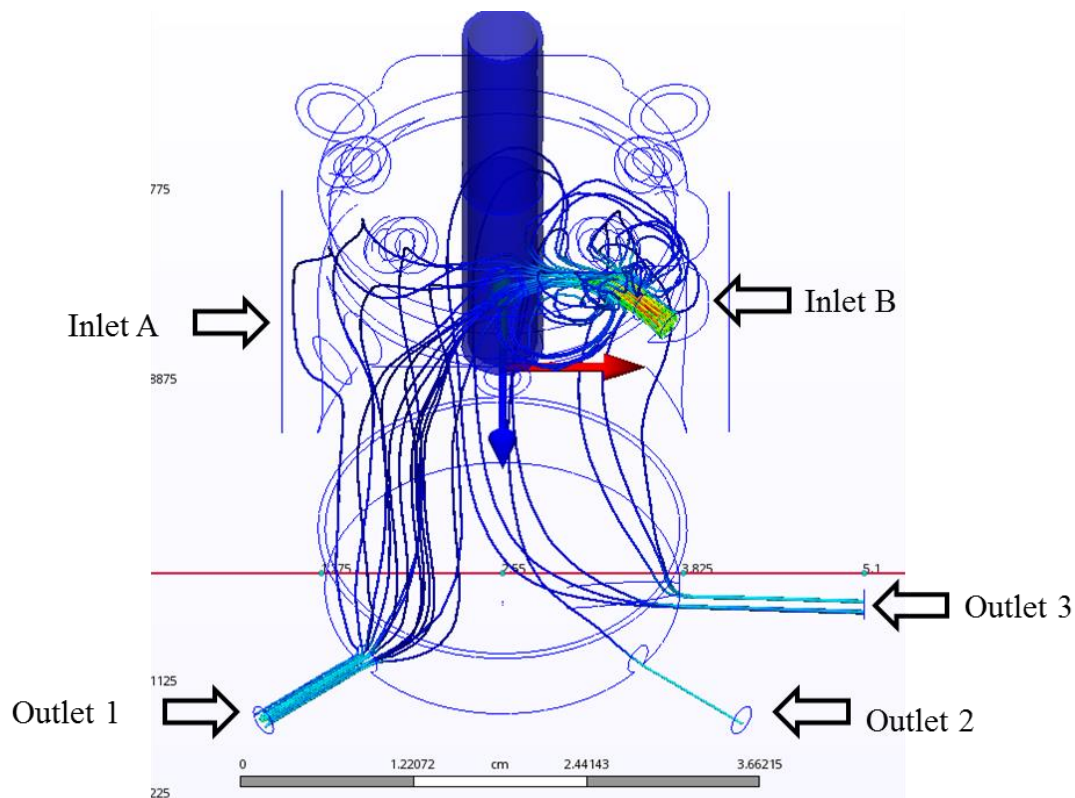
**Figure 31 The inlets and outlets of the optical chamber of the Z.1** A) Left side of the optical chamber. It shows the inlet A and the outlet 1. B) The right side shows the inlet B and the outlets 2 and 3

Using a Computational Fluid Dynamics program (CFD), it was possible to simulate all the possible combinations for Ringer solution sub system described above. The visualization of the flow, the appropriate Reynold's number of the inlets and the outlets fluids and the residence time of the simulated particles within the Z.1 revealed optimal combined scenarios for the Ringer solution flow.

The pressure in the inlet B is higher than on the inlet A due to the difference of the diameter while having with the same flow rate. It is important to mention that the pressure does not represent a relevant aspect due to the low flow rates that the system is going to handle during experimentation. Since the experiments require a stable and slow flow to sustain the live probe and not to create turbulences within the optical chamber.

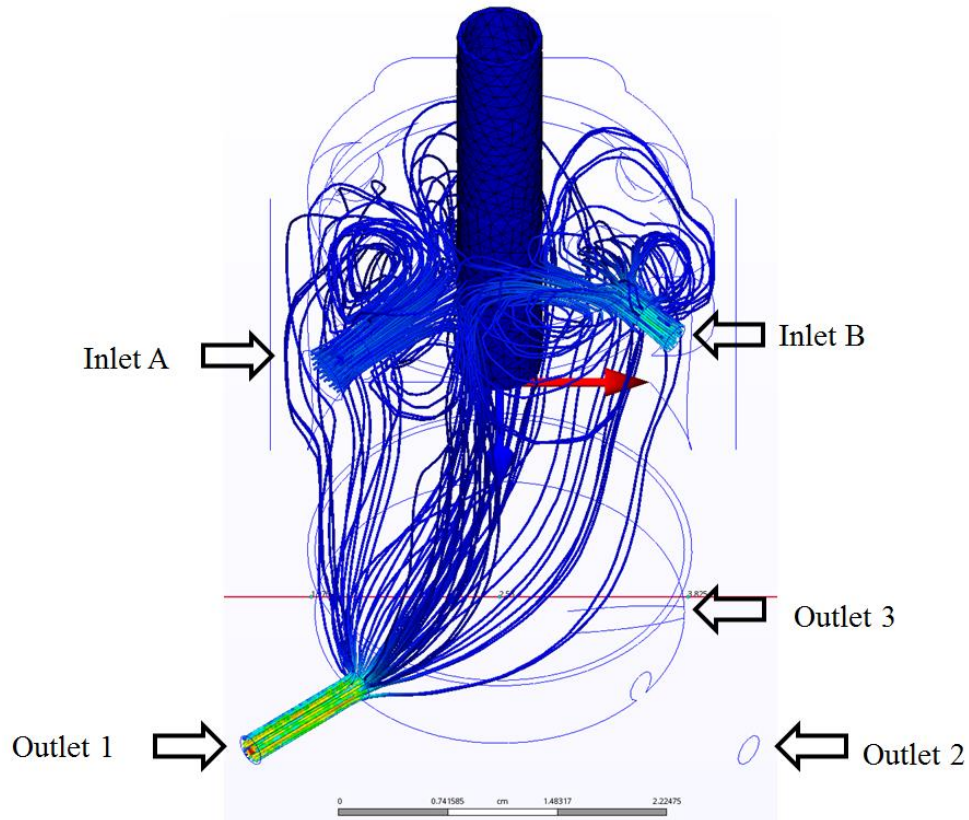
### 6.3.6.2 Undesired Flow Distribution

Utilizing only one of the optical chamber inlets forces the flow in one direction (**Figure 32**). Therefore, the combinations of inlets and outlets utilizing only one inlet of the flow do not show the basic flow characteristics required. This happens because the flow, as seen on the figure 32, does not reach the whole volume inside the optical chamber.



**Figure 32 Simulation of ringer solution flow using Inlet B and Outlets 1, 2 and 3**

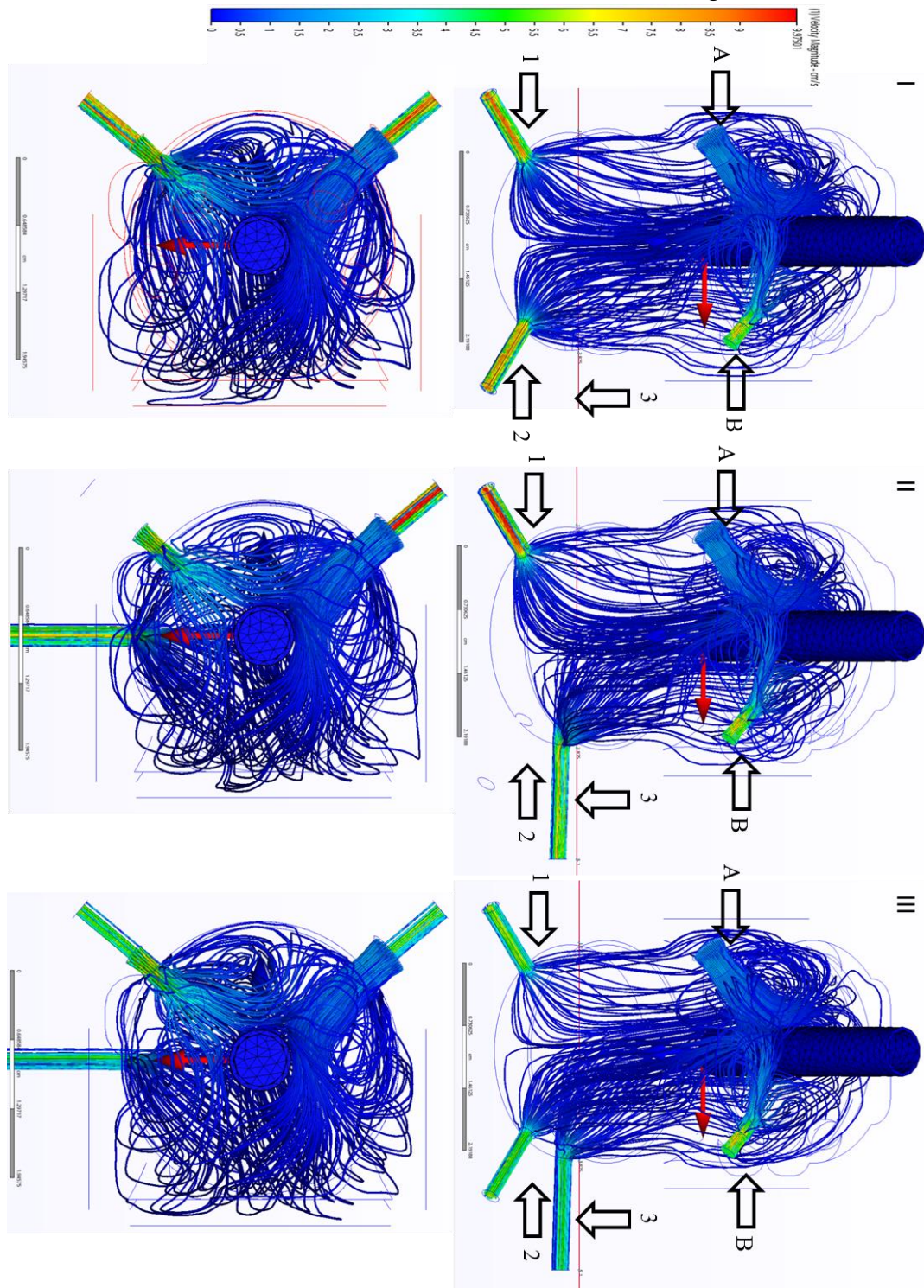
The simulations showed that using the two inlets provide a more controllable flow that also fills the chamber, ideal to wash the remaining odour away after the exposure time. This reduces the possibilities to seven for all the possible combinations of in-and outlets.



**Figure 33 Example of one Ringer solution flow simulation utilizing the inlets A and B, and the outlet 1**

Therefore, all the possibilities with only one outlet are not taken into account. Utilizing the outlets two and three has the same effect due to their location on the under right side of the chamber.

6.3.6.3 Possible Solutions Simulation for the Ringer Flow



**Figure 34 3 Possible combinations for the Ringer solution distribution system utilizing two inlets.** A) Outlets 1 and 2 allow the flow to the whole chamber. B) The combination of the outlets 1 and 3 cause a similar effect that the combination 1 and 2. The flow spreads along the whole volume inside the optical chamber C) Utilizing the outlets 1, 2 and 3 allows the flow to reach the whole chamber while having a lower out volume flow in comparison with the other possibilities

## 6.3.6.4 Ringer Solution Flow Simulation Results

**Table 3 Simulation results utilizing the inlets A and B and the outlets 1 and 2**

Inlet A Reynold's number	45.6023
Inlet B Reynold's number	87.0589
Outlet 1 Reynold's number	87.5053
Outlet 2 Reynold's number	84.8482
Outlet 3 Reynold's number	0
Max residence time	2702.5 s
Min residence time	26.72
Average residence time	123.83s
Speed range of the highest volume	0.000000 - 0.498750 cm/s 98.90%

**Table 4 Simulation results utilizing the inlets A and B and the outlets 1 and 3**

Inlet A Reynold's number	45.6023
Inlet B Reynold's number	87.0589
Outlet 1 Reynold's number	93.8549
Outlet 2 Reynold's number	0
Outlet 3 Reynold's number	78.298
Max residence time	2148.6 s
Min residence time	27.7 s
Average residence time	103.2 s
Speed range of the highest volume	0.000000 - 0.534276 cm/s 98.98%

**Table 5 Simulation results utilizing the inlets A and B and the outlets 1, 2 and 3**

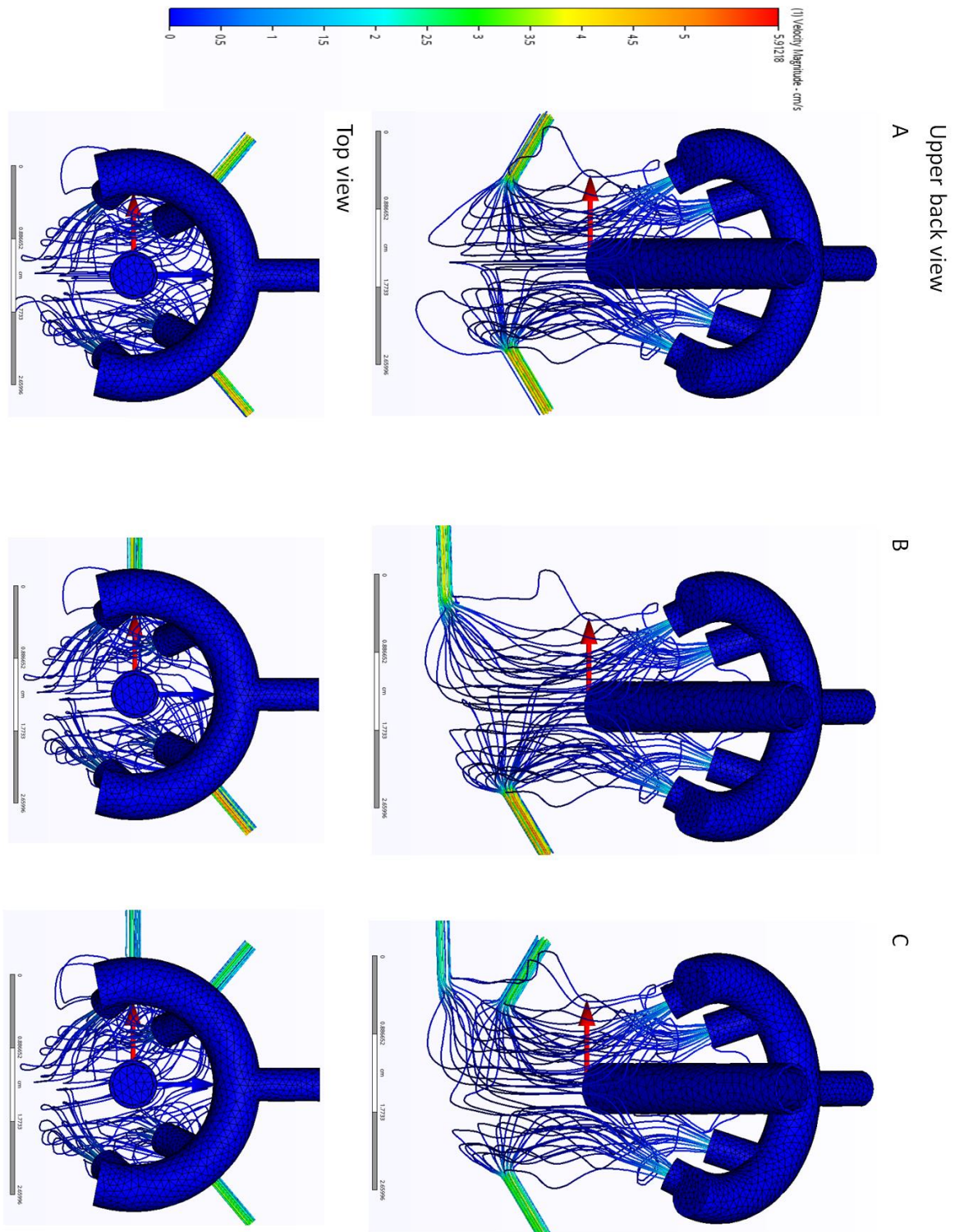
Inlet A Reynold's number	45.6023
Inlet B Reynold's number	87.0589
Outlet 1 Reynold's number	61.911
Outlet 2 Reynold's number	60.1199
Outlet 3 Reynold's number	50.0661
Max residence time	6038.3 s
Min residence time	23.7 s
Average residence time	168.8 s
Speed range of the highest volume	0.000000 - 0.433276 cm/s 98.68%

The results of the chosen combinations of Inlets and Outlets show the results shown above. They all possess a laminar flow with subtle revolutions at the inlets due to the probe hanging close to the inlets. This

### 6.3.6.5 Simulation Odour Flow within the Z.1 Optical Chamber

Equally important is the behaviour of the odour within the chamber. Therefore, simulations of the odour distribution were carried out utilizing the special designed odour distributor model while maintaining a constant volume entrance flow rate of  $10 \text{ cm}^3/\text{min}$ . Then the flow is directed to the four outlets (**Figure 35**). The odour outlets are positioned in a symmetrically way to guarantee that the same amount of odour travels to both sides

The odour flow is going to run only for a couple of seconds to induce a reaction of the olfactory receptor neurons of the fly's antenna. Thus maintaining a constant flow during the imaging process is crucial to obtain reliable results.



**Figure 35 3 Possible combinations for the odour distribution. A) Outlets 1 and 2 allow the flow to the whole chamber. B) The outlets 1 and 3 cause a similar effect that the combination 1 and 2. C) Utilizing the three outlets allow the flow to reach all the chamber while having a lower out volume flow in comparison with the other possibilities**

## 6.3.6.6 Odour Solution Flow Simulation Results

**Table 6 Odour simulation result utilizing the outlets 1 and 2**

Inlet Odour Reynold's number	73.6652	
Outlet 1 Reynold's number	41.8965	
Outlet 2 Reynold's number	43.8096	
Outlet 3 Reynold's number	0	
Max residence time	2834.9	
Min residence time	58.4	
Average residence time	276.23	
Speed range of the highest volume	0.000000 - 0.295609	99.069825%

**Table 7 Odour simulation result utilizing the outlets 1 and 3**

Inlet Odour Reynold's number	73.6652	
Outlet 1 Reynold's number	48.4738	
Outlet 2 Reynold's number	0	
Outlet 3 Reynold's number	37.1501	
Max residence time	2742.8 s	
Min residence time	58.4 s	
Average residence time	161.9 s	
Speed range of the highest volume	0.000000 - 0.498750	cm/s 98.90%

**Table 8 Odour simulation result utilizing the outlets 1, 2 and 3**

Inlet Odour Reynold's number	73.6652	
Outlet 1 Reynold's number	30.3517	
Outlet 2 Reynold's number	31.5989	
Outlet 3 Reynold's number	23.7278	
Max residence time	5259.7 s	
Min residence time	20.5 s	
Average residence time	300.2 s	
Speed range of the highest volume	0.0 - 0.295613	cm/s 99.034659%



## 6.4 Development of Possible Active Structures

By considering the sub systems on their adaptability for odour exposure experiments and ways of optimizing it, solution proposals can be transmitted in the morphological box according to VDI 2221. Each resulting active structure results in a solution alternative for the entire system, which will subsequently evaluate according to its technical capabilities.

### 6.4.1 Morphological Box and Defining Active Structures




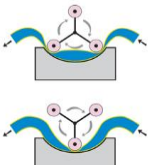
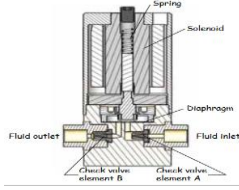







Separating the sub function aids to define the best possible combination of each system. After reviewing different solutions for of the two sub functions, i.e. odour and Ringer solution distribution, which are suitable for the odour exposure experiments, the morphological box propose in the VDI 2221 allows combining the solutions into different active structures. Every individual modular structure gives out a different alternative to solve the problem in the whole system. Afterwards each individual structure gets a score according to different and important economic and technical points. The total score of each active structure will show which active is the best to adapt the current microscope with an odour exposure setup.

Only combination of inlets and outlets that fulfilled the desired characteristics for odour exposure experiment was taken into account during the selection process.

6.4.2 Morphological Box of the Ringer Solution Flow

**Table 9 Morphological box of the Ringer solution flow sub function**

The morphological box helps to combine the different solutions for each sub system and guarantees that the outcome of each possible solution still fulfils the requirements of the Ringer solution flow sub function.

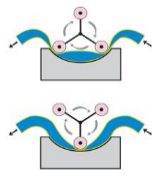
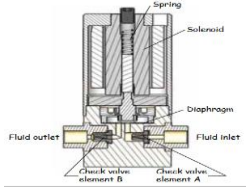

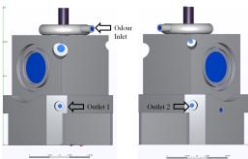
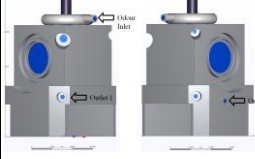
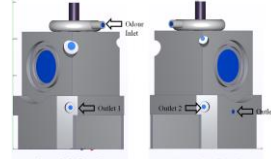
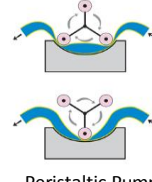
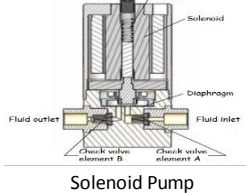




	Option 1	Option 2	Option 3
Ringer Storage	 Polypropylene	 Glass	 Fluoropolymer
Ringer Transport	 Peristaltic Pump	 Solenoid Pump	 Syringe Pump
Ringer Distribution	 Inlets A and B/ Outlets 1 and 2	 Inlets A and B/ Outlets 1 and 3	 Inlets A and B/ Outlets 1, 2 and 3
Odour Storage	 Polypropylene	 Glass	 Fluoropolymer

[48, 50, 54] [49, 51, 55]

6.4.3 Morphological Box of the Odour Flow















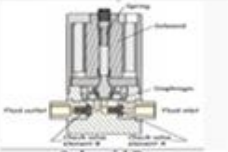



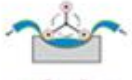
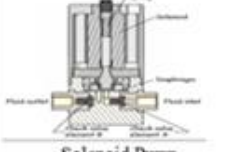




**Table 10 Morphological box of the odour flow sub function**

The morphological box helps to combine the different solutions for each sub system and guarantees that the outcome of each possible solution still fulfils the requirements of the Ringer solution flow sub function.

	Option 1	Option 2	Option 3
Odour Transport	 <p>Peristaltic Pump</p>	 <p>Solenoid Pump</p>	 <p>Syringe Pump</p>
Odour Distribution	 <p>Odour Inlet / Outlets 1 and 2</p>	 <p>Odour Inlet / Outlets 1 and 3</p>	 <p>Odour Inlet / Outlets 1, 2 and 3</p>
Waste Transport	 <p>Peristaltic Pump</p>	 <p>Solenoid Pump</p>	 <p>Syringe Pump</p>
Waste Storage	 <p>Polypropylene</p>	 <p>Glass</p>	 <p>Fluoropolymer</p>

[48, 50, 54] [49, 51, 55]

Table 11 Active structures displaying different alternatives to solve the main issue

	Active structure 1	Active structure 2	Active structure 3
Ringer Storage	 Polypropylene	 Glass	 Fluoropolymer
Ringer Trasport	 Peristaltic Pump	 Peristaltic Pump	 Peristaltic Pump
Ringer Distribution	 Inlets A and B/ Outlets 1 and 2	 Inlets A and B/ Outlets 1 and 3	 Inlets A and B/ Outlets 1, 2 and 3
Odour Storage	 Syringe	 Syringe	 Fluoropolymer
Odour Trasport	 Syringe Pump	 Syringe Pump	 Solenoid Pump
Odour Distribution	 Odour Inlet / Outlets 1 and 2	 Odour Inlet / Outlets 1 and 3	 Odour Inlet / Outlets 1, 2 and 3
Waste Trasport	 Peristaltic Pump	 Solenoid Pump	 Peristaltic Pump
Waste Storage	 Polypropylene	 Glass	 Fluoropolymer

[48, 50, 54] [49, 51, 55, 69]

## 6.4.4 Active structures

Given the fact that the main system is a combination of three sub functions therefore, we can appreciate a similarity of sub function for each one of the sub systems.

### 6.4.4.1 Active Structure 1

- The Ringer solution and the waste, i.e. odour plus Ringer solution would be stored utilizing the same bottle materials. The polypropylene bottles are autoclavable as all the other components in the system are which ensure the removal of any odour residues. This material can also endure temperatures down to -40c
- The peristaltic pump is suitable to control small volume flows and also does not have any contact with the Ringer solution avoiding any contamination risks. It manages to control the required volume flow rate of 20 mL/min but it can also operate at lower rates while having the minor disadvantage of the pulsation
- Utilizing the inlets A and B in combination with the outlets 1 and 2 of the optical chamber of the Z.1 gives us an average residence time of 123.8 second for the Ringer solution flow
- The storage of the odour inside a syringe helps keeping the odour away from any external impurities. It also helps to control the exact amount of odour used during the odour exposure. The syringes are autoclavable but also disposable
- The syringe pump for the odour flow provides, as the peristaltic pumps do, a pumping system that does not come in contact with the transported liquid. This pump can also control very small volume flow rates such as 10 microliter per minute
- Utilizing the same outlets for the odour extraction revealed an average residence time of 276.2 seconds
- The peristaltic pump for the extraction provides a relatively constant flow of extraction and can be connected to all the outlets

### 6.4.4.2 Active Structure 2

- The Ringer solution and the waste would be stored utilizing the same bottle materials. The glass bottles are autoclavable as all the other components in the system are which ensure the removal of any odour residues
- The peristaltic pump is suitable to control small volume flows and also does not have any contact with the Ringer solution avoiding any contamination risks. It manages to control the required volume flow rate of 20 mL/min but it can also operate at lower rates

- Using the Inlets A and B and the outlets 1 and 3 of the optical chamber of the Z.1 give the Ringer solution flow an average residence time of 103.2 second
- The storage of the odour inside a syringe helps keeping the odour away from any external impurities. It also helps to control the exact amount of odour used during the odour exposure. The syringes are autoclavable but also disposable
- The syringe pump for the odour flow provides, as the peristaltic pumps do, a pumping system that does not come in contact with the transported liquid. This pump can also control very small volume flow rates such as 10 microliter per minute
- Utilizing the same outlets for the odour extraction revealed an average residence time of 161.9 seconds
- Another solenoid pump is responsible of extracting the waste out of the optical chamber with a similar rate that the one pumping the Ringer solution. This pump cannot be adjusted to extract at a different rate during the odour exposure

### 6.4.4.3 Active Structure 3

- All the liquids would be stored utilizing the same bottle materials. The fluoropolymer bottles are autoclavable as all the other components in the system are which ensure the removal of any odour residues. This material can also withdraw temperatures down to -240c up to 250 C
- The peristaltic pump is suitable to control small volume flows and also does not have any contact with the Ringer solution avoiding any contamination risks. It manages to control the required volume flow rate of 20 mL/min but it can also operate at smaller rates
- Utilizing the inlets A and B in combination with the outlets 1, 2 and 3 of the optical chamber of the Z.1 give us an average residence time of 168.8 second for the Ringer solution flow
- The peristaltic pump for the odour flow provides a pumping system that does not come in contact with the transported liquid, while controlling the pumping of the desired volume flow rate. This pump however does not provide a constant flow due to the pulsations caused by the rolls
- Utilizing the same outlets for the odour extraction revealed an average residence time of 300.2s seconds
- The peristaltic pump for the extraction provides a relatively constant flow of extraction and can be connected to all the outlets This pump can also be

programmed to extract at different rates depending on which phase is the experiment on

All the modular structures are suitable to enable the optical chamber of the Light-Sheet-Fluorescence-Microscope Z.1 for odour exposure experiments. The syringe main component is glass.

## 6.5 Scoring Method for the Optimal Modular Structure

The most reliable way to differentiate the modular structures and to determine which the best one, a scoring method is has to be used. This gives us a clear understanding for the best module. The scoring method according to the VDI 2221 guideline gives scores for specific characteristics of the modular structures. These characteristics have specific values according to the relevancy in the system, therefore, simplifying the comparison between the systems. This method is suitable for any system, due to its flexibility and adaptation to any future imaging project.

The values are directly related to their importance for the whole system. Therefore, the average residence time of the Ringer solution in the system represents with a 50% the most important aspect. The Reynolds's number on the outlets gives out if the flow is laminar and this is valued with 30%. The control over the pumps and their flow is a valued with 25% due to its direct effect on the optical chambers internal flow. The maintenance required has a direct impact on the performance of each system, but due to the low usage it is only valued with 5%.

## 6.5.1 Requirements for the Scores

Table 12 Table of requirements for the values

Points	Attribute	Active Structure 1	Active Structure 2	Active Structure 3
Residence time of the Ringer solution flow				
0	>160s	An average on 123.8 s for the residence time ensure that the remaining odour would be washed away in an acceptable time	An average on 103.2 s for the residence time ensure that the remaining odour would be washed away in a more than acceptable time	An average on 168.8 s for the residence time implies that the washing process of the remaining odour molecules would be to slow
1	<=160s			
2	<=140s			
3	<=120s			
4	<100s			
Reynold´s number of the dour flow in the outlets				
0	<=50	A Reynold´s number of 41.89 for the outlet 1 and 43.80 for the outlet 2 give away that the flow remains laminar inside the chamber	A Reynold´s number of 41.89 for the outlet 1 and 37.15 for the outlet 3 give away that the flow remains laminar inside the chamber	A Reynold´s number of 30.35 for the outlet 1, 31.59 for the outlet 2 and 23.72 give away that the flow remains laminar inside the chamber
1	<=45			
2	<=40			
3	<=35			
4	<30			
Control over the pump systems				
0	None	The peristaltic pump creates a pulsation on the Ringer solution flow created by the rolls. The odour flow on the other hand is very	The peristaltic pump creates a pulsation on the Ringer solution flow created by the rolls. The odour flow on	The peristaltic pump creates a pulsation on the Ringer solution flow created by the rolls. The solenoid pump



1	low	<p>reliable and controllable. The syringe pump simplifies the task of adding the odour at a constant volume flow rate. The peristaltic extraction pump also causes a pulsation of the flow, which is not so relevant since it only pumps out the waste. This pump can also be programmed to work at different rates</p>	<p>the other hand is very reliable and controllable. The odour flow on the other hand is very reliable and controllable. The syringe pump simplifies the task of adding the odour at a constant volume flow rate. The peristaltic extraction pump also causes a small pulsation of the flow, which is not so relevant since it only pumps out the waste. This pump can only work at flow rates higher than 20 mL/min</p>	<p>works at a pulsation constant rate. This flow is however not lower than 20 mL/min. The peristaltic extraction pump also causes a pulsation of the flow, which is not so relevant since it only pumps out the waste. This pump can also be programmed to work at different flow rates.</p>
2	Medium			
3	High			
4	Total			
Maintenance needed				
0	Very high	<p>The peristaltic pump requires constant changes of the tubes needed due to the pressure applied on the by the rolls. New syringes should be used after every experiment to guarantee the cleanliness of the system. The bottles are autoclavable and should not represent a problem</p>	<p>The solenoid pump has a high amount of work hours before it has to be changed. New syringes should be used after every experiment to guarantee the cleanliness of the system. The bottles are autoclavable and should not represent a problem</p>	<p>The peristaltic pump requires constant changes of the tubes needed due to the pressure applied on the by the rolls. The solenoid pump has a high amount of work hours before it has to be chained. The bottles are autoclavable and should not represent a problem</p>
1	High			
2	Medium			
3	Low			
4	None			

### 6.5.2 Results of the Scoring Method

The scoring method gives us the best modular structure to solve the main function. The second modular structure is with 71.25 % of the possible points the best option of the ones taken into account. Utilizing the Inlets A and B and the outlets 1 and 3 of the optical chamber of the Z.1 give the Ringer solution flow an average residence time of 103.2 second, which represent the best time for the most important aspect

**Table 13 Scoring table.** Evaluation of combinations of system characteristics (modular structures) depicted in a cross diagram.

Criteria \ Version	Quantifier in % (Q)	Active Structure 1		Active Structure 2		Active Structure 3		Ideal Solution	
		Points	Points x Q	Points	Points x Q	Points	Points x Q	Points	Points x Q
Residence time of the ringer flow	50	2	100	3	150	0	0	4	200
Reynold's number of the odour flow in the outlets	25	2	50	2	50	4	100	4	100
Controll over the pumps	20	3	60	4	80	2	40	4	80
Maintenance needed	5	1	5	1	5	3	15	4	20
Sum	100	8	215	10	285	9	155	16	400
Value			53.75		71.25		38.75		100

The storage of the odour inside a syringe helps keeping the odour away from any external impurities. It also helps to control the exact amount of odour used during the odour exposure. The syringes are autoclavable but also disposable.

The pulsation of the solenoid pump generates some pulsation which does not affect the flow in such a way that it turns unreliable. The syringe pump while maintaining a laminar flow which contacts directly on the probe also provides a reliable system to control the odour flow.

## 7 Conclusion

The thesis represents an effort to adapt the optical chamber of the Z.1 microscope in order to expand its capabilities. This would enable the exposure to odour stimuli for *in-vivo* probes without destroying the structural integrity and damaging the specimen. With the aid of the odour distributor model it was possible to expose the probe to an odour diluted in Ringer solution within the optical chamber of the Z.1. The position and the shape of the odour distributor model ensure that the LFSM does function properly and can be attached and detached without having to modify the optical chamber. The syringe pump keeps a constant and accurate odour flow during the exposure. The combination of the outlets 1 and 3 give us an average residence time of 161 seconds while maintaining an optimal laminar flow, which helps to control the odour in and out flux. In combination with the Ringer solution flow with an average residence time of 100 seconds provides the system with an adequate flow exchange within the chamber for consecutive odour exposures and imaging processes. This leaves the probe intact while assuring that the odour does not exceed the desired residence time and is properly washed away.

Even though the simulations proved the feasibility of this task, further *in-vivo* experiments should be conducted to test the proposed system and be adapted if needed. For this a fluorescence dye could be used while the Z.1 images to be able to trace the flow. After the flow tests have been conducted further test on live genetically modified probes can be conducted to image its reactions.

Although the system enables the odour exposure and the washing of the remnants within the optical chamber, while keeping a constant level of Ringer solution, the cuticle remains too thick to image internal structures without damaging the probe. This can be avoided by utilizing some genetically modified organisms with a clear cuticle to enable the visualisation of internal structures and interactions.

## References

### Web Sites

7. University, M. *The Compound Light Microscope*. [cited 2018 19/08/2018]; Available from: <https://www.cas.miamioh.edu/mbiws/microscopes/compoundscope.html>.
8. Rice, G. *Fluorescence Microscopy*. 2018 6/11/2018]; Available from: [https://serc.carleton.edu/microbelife/research\\_methods/microscopy/fluomic.html](https://serc.carleton.edu/microbelife/research_methods/microscopy/fluomic.html).
16. Olenych, S. *In Vivo and Cleared Tissue Imaging for Light-sheet Microscopy*. 2015 [cited 2018 19/08/2018]; Webinar]. Available from: <https://bitesizebio.com/webinar/in-vivo-and-cleared-tissue-imaging-for-light-sheet-microscopy/>.
20. Zeiss. *Lightsheet Z.1*. 2014 [cited 2018 19/08/2018]; Available from: <https://www.zeiss.com/microscopy/us/products/imaging-systems/lightsheet-z-1.html>.
48. Fisher, T. *Polypropylene (PPCO) Bottles*. 2018 6/11/2018]; Available from: <https://www.thermofisher.com/de/en/home/life-science/lab-plasticware-supplies/reusable-plasticware/laboratory-bottles/polypropylene-ppco-bottles.html>.
49. Groups, D. *Laboratory glass bottles* 2018 27/11/2018]; Available from: <http://www.duran-group.com/en/products-solutions/laboratory-glassware/products/laboratory-glass-bottles.html>.
50. Fisher, T. *Fluoropolymer FEP and PFA Bottles*. 2018 6/11/2018]; Available from: <https://www.thermofisher.com/de/de/home/life-science/lab-plasticware-supplies/reusable-plasticware/laboratory-bottles/fluoropolymer-fep-pfa-bottles.html>.
52. Marlon, W. *How do peristaltic pumps work - industrial*. 2018 07/11/2018]; Available from: <http://www.watson-marlow.com/id-en/support/how-do-peristaltic-pumps-work-industrial/>.
53. Digital, R. *Operating Manual*. 2009 07/11/2018]; Available from: [https://wikisites.mcgill.ca/djgroup/images/0/0c/Reglo\\_Digital\\_new.pdf](https://wikisites.mcgill.ca/djgroup/images/0/0c/Reglo_Digital_new.pdf).
54. Fluidics, B.-C. *Solenoid Operated Micro Pumps*. 2018 7/11/2018]; Available from: <https://biochemfluidics.com/products/solenoid-operated-micro-pumps>.
55. Chemyx. *Fusion 4000 Independent Channels Syringe Pump*. 2018 07/11/2018 ]; Available from: <https://www.chemyx.com/syringe-pumps/fusion-4000/>.
64. Autodesk. *Autodesk CFD*. 2018 28/11/2018 ]; Available from: <https://www.autodesk.com/products/cfd/overview>.

66. Autodesk. *Tools for computational fluid dynamics*. 2018 [2/11/2018]; Available from: <https://www.autodesk.com/products/cfd/features>.
68. Autodesk. *Surface wrapping*. [06/11/2018]; Available from: <https://knowledge.autodesk.com/support/cfd/learn-explore/caas/CloudHelp/cloudhelp/2019/ENU/SimCFD-UsersGuide/files/GUID-D1BAC116-AADE-4A1A-96CA-98A857F07090-htm.html>.
69. Analytica, C. *Hamilton Microliter Syringe, Cemented Needle volume 10ul*. 2018 [27/11/2018]; Available from: <https://www.capitalanalytical.com/index.php?c=product&product=944>.

### Thesis

32. Farley, L., *Nitric Oxide in the Olfactory Bulb: Potential Roles in Physiology and Pathology*, in *Physiology*. 2013, University Otago: Dunedin, New Zealand. p. 122.
42. Grabe, V., *In vivo visualization of inhibitory odor responses in the olfactory system of the fruit fly *Drosophila melanogaster**. 2010, Friedrich-Schiller-Universität. p. 78.
51. Chang, Y.-Y., *The Development of the Simple Syringe Pump*, in *Materials Science and Engineering*. 2009, I-Shou University: Kaohsiung, Taiwan, Republic of China.

### Books

3. Pahl, G., *Fundamentals of engineering design*, in *Dubbel: Taschenbuch für den Maschinenbau*, W. Beitz and K.-H. Küttner, Editors. 1987, Springer Berlin Heidelberg: Berlin, Heidelberg. p. 385-417.
5. Rochow, T.G. and P.A. Tucker, *A Brief History of Microscopy*, in *Introduction to Microscopy by Means of Light, Electrons, X Rays, or Acoustics*. 1994, Springer US: Boston, MA. p. 1-21.
13. Webb, D.J. and C.M. Brown, *Epi-Fluorescence Microscopy*, in *Cell Imaging Techniques: Methods and Protocols*, D.J. Taatjes and J. Roth, Editors. 2013, Humana Press: Totowa, NJ. p. 29-59.
27. Mori, I., *Olfaction A2 - Maloy, Stanley*, in *Brenner's Encyclopedia of Genetics (Second Edition)*, K. Hughes, Editor. 2013, Academic Press: San Diego. p. 161-163.
28. Thum, A., *Sugar reward learning in *Drosophila* : neuronal circuits in *Drosophila* associative olfactory learning*. 2006.
43. Strutz, A., et al., *Calcium Imaging of Neural Activity in the Olfactory System of *Drosophila**, in *Genetically Encoded Functional Indicators*, J.-R. Martin, Editor. 2012, Humana Press: Totowa, NJ. p. 43-70.

47. Feldhusen, J., et al., *Grundlagen der Konstruktionstechnik*, in *Dubbel: Taschenbuch für den Maschinenbau*, K.-H. Grote and J. Feldhusen, Editors. 2007, Springer Berlin Heidelberg: Berlin, Heidelberg. p. F1-F49.
57. Anderson, J.D., *Governing Equations of Fluid Dynamics*, in *Computational Fluid Dynamics*, J.F. Wendt, Editor. 2009, Springer Berlin Heidelberg: Berlin, Heidelberg. p. 15-51.
59. R.F.Boucher, Y.N., *Introduction to Fluid Mechanics* ed. Butterworth-Heinemann. 1998, Great Britain by MPG, Bodmin, Cornwall
62. Nakayama, Y. and R.F. Boucher, *4 - Fundamentals of flow*, in *Introduction to Fluid Mechanics*, Y. Nakayama and R.F. Boucher, Editors. 1998, Butterworth-Heinemann: Oxford. p. 41-54.
67. Rapp, B.E., *Chapter 9 - Fluids*, in *Microfluidics: Modelling, Mechanics and Mathematics*, B.E. Rapp, Editor. 2017, Elsevier: Oxford. p. 243-263.

#### Journal Article

1. Keller, P.J., M.B. Ahrens, and J. Freeman, *Light-sheet imaging for systems neuroscience*. Nature Methods, 2014. **12**: p. 27.
2. Group, N.P., *Method of the Year 2014*. Nature Methods, 2014. **12**: p. 1.
4. Engineers, V.D.I.A.o.G., *VDI 2221 - Systematic approach to the development and design of technical systems and products*. 1993.
6. Lichtman, J.W. and J.-A. Conchello, *Fluorescence microscopy*. Nature Methods, 2005. **2**: p. 910.
9. Huisken, J. and D.Y. Stainier, *Selective plane illumination microscopy techniques in developmental biology*. Development, 2009. **136**(12): p. 1963-75.
10. Conchello, J.-A. and J.W. Lichtman, *Optical sectioning microscopy*. Nature Methods, 2005. **2**: p. 920.
11. Huisken, J., et al., *Optical Sectioning Deep Inside Live Embryos by Selective Plane Illumination Microscopy*. Science, 2004. **305**(5686): p. 1007-1009.
12. Dan, D., et al., *DMD-based LED-illumination Super-resolution and optical sectioning microscopy*. Scientific Reports, 2013. **3**: p. 1116.
14. Robert, H.W., *Confocal optical microscopy*. Reports on Progress in Physics, 1996. **59**(3): p. 427.
15. Olaf selchow, J.H., *Light sheet fluorescence microscopy and revolutionary 3 D analyses of live specimens*. Photonik international, 2013: p. 4.

17. Siedentopf, H. and R. Zsigmondy, *Über Sichtbarmachung und Größenbestimmung ultramikroskopischer Teilchen, mit besonderer Anwendung auf Goldrubingläser*. Annalen der Physik, 1902. **315**(1): p. 1-39.
18. VOIE, A.H., D.H. BURNS, and F.A. SPELMAN, *Orthogonal-plane fluorescence optical sectioning: Three-dimensional imaging of macroscopic biological specimens*. Journal of Microscopy, 1993. **170**(3): p. 229-236.
19. Huisken, J., et al., *Optical Sectioning Deep Inside Live Embryos by Selective Plane Illumination Microscopy*. Science, 2004. **305**(5686): p. 1007.
21. Olarte, O.E., et al., *Light-sheet microscopy: a tutorial*. Advances in Optics and Photonics, 2018. **10**(1): p. 111-179.
22. Brattoli, M., et al., *Odour detection methods: olfactometry and chemical sensors*. Sensors (Basel), 2011. **11**(5): p. 5290-322.
23. Fleischer, J., et al., *Access to the odor world: olfactory receptors and their role for signal transduction in insects*. Cell Mol Life Sci, 2018. **75**(3): p. 485-508.
24. de Bruyne, M., K. Foster, and J.R. Carlson, *Odor coding in the Drosophila antenna*. Neuron, 2001. **30**(2): p. 537-52.
25. Prasad, B.C. and R.R. Reed, *Chemosensation: molecular mechanisms in worms and mammals*. Trends Genet, 1999. **15**(4): p. 150-3.
26. Shi, P. and J. Zhang, *Extraordinary diversity of chemosensory receptor gene repertoires among vertebrates*. Results Probl Cell Differ, 2009. **47**: p. 1-23.
29. Adams, M.D., et al., *The genome sequence of Drosophila melanogaster*. Science, 2000. **287**(5461): p. 2185-95.
30. Beckingham, K.M., et al., *Drosophila melanogaster--the model organism of choice for the complex biology of multi-cellular organisms*. Gravit Space Biol Bull, 2005. **18**(2): p. 17-29.
31. Jennings, B.H., *Drosophila – a versatile model in biology & medicine*. Materials Today, 2011. **14**(5): p. 190-195.
33. Shanbhag, S.R., B. Muller, and R.A. Steinbrecht, *Atlas of olfactory organs of Drosophila melanogaster 2. Internal organization and cellular architecture of olfactory sensilla*. Arthropod Struct Dev, 2000. **29**(3): p. 211-29.
34. Vosshall, L.B. and R.F. Stocker, *Molecular architecture of smell and taste in Drosophila*. Annu Rev Neurosci, 2007. **30**: p. 505-33.
35. Joseph, R.M. and J.R. Carlson, *Drosophila Chemoreceptors: A Molecular Interface Between the Chemical World and the Brain*. Trends in Genetics, 2015. **31**(12): p. 683-695.

36. Olsson, S.B. and B.S. Hansson, *Electroantennogram and single sensillum recording in insect antennae*. Methods Mol Biol, 2013. **1068**: p. 157-77.
37. Miller, D.J., *Sydney Ringer; physiological saline, calcium and the contraction of the heart*. J Physiol, 2004. **555**(Pt 3): p. 585-7.
38. Russell, J.T., *Imaging calcium signals in vivo: a powerful tool in physiology and pharmacology*. Br J Pharmacol, 2011. **163**(8): p. 1605-25.
39. Paredes, R.M., et al., *Chemical calcium indicators*. Methods (San Diego, Calif.), 2008. **46**(3): p. 143-151.
40. Pérez Koldenkova, V. and T. Nagai, *Genetically encoded Ca<sup>2+</sup> indicators: Properties and evaluation*. Biochimica et Biophysica Acta (BBA) - Molecular Cell Research, 2013. **1833**(7): p. 1787-1797.
41. Yuste, R., *Fluorescence microscopy today*. Nature Methods, 2005. **2**: p. 902.
44. Mukunda, L., et al., *Calmodulin modulates insect odorant receptor function*. Cell Calcium, 2014. **55**(4): p. 191-9.
45. Pentzold, S., et al., *Silencing cuticular pigmentation genes enables RNA FISH in intact insect appendages*. The Journal of Experimental Biology, 2018. **221**(18).
46. Ciddor, P.E., *Refractive index of air: new equations for the visible and near infrared*. Applied Optics, 1996. **35**(9): p. 1566-1573.
56. Buchdahl, G., *SCIENCE AND LOGIC: SOME THOUGHTS ON NEWTON'S SECOND LAW OF MOTION IN CLASSICAL MECHANICS\**. The British Journal for the Philosophy of Science, 1951. **II**(7): p. 217-235.
58. Flynn, M.R. and E.D. Sills, *On the use of computational fluid dynamics in the prediction and control of exposure to airborne contaminants-an illustration using spray painting*. Ann Occup Hyg, 2000. **44**(3): p. 191-202.
60. Gentry, R.A., R.E. Martin, and B.J. Daly, *An Eulerian differencing method for unsteady compressible flow problems*. Journal of Computational Physics, 1966. **1**(1): p. 87-118.
61. Zhang, Z. and Q. Chen, *Comparison of the Eulerian and Lagrangian methods for predicting particle transport in enclosed spaces*. Atmospheric Environment, 2007. **41**(25): p. 5236-5248.
63. Reynolds, O., *An Experimental Investigation of the Circumstances Which Determine Whether the Motion of Water Shall Be Direct or Sinuous, and of the Law of Resistance in Parallel Channels*. Philosophical Transactions of the Royal Society of London, 1883. **174**: p. 935-982.



65. Hughes, H.C. and S. Reynolds, *The use of computational fluid dynamics for modeling airflow design in a kennel facility*. Contemp Top Lab Anim Sci, 1995. **34**(2): p. 49-53.



## Appendix

1. <u>Protocols</u> .....	XIII
A. <u>Ringer Flow Simulations within the Optical Chamber of the Z.1 Microscope</u> .....	XIII
B. <u>Simulation within Odour Distributor Model</u> .....	XXXIV
C. <u>Odour Simulation within the optical chamber</u> .....	XLII
2. <u>Appendix of Blue Prints of the Optical Chamber of the Light-Sheet-Fluorescence-Microscope</u>	
<u>Z.1</u> LXI	

## 1. Protocols

### A. Ringer Flow Simulations within the Optical Chamber of the Z.1 Microscope

Inlets flow rate: 10 cm<sup>3</sup>/s

Prepared by: Eckard Schumann

Requested by: Dr. Jürgen Rybak

Date: Thursday, November 29, 2018

#### Summary

#### Description

The optical chamber of the Z.1 possesses 2 inlets and 3 outlets which can be used for the Ringer solution flow subs function. The distribution of the Ringer solution liquid into the chamber is done in a controlled manner and is also used to transport the remaining odour (the 'waste') to the Z.1 outlets. The Z.1 chamber inlets are located on the frontal upper part of the chamber, one on the left side and the other on the right part. The outlets are positioned on the frontal under part of the chamber. This allows the flow to stream downwards. The outlets are distributed on the left frontal side, the right frontal side with another one on the right side which connects to the centre of the chamber. This provides the system with 21 possible combinations to create the Ringer solution flow, from which 3 are shown on this protocol, because they possess desired visual characteristics.

# Ringer Flow Simulations within the Optical Chamber of the Z.1 Microscope

XIV

## Software information

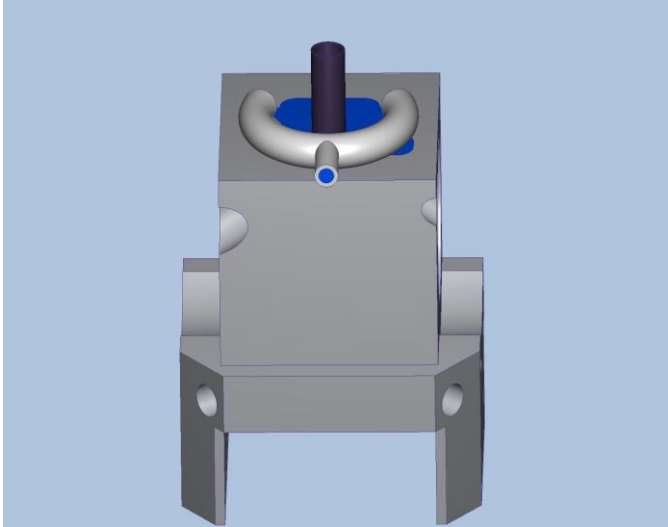
Simulation CFD version	18.0
Simulation CFD build code	20170328

## Design 1

Length units	cm
Coordinate system	Cartesian 3D

## Scenario Ringer solution simulation using the inlets A and B and the outlets 1 and 2

## Materials

		
Name	ASSIGNED TO	PROPERTIES
Titanium	Chamber:1@Duftverteiler_ASME\Chamber_1:1 Chamber:1@Duftverteiler_ASME\Chamber_1:1 Volumen:1@Duftverteiler_ASME\Chamber_1:1 Chamber:1@Duftverteiler_ASME\Chamber_1:1	X-Direction 21.9 W/m-K Y-Direction Same as X-dir. Z-Direction Same as X-dir. Density 4500.0 kg/m3 Specific heat 522.0 J/kg-K Emissivity 0.5 Transmissivity 0.0 Electrical 4.2e-07 ohm-m Wall 0.0 meter

# Ringer Flow Simulations within the Optical Chamber of the Z.1 Microscope

XV

Stainless Steel (316)	Duftverteiler_ASME Volumen:1@Duftverteiler_ASME\Chamber_1:1_U_Duftverteiler_ASME Volumen:1@Duftverteiler_ASME\Chamber_1:1_U_Duftverteiler_ASME Duftverteiler_ASME_U_Chamber:1@Duftverteiler_ASME\Chamber_1:1 Duftverteiler_ASME_U_Chamber:1@Duftverteiler_ASME\Chamber_1:1 Volumen:1@Duftverteiler_ASME\Chamber_1:1_U_Duftverteiler_ASME Volumen:1@Duftverteiler_ASME\Chamber_1:1_U_Duftverteiler_ASME	X- 16.3 Y- Same as Z- Same as Density 8.0 Specific 0.5 J/g-K Emissivit 0.35 Transmis 0.0 Electrical 7.4e-05 Wall 0.0
Water	Volumen:1@Duftverteiler_ASME\Chamber_1:1 Volumen_odour:1@Duftverteiler_ASME Volumen_odour:1@Duftverteiler_ASME_U_Volumen:1@Duftverteiler_ASME\Chamber_1:1 Volumen_odour:1@Duftverteiler_ASME_U_Volumen:1@Duftverteiler_ASME\Chamber_1:1 Volumen_odour:1@Duftverteiler_ASME_U_Volumen:1@Duftverteiler_ASME\Chamber_1:1 Volumen_odour:1@Duftverteiler_ASME_U_Volumen:1@Duftverteiler_ASME\Chamber_1:1	Density Piecewis Viscosity 0.001003 Conducti 0.6 W/m- Specific 4182.0 Compres 2185650 Emissivit 1.0 Wall 0.0 Phase Linked
Glass	Chamber_1:1@Duftverteiler_ASME Volumen:1@Duftverteiler_ASME\Chamber_1:1 Volumen:1@Duftverteiler_ASME\Chamber_1:1_U_Chamber_1:1@Duftverteiler_ASME	X-Direction 0.78 W/m-K Y-Direction Same as X- Z-Direction Same as X- Density 2700.0 Specific heat 840.0 J/kg-K Emissivity 0.92 Transmissivit 0.0 Electrical 50000000.0 Wall 0.0 meter

## Boundary conditions

Type	ASSIGNED TO
Pressure(0 dyne/cm2 Gage)	Surface:32 Surface:33
Velocity Normal(0 cm/s)	Surface:45 Surface:46 Surface:60 Surface:61

# Ringer Flow Simulations within the Optical Chamber of the Z.1 Microscope

XVI

Volume Flow Rate(10 cm <sup>3</sup> /min)	Surface:51 Surface:55
---	--------------------------

## Mesh

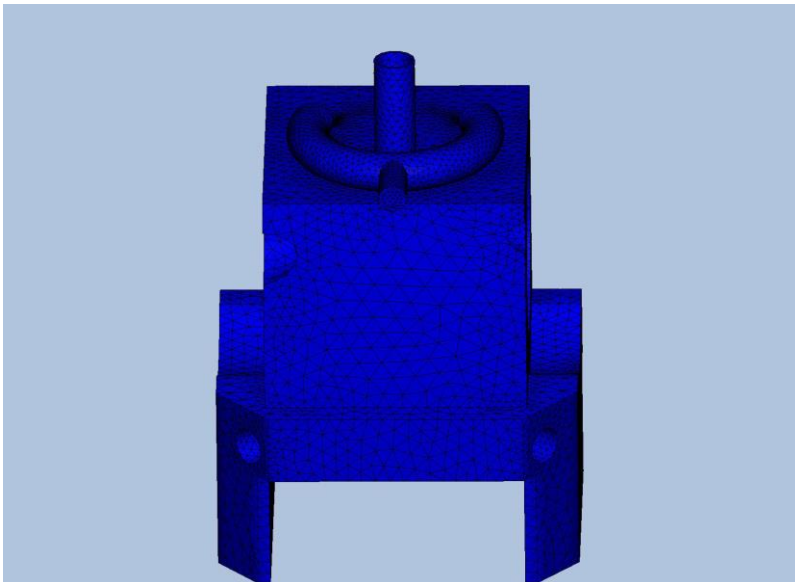
### Automatic Meshing Settings

Surface refinement	0
Gap refinement	0
Resolution factor	1.0
Edge growth rate	1.1
Minimum points on edge	2
Points on longest edge	10
Surface limiting aspect ratio	20

### Mesh Enhancement Settings

Mesh enhancement	1
Enhancement blending	0
Number of layers	3
Layer factor	0.45
Layer gradation	1.05

## Meshed Model



Number of Nodes	110179
Number of Elements	463936

## Physics

# Ringer Flow Simulations within the Optical Chamber of the Z.1 Microscope

XVII

Flow	On
Compressibility	Incompressible
Heat Transfer	Off
Auto Forced Convection	Off
Gravity Components	0.0, 0.0, 0.0
Radiation	Off
Scalar	No scalar
Turbulence	On

## Solver Settings

Solution mode	Steady State
Solver computer	MyComputer
Intelligent solution control	On
Advection scheme	ADV 5
Turbulence model	k-epsilon

## Convergence

Iterations run	182
Solve time	348 seconds
Solver version	18.0.20170328

## Energy Balance

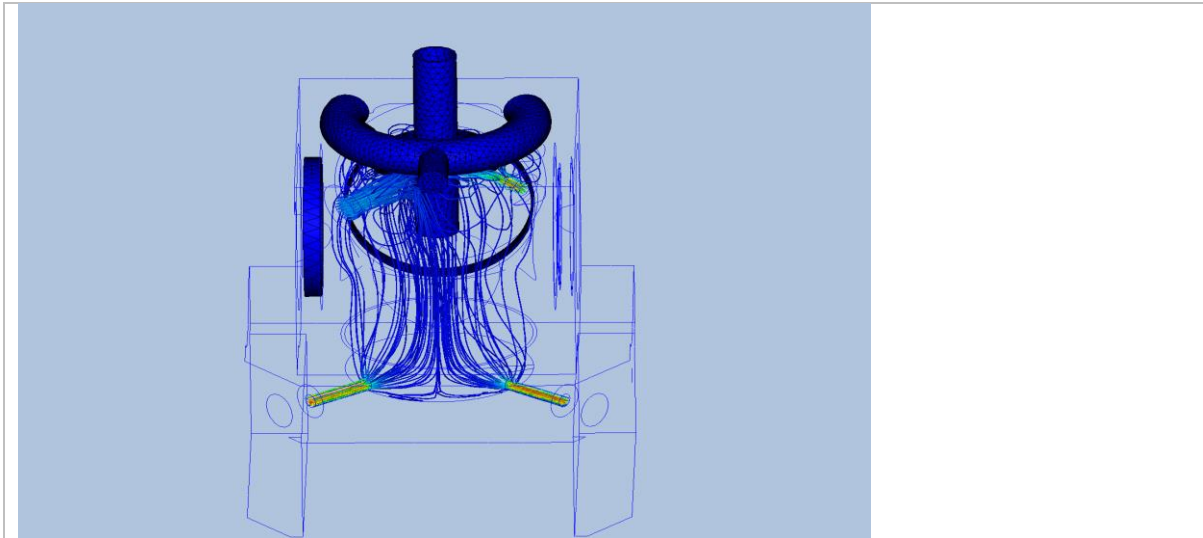

## Mass Balance

	In	Out
Mass flow	0.332734 g/s	-0.329284 g/s
Volume flow	0.333334 cm <sup>3</sup> /s	-0.329878 cm <sup>3</sup> /s

**Results of the Scenario Ringer solution simulation using the inlets A and B and the outlets 1 and 2**

# Ringer Flow Simulations within the Optical Chamber of the Z.1 Microscope

XVIII



Inlets and Outlets

inlet 1	inlet bulk pressure 83.1712 inlet bulk 0.0 C inlet mach number 2.7475e-10 mass flow in 0.166367 g/s minimum x,y,z of 0.0 node near minimum 12390.0 reynolds number 45.6023 surface id 51.0 volume flow in 0.166667 cm <sup>3</sup> /s
inlet 2	inlet bulk pressure 121.398 inlet bulk 0.0 C inlet mach number 1.00785e-09 mass flow in 0.166367 g/s minimum x,y,z of 0.0 node near minimum 12643.0 reynolds number 87.0589 surface id 55.0 total mass flow in 0.332734 g/s total vol. flow in 0.333334 cm <sup>3</sup> /s volume flow in 0.166667 cm <sup>3</sup> /s
outlet 1	mass flow out -0.167329 g/s minimum x,y,z of 0.0 node near minimum 8550.0 outlet bulk pressure -0.0 dyne/cm <sup>2</sup> outlet bulk -0.0 C outlet mach number 4.36171e-10 reynolds number 87.5623



# Ringer Flow Simulations within the Optical Chamber of the Z.1 Microscope

XIX

	surface id	32.0
	volume flow out	-0.167631 cm <sup>3</sup> /s
outlet 2	mass flow out	-0.161955 g/s
	minimum x,y,z of	0.0
	node near minimum	8559.0
	outlet bulk pressure	-0.0 dyne/cm <sup>2</sup>
	outlet bulk	-0.0 C
	outlet mach number	4.24186e-10
	reynolds number	84.7499
	surface id	33.0
	total mass flow out	-0.329284 g/s
	total vol. flow out	-0.329877 cm <sup>3</sup> /s
	volume flow out	-0.162247 cm <sup>3</sup> /s

## Field Variable Results

Variable	Max	Min
cond	0.219 W/cm-K	0.006 W/cm-K
dens	8.0 g/cm <sup>3</sup>	0.9982 g/cm <sup>3</sup>
econd	1544.07 W/cm-K	0.0 W/cm-K
emiss	1.0	0.0
evisc	598.124 g/cm-s	0.0 g/cm-s
gent	24089.3 1/s	8.19641e-11 1/s
press	151.17 dyne/cm <sup>2</sup>	0.0 dyne/cm <sup>2</sup>
ptotl	161.819 dyne/cm <sup>2</sup>	0.0 dyne/cm <sup>2</sup>
scal1	0.0	0.0
seebeck	0.0 V/K	0.0 V/K
shgc	0.0	0.0
spech	4.182 J/g-K	0.5 J/g-K
temp	0.0 C	0.0 C
transmiss	0.0	0.0
turbd	235434.0 cm <sup>2</sup> /s <sup>3</sup>	2e-15 cm <sup>2</sup> /s <sup>3</sup>
turbk	59.2234 cm <sup>2</sup> /s <sup>2</sup>	1.00306e-06 cm <sup>2</sup> /s <sup>2</sup>
ufactor	0.0	0.0
visc	0.01003 g/cm-s	0.0 g/cm-s
vx vel	7.23466 cm/s	-7.65506 cm/s
vy vel	1.96961 cm/s	-2.23741 cm/s
vz vel	6.41514 cm/s	-5.6671 cm/s
wrough	0.0 cm	0.0 cm

## Fluid Forces on Walls

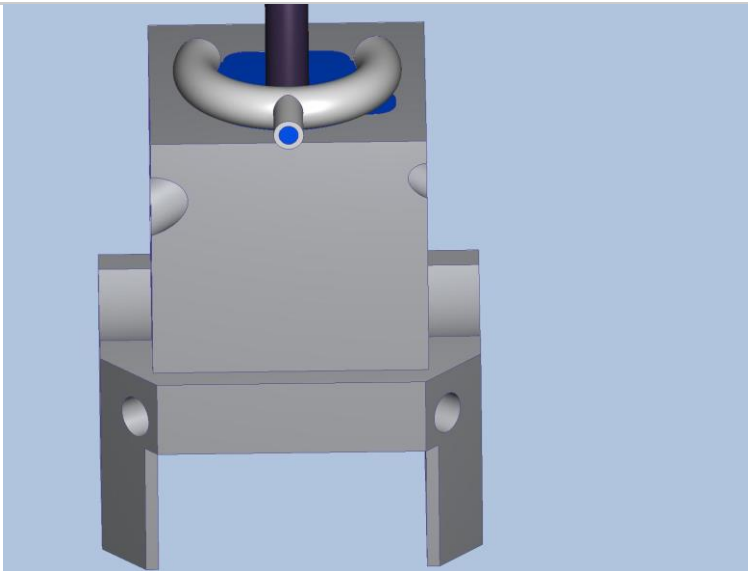
pressx	5.3524 dynes
pressy	2.8021 dynes
pressz	-12.913 dynes
shearx	-0.36812 dynes
sheary	-0.19259 dynes
shearz	0.41447 dynes

# Ringer Flow Simulations within the Optical Chamber of the Z.1 Microscope

XX

## Scenario Ringer solution using the inlets A and B with the outlet 1 and 3

### Materials



Name	ASSIGNED TO	PROPERTIES
Titanium	Chamber:1@Duftverteiler_ASME\Chamber_1:1 Chamber:1@Duftverteiler_ASME\Chamber_1:1 Volumen:1@Duftverteiler_ASME\Chamber_1:1 Chamber:1@Duftverteiler_ASME\Chamber_1:1	X-Direction 21.9 W/m-K Y-Direction Same as X-dir. Z-Direction Same as X-dir. Density 4500.0 kg/m3 Specific heat 522.0 J/kg-K Emissivity 0.5 Transmissivity 0.0 Electrical 4.2e-07 ohm-m Wall 0.0 meter
Stainless Steel (316)	Duftverteiler_ASME Volumen:1@Duftverteiler_ASME\Chamber_1:1_U_Duftverteiler_ASME Volumen:1@Duftverteiler_ASME\Chamber_1:1_U_Duftverteiler_ASME Duftverteiler_ASME_U_Chamber:1@Duftverteiler_ASME\Chamber_1:1 Duftverteiler_ASME_U_Chamber:1@Duftverteiler_ASME\Chamber_1:1 Volumen:1@Duftverteiler_ASME\Chamber_1:1_U_Duftverteiler_ASME Volumen:1@Duftverteiler_ASME\Chamber_1:1_U_Duftverteiler_ASME	X- 16.3 Y- Same as Z- Same as Density 8.0 Specific 0.5 J/g-K Emissivit 0.35 Transmis 0.0 Electrical 7.4e-05 Wall 0.0

# Ringer Flow Simulations within the Optical Chamber of the Z.1 Microscope

Water	Volumen:1 @Duftverteiler_ASME\Chamber_1:1 Volumen_odour:1 @Duftverteiler_ASME Volumen_odour:1 @Duftverteiler_ASME_U_Volumen:1 @Duftverteiler_ASME\Chamber_1:1 Volumen_odour:1 @Duftverteiler_ASME_U_Volumen:1 @Duftverteiler_ASME\Chamber_1:1 Volumen_odour:1 @Duftverteiler_ASME_U_Volumen:1 @Duftverteiler_ASME\Chamber_1:1 Volumen_odour:1 @Duftverteiler_ASME_U_Volumen:1 @Duftverteiler_ASME\Chamber_1:1	Density      Piecewis Viscosity     0.001003 Conducti     0.6 W/m- Specific      4182.0 Compres     2185650 Emissivit    1.0 Wall          0.0 Phase        Linked
Glass	Chamber_1:1 @Duftverteiler_ASME Volumen:1 @Duftverteiler_ASME\Chamber_1:1 Volumen:1 @Duftverteiler_ASME\Chamber_1:1_U_Chamber_1:1 @Duftverteiler_ASME	X-Direction    0.78 W/m-K Y-Direction    Same as X- Z-Direction    Same as X- Density        2700.0 Specific heat   840.0 J/kg-K Emissivity     0.92 Transmissivit 0.0 Electrical     50000000.0 Wall            0.0 meter

## Boundary conditions

Type	ASSIGNED TO
Pressure(0 dyne/cm2 Gage)	Surface:32 Surface:34
Velocity Normal(0 cm/s)	Surface:45 Surface:46 Surface:60 Surface:61
Volume Flow Rate(10 cm3/min)	Surface:51 Surface:55

## Mesh

### Automatic Meshing Settings

# Ringer Flow Simulations within the Optical Chamber of the Z.1 Microscope

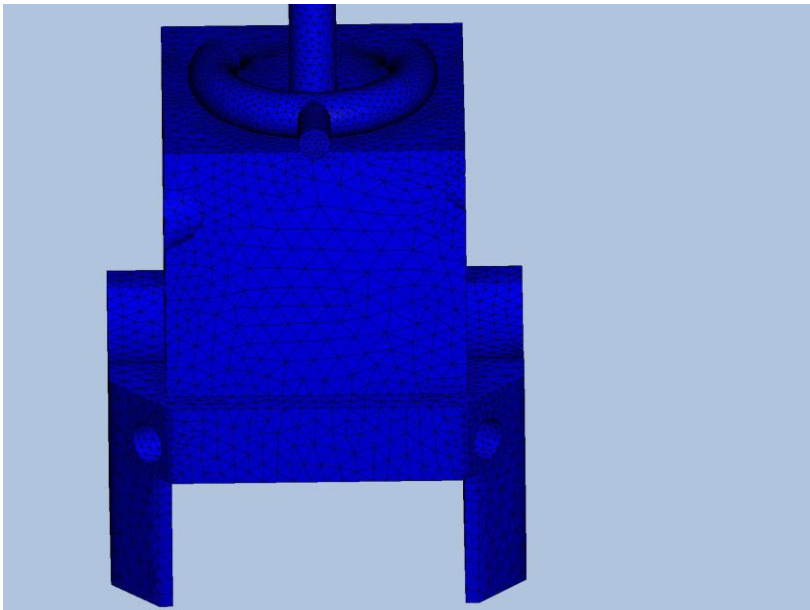
XXII

Surface refinement	0
Gap refinement	0
Resolution factor	1.0
Edge growth rate	1.1
Minimum points on edge	2
Points on longest edge	10
Surface limiting aspect ratio	20

## Mesh Enhancement Settings

Mesh enhancement	1
Enhancement blending	0
Number of layers	3
Layer factor	0.45
Layer gradation	1.05

## Meshed Model



Number of Nodes	110153
Number of Elements	463868

## Physics

Flow	On
Compressibility	Incompressible
Heat Transfer	Off
Auto Forced Convection	Off
Gravity Components	0.0, 0.0, 0.0
Radiation	Off
Scalar	No scalar

# Ringer Flow Simulations within the Optical Chamber of the Z.1 Microscope

XXIII

Turbulence	On
------------	----

## Solver Settings

Solution mode	Steady State
Solver computer	MyComputer
Intelligent solution control	On
Advection scheme	ADV 5
Turbulence model	k-epsilon

## Convergence

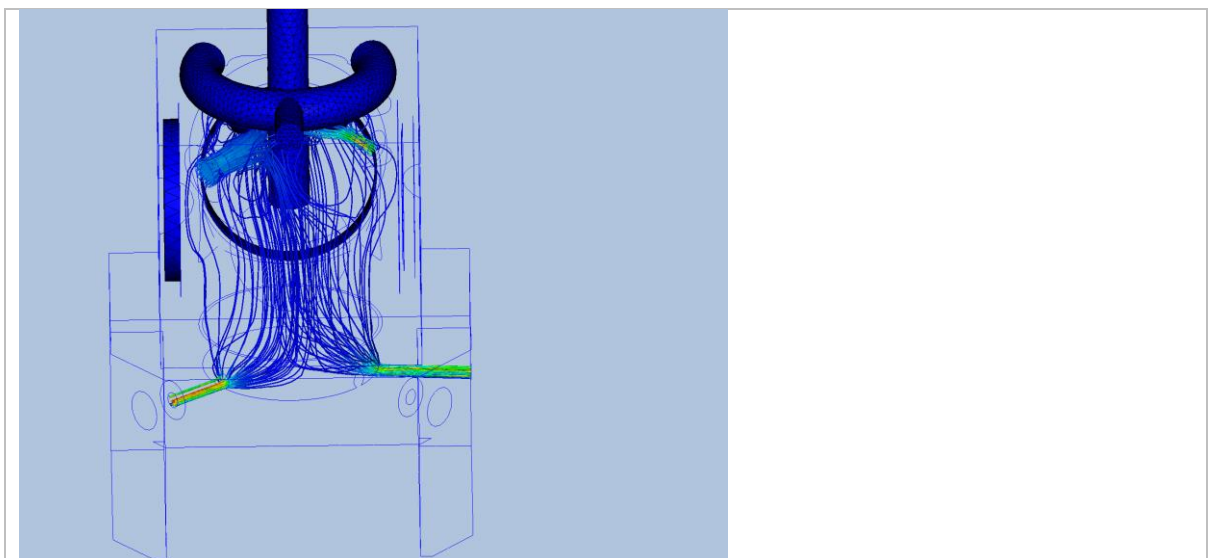
Iterations run	200
Solve time	374 seconds
Solver version	18.0.20170328

## Energy Balance


## Mass Balance

	In	Out
Mass flow	0.332734 g/s	-0.329277 g/s
Volume flow	0.333334 cm <sup>3</sup> /s	-0.329872 cm <sup>3</sup> /s

## Results of the Scenario Ringer solution using the inlets A and B with the outlet 1 and 3



Inlets and Outlets

# Ringer Flow Simulations within the Optical Chamber of the Z.1 Microscope

XXIV

inlet 1	inlet bulk pressure	92.2786
	inlet bulk	0.0 C
	inlet mach number	2.7475e-10
	mass flow in	0.166367 g/s
	minimum x,y,z of	0.0
	node near minimum	12389.0
	reynolds number	45.6023
	surface id	51.0
	volume flow in	0.166667 cm <sup>3</sup> /s
inlet 2	inlet bulk pressure	130.538
	inlet bulk	0.0 C
	inlet mach number	1.00785e-09
	mass flow in	0.166367 g/s
	minimum x,y,z of	0.0
	node near minimum	12642.0
	reynolds number	87.0589
	surface id	55.0
	total mass flow in	0.332734 g/s
	total vol. flow in	0.333334 cm <sup>3</sup> /s
	volume flow in	0.166667 cm <sup>3</sup> /s
outlet 1	mass flow out	-0.17935 g/s
	minimum x,y,z of	0.0
	node near minimum	8550.0
	outlet bulk pressure	-0.0 dyne/cm <sup>2</sup>
	outlet bulk	-0.0 C
	outlet mach number	4.68152e-10
	reynolds number	93.853
	surface id	32.0
	volume flow out	-0.179674 cm <sup>3</sup> /s
outlet 2	mass flow out	-0.149927 g/s
	minimum x,y,z of	0.0
	node near minimum	819.0
	outlet bulk pressure	-0.0 dyne/cm <sup>2</sup>
	outlet bulk	-0.0 C
	outlet mach number	4.14844e-10
	reynolds number	78.3007
	surface id	34.0
	total mass flow out	-0.329278 g/s
	total vol. flow out	-0.329871 cm <sup>3</sup> /s
	volume flow out	-0.150198 cm <sup>3</sup> /s

## Field Variable Results

Variable	Max	Min
cond	0.219 W/cm-K	0.006 W/cm-K

# Ringer Flow Simulations within the Optical Chamber of the Z.1 Microscope

XXV

dens	8.0 g/cm <sup>3</sup>	0.9982 g/cm <sup>3</sup>
econd	1544.33 W/cm-K	0.0 W/cm-K
emiss	1.0	0.0
evisc	598.221 g/cm-s	0.0 g/cm-s
gent	34708.2 1/s	3.12857e-11 1/s
press	160.341 dyne/cm <sup>2</sup>	0.0 dyne/cm <sup>2</sup>
ptotl	170.99 dyne/cm <sup>2</sup>	0.0 dyne/cm <sup>2</sup>
scal1	0.0	0.0
seebeck	0.0 V/K	0.0 V/K
shgc	0.0	0.0
spech	4.182 J/g-K	0.5 J/g-K
temp	0.0 C	0.0 C
transmiss	0.0	0.0
turbd	478444.0 cm <sup>2</sup> /s <sup>3</sup>	2e-15 cm <sup>2</sup> /s <sup>3</sup>
turbk	60.517 cm <sup>2</sup> /s <sup>2</sup>	1.0235e-06 cm <sup>2</sup> /s <sup>2</sup>
ufactor	0.0	0.0
visc	0.01003 g/cm-s	0.0 g/cm-s
vx vel	8.71244 cm/s	-8.19029 cm/s
vy vel	1.95633 cm/s	-4.38527 cm/s
vz vel	6.8629 cm/s	-5.66675 cm/s
wrough	0.0 cm	0.0 cm

## Fluid Forces on Walls

pressx	5.2893 dynes
pressy	3.3287 dynes
pressz	-12.115 dynes
shearx	0.90438 dynes
sheary	-0.18079 dynes
shearz	-0.1097 dynes

# Ringer Flow Simulations within the Optical Chamber of the Z.1 Microscope

## Scenario Ringer solution using the inlets A and B with the outlets 1, 2 and 3

### Materials

Name	ASSIGNED TO	PROPERTIES	
Titanium	Chamber:1@Duftverteiler_ASME\Chamber_1:1 Chamber:1@Duftverteiler_ASME\Chamber_1:1 Volumen:1@Duftverteiler_ASME\Chamber_1:1 Chamber:1@Duftverteiler_ASME\Chamber_1:1	X-Direction Y-Direction Z-Direction Density Specific heat Emissivity Transmissivity Electrical Wall	21.9 W/m-K Same as X-dir. Same as X-dir. 4500.0 kg/m3 522.0 J/kg-K 0.5 0.0 4.2e-07 ohm-m 0.0 meter
Stainless Steel (316)	Duftverteiler_ASME Volumen:1@Duftverteiler_ASME\Chamber_1:1_U_Duftverteiler_ASME Volumen:1@Duftverteiler_ASME\Chamber_1:1_U_Duftverteiler_ASME Duftverteiler_ASME_U_Chamber:1@Duftverteiler_ASME\Chamber_1:1 Duftverteiler_ASME_U_Chamber:1@Duftverteiler_ASME\Chamber_1:1 Volumen:1@Duftverteiler_ASME\Chamber_1:1_U_Duftverteiler_ASME Volumen:1@Duftverteiler_ASME\Chamber_1:1_U_Duftverteiler_ASME	X- Y- Z- Density Specific Emissivit Transmis Electrical Wall	16.3 Same as Same as 8.0 0.5 J/g-K 0.35 0.0 7.4e-05 0.0



# Ringer Flow Simulations within the Optical Chamber of the Z.1 Microscope

XXVII

Water	Volumen:1 @Duftverteiler_ASME\Chamber_1:1 Volumen_odour:1 @Duftverteiler_ASME_U_V Volumen_odour:1 @Duftverteiler_ASME_U_V olumen:1 @Duftverteiler_ASME\Chamber_1:1 Volumen_odour:1 @Duftverteiler_ASME_U_V olumen:1 @Duftverteiler_ASME\Chamber_1:1 Volumen_odour:1 @Duftverteiler_ASME_U_V olumen:1 @Duftverteiler_ASME\Chamber_1:1 Volumen_odour:1 @Duftverteiler_ASME_U_V olumen:1 @Duftverteiler_ASME\Chamber_1:1	Density Viscosity Conducti Specific Compres Emissivit Wall Phase	Pieewis 0.001003 0.6 W/m- 4182.0 2185650 1.0 0.0 Linked
Glass	Chamber_1:1 @Duftverteiler_ASME Volumen:1 @Duftverteiler_ASME\Chamber_1:1 Volumen:1 @Duftverteiler_ASME\Chamber_1:1_U_Chamber_1:1 @Duftverteiler_ASME	X-Direction Y-Direction Z-Direction Density Specific heat Emissivity Transmissivit Electrical Wall	0.78 W/m-K Same as X- Same as X- 2700.0 840.0 J/kg-K 0.92 0.0 50000000.0 0.0 meter

## Boundary conditions

Type	ASSIGNED TO
Pressure(0 dyne/cm2 Gage)	Surface:32 Surface:33 Surface:34
Velocity Normal(0 cm/s)	Surface:45 Surface:46 Surface:60 Surface:61
Volume Flow Rate(10 cm3/min)	Surface:51 Surface:55

## Mesh

### Automatic Meshing Settings

Surface refinement	0
Gap refinement	0

# Ringer Flow Simulations within the Optical Chamber of the Z.1 Microscope

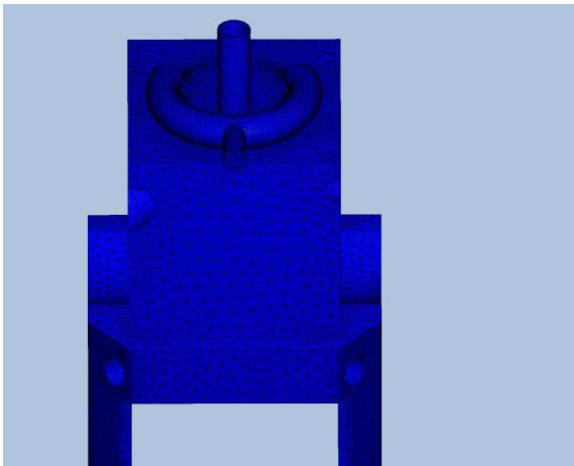
XXVIII

Resolution factor	1.0
Edge growth rate	1.1
Minimum points on edge	2
Points on longest edge	10
Surface limiting aspect ratio	20

## Mesh Enhancement Settings

Mesh enhancement	1
Enhancement blending	0
Number of layers	3
Layer factor	0.45
Layer gradation	1.05

## Meshed Model



Number of Nodes	110103
Number of Elements	463710

## Physics

Flow	On
Compressibility	Incompressible
Heat Transfer	Off
Auto Forced Convection	Off
Gravity Components	0.0, 0.0, 0.0
Radiation	Off
Scalar	No scalar
Turbulence	On

## Solver Settings

Solution mode	Steady State
---------------	--------------

# Ringer Flow Simulations within the Optical Chamber of the Z.1 Microscope

XXIX

Solver computer	MyComputer
Intelligent solution control	On
Advection scheme	ADV 5
Turbulence model	k-epsilon

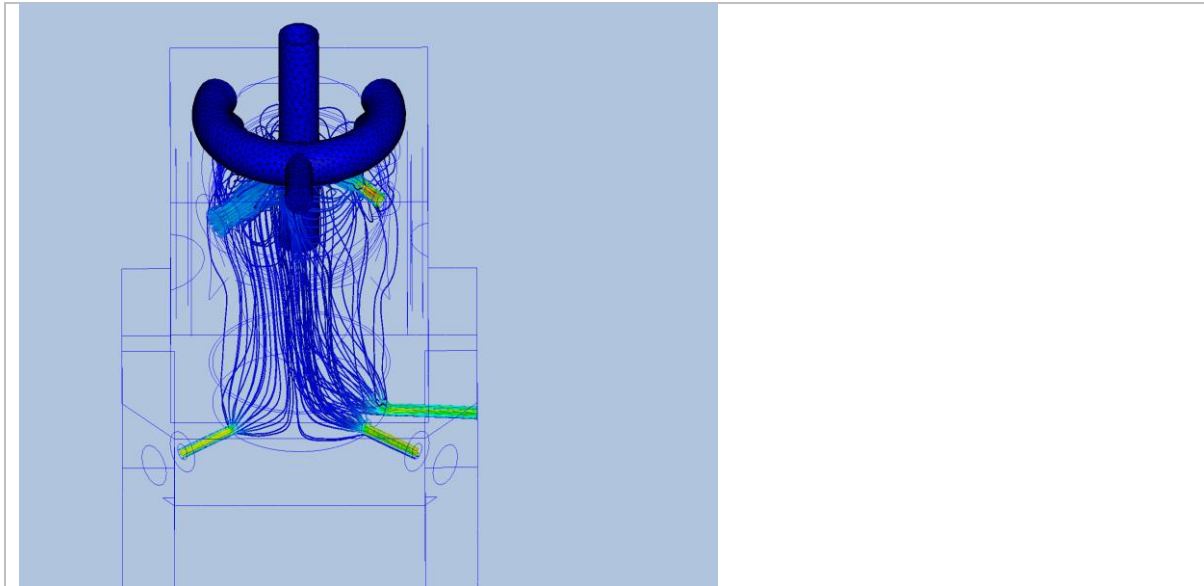
## Convergence

Iterations run	152
Solve time	309 seconds
Solver version	18.0.20170328

## Mass Balance

	In	Out
Mass flow	0.332734 g/s	-0.3289438 g/s
Volume flow	0.333334 cm <sup>3</sup> /s	-0.3295374 cm <sup>3</sup> /s

## Results of the Scenario Ringer solution using the inlets A and B with the outlets 1, 2 and 3



## Inlets and Outlets

inlet 1	inlet bulk pressure	51.0212	
	inlet bulk	0.0 C	
	inlet mach number	2.7475e-10	

# Ringer Flow Simulations within the Optical Chamber of the Z.1 Microscope

XXX

	mass flow in 0.166367 g/s minimum x,y,z of 0.0 node near minimum 12420.0 reynolds number 45.6023 surface id 51.0 volume flow in 0.166667 cm <sup>3</sup> /s
inlet 2	inlet bulk pressure 89.2948 inlet bulk 0.0 C inlet mach number 1.00785e-09 mass flow in 0.166367 g/s minimum x,y,z of 0.0 node near minimum 12673.0 reynolds number 87.0589 surface id 55.0 total mass flow in 0.332734 g/s total vol. flow in 0.333334 cm <sup>3</sup> /s volume flow in 0.166667 cm <sup>3</sup> /s
outlet 1	mass flow out -0.118345 g/s minimum x,y,z of 0.0 node near minimum 8550.0 outlet bulk pressure -0.0 dyne/cm <sup>2</sup> outlet bulk -0.0 C outlet mach number 3.07208e-10 reynolds number 61.9292 surface id 32.0 volume flow out -0.118558 cm <sup>3</sup> /s
outlet 2	mass flow out -0.114881 g/s minimum x,y,z of 0.0 node near minimum 8559.0 outlet bulk pressure -0.0 dyne/cm <sup>2</sup> outlet bulk -0.0 C outlet mach number 2.99853e-10 reynolds number 60.1168 surface id 33.0 volume flow out -0.115089 cm <sup>3</sup> /s
outlet 3	mass flow out -0.0957178 g/s minimum x,y,z of 0.0 node near minimum 819.0 outlet bulk pressure -0.0 dyne/cm <sup>2</sup> outlet bulk -0.0 C outlet mach number 2.64101e-10 reynolds number 49.9894 surface id 34.0 total mass flow out -0.328944 g/s

# Ringer Flow Simulations within the Optical Chamber of the Z.1 Microscope

XXXI

	total vol. flow out	-0.329537 cm <sup>3</sup> /s
	volume flow out	-0.0958904 cm <sup>3</sup> /s

## Field Variable Results

Variable	Max	Min
cond	0.219 W/cm-K	0.006 W/cm-K
dens	8.0 g/cm <sup>3</sup>	0.9982 g/cm <sup>3</sup>
econd	1480.24 W/cm-K	0.0 W/cm-K
emiss	1.0	0.0
evisc	570.502 g/cm-s	0.0 g/cm-s
gent	23253.8 1/s	1.23641e-10 1/s
press	119.066 dyne/cm <sup>2</sup>	0.0 dyne/cm <sup>2</sup>
ptotl	129.715 dyne/cm <sup>2</sup>	0.0 dyne/cm <sup>2</sup>
scal1	0.0	0.0
seebeck	0.0 V/K	0.0 V/K
shgc	0.0	0.0
spech	4.182 J/g-K	0.5 J/g-K
temp	0.0 C	0.0 C
transmiss	0.0	0.0
turbd	233520.0 cm <sup>2</sup> /s <sup>3</sup>	2.08311e-15 cm <sup>2</sup> /s <sup>3</sup>
turbk	58.7412 cm <sup>2</sup> /s <sup>2</sup>	1.02158e-06 cm <sup>2</sup> /s <sup>2</sup>
ufactor	0.0	0.0
visc	0.01003 g/cm-s	0.0 g/cm-s
vx vel	5.57033 cm/s	-6.42581 cm/s
vy vel	1.9648 cm/s	-2.97764 cm/s
vz vel	4.57461 cm/s	-5.65102 cm/s
wrough	0.0 cm	0.0 cm

## Fluid Forces on Walls

pressx	1.2326 dynes
pressy	1.9779 dynes
pressz	-7.8288 dynes
shearx	0.94602 dynes
sheary	-0.1822 dynes
shearz	0.0040643 dynes

# Ringer Flow Simulations within the Optical Chamber of the Z.1 Microscope

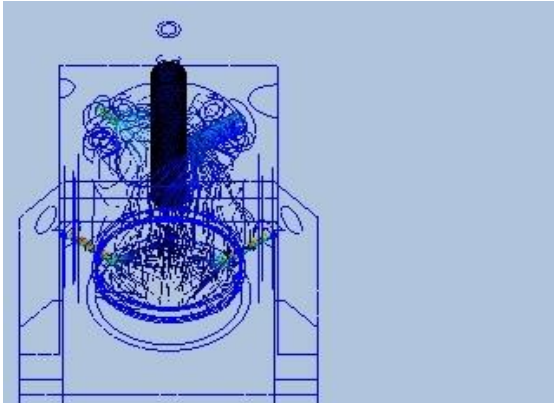
XXXII

## Decision Centre

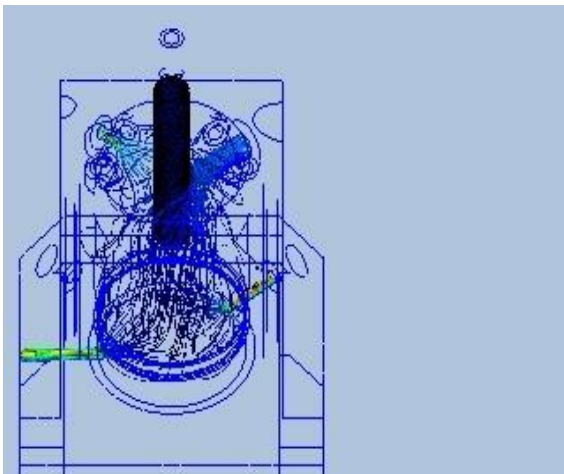
### Summary images

Image 01

Design 1::18Scenario Ringer solution inlet AB outlet 1&2



Design 1::Scenario Ringer solution inlet AB outlet 1&3



Design 1::Scenario Ringer solution inlet AB outlet 1&2&3

# Ringer Flow Simulations within the Optical Chamber of the Z.1 Microscope

XXXIII

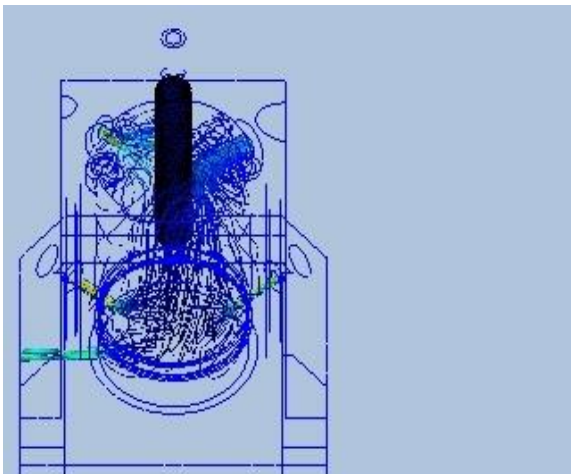
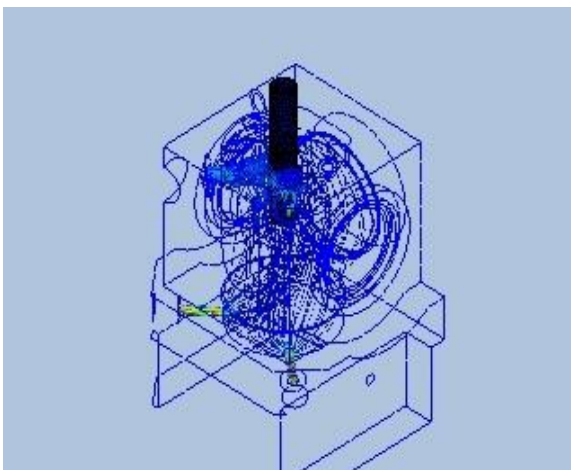
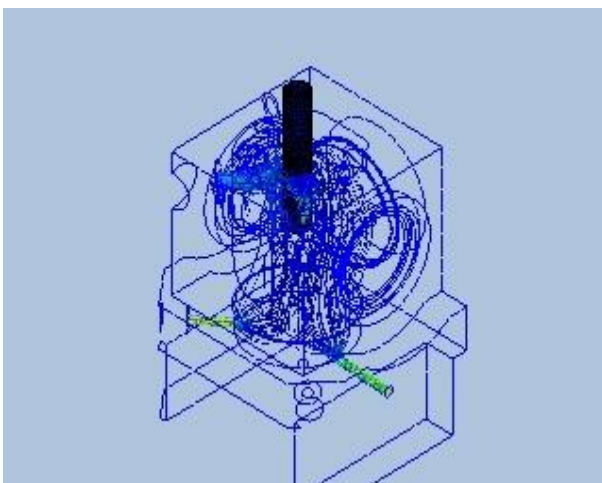


Image 02

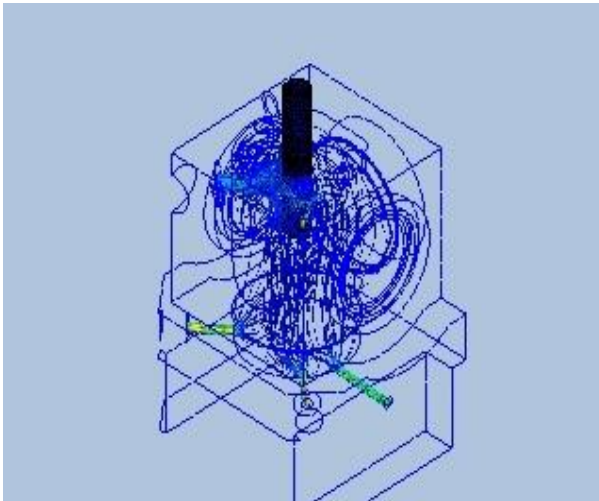
Design 1::Scenario Ringer solution inlet AB outlet 1&2



Design 1::Scenario Ringer solution inlet AB outlet 1&3



Design 1::Scenario Ringer solution inlet AB outlet 1&2&3



## B. Simulation within Odour Distributor Model

Inlet flow rate: 10 cm<sup>3</sup>/min

Prepared by: Eckard Schumann

Requested by: Dr. Jürgen Rybak

Date: Thursday, November 29, 2018

### Summary

#### Description

To test the function of the odour distributor model I had to simulate the internal flow of the diluted odour. I used water since it has similar characteristics to the diluted odour in Ringer solution. A flow rate of 10 cm<sup>3</sup>/min was used to simulate the ingoing flow in the odour distributor model.

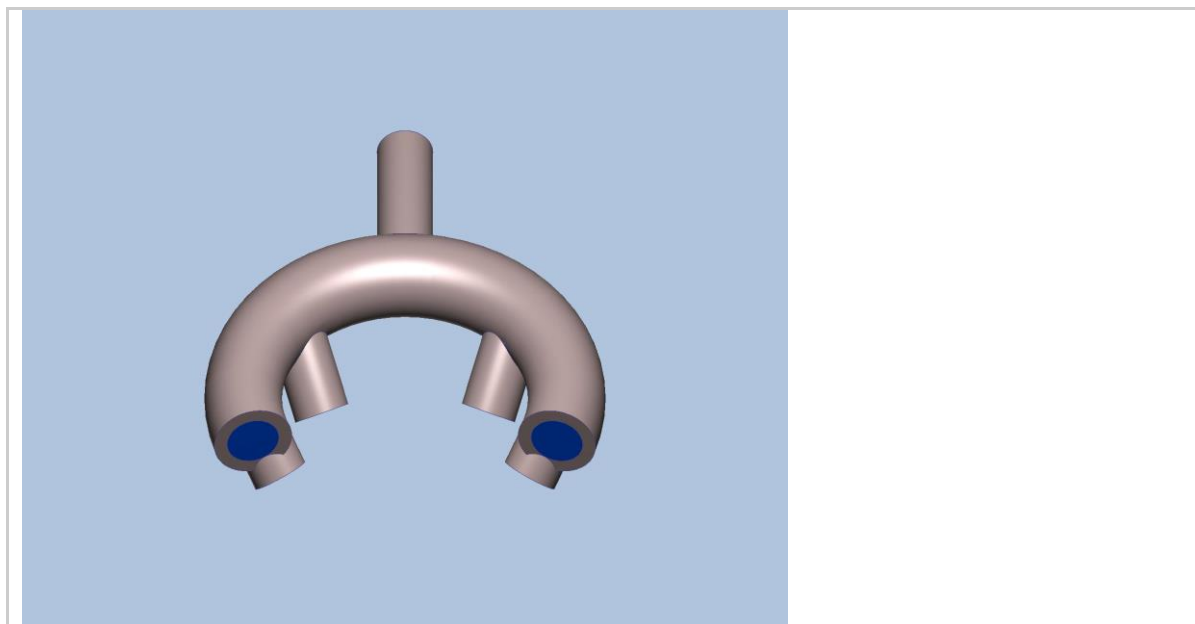
#### Design 1

Length units	cm
Coordinate system	Cartesian 3D



## Odour Distributor Model

### Materials



Name	ASSIGNED TO	PROPERTIES	
Aluminium	finished	X-Direction	204.0 W/m-K
		Y-Direction	Same as X-dir.
		Z-Direction	Same as X-dir.
		Density	2707.0 kg/m3
		Specific heat	896.0 J/kg-K
		Emissivity	0.2
		Transmissivity	0.0
		Electrical resistivity	2.7e-08 ohm-m
		Wall roughness	0.0 meter

# Simulation within Odour Distributor Model

XXXVI

Water	Component9:1 @finished	Density	Piecewise Linear
		Viscosity	0.001003 Pa-s
		Conductivity	0.6 W/m-K
		Specific heat	4182.0 J/kg-K
		Compressibility	2185650000.0 Pa
		Emissivity	1.0
		Wall roughness	0.0 meter
		Phase	Linked Vapor

## Boundary conditions

Type	ASSIGNED TO
Volume Flow Rate(10 cm <sup>3</sup> /min)	Surface:1
Pressure(0 dyne/cm <sup>2</sup> Gage)	Surface:2 Surface:3 Surface:4 Surface:5

## Mesh

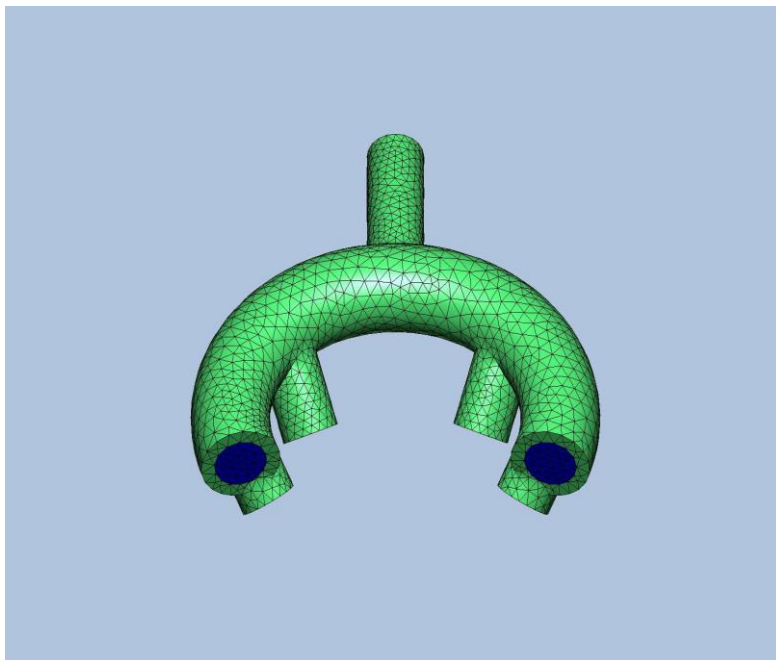
### Automatic Meshing Settings

Surface refinement	0
Gap refinement	0
Resolution factor	1.0
Edge growth rate	1.1
Minimum points on edge	2
Points on longest edge	10
Surface limiting aspect ratio	20

### Mesh Enhancement Settings

Mesh enhancement	1
Enhancement blending	0
Number of layers	3
Layer factor	0.45
Layer gradation	1.05

### Meshed Model



Number of Nodes	11955
Number of Elements	41793

## Physics

Flow	On
Compressibility	Incompressible
Heat Transfer	Off
Auto Forced Convection	Off
Gravity Components	0.0, 0.0, 0.0
Radiation	Off
Scalar	No scalar
Turbulence	On

## Solver Settings

Solution mode	Steady State
Solver computer	MyComputer
Intelligent solution control	On
Advection scheme	ADV 5
Turbulence model	k-epsilon

## Convergence

Iterations run	100
Solve time	38 seconds
Solver version	18.0.20170328

## Mass Balance

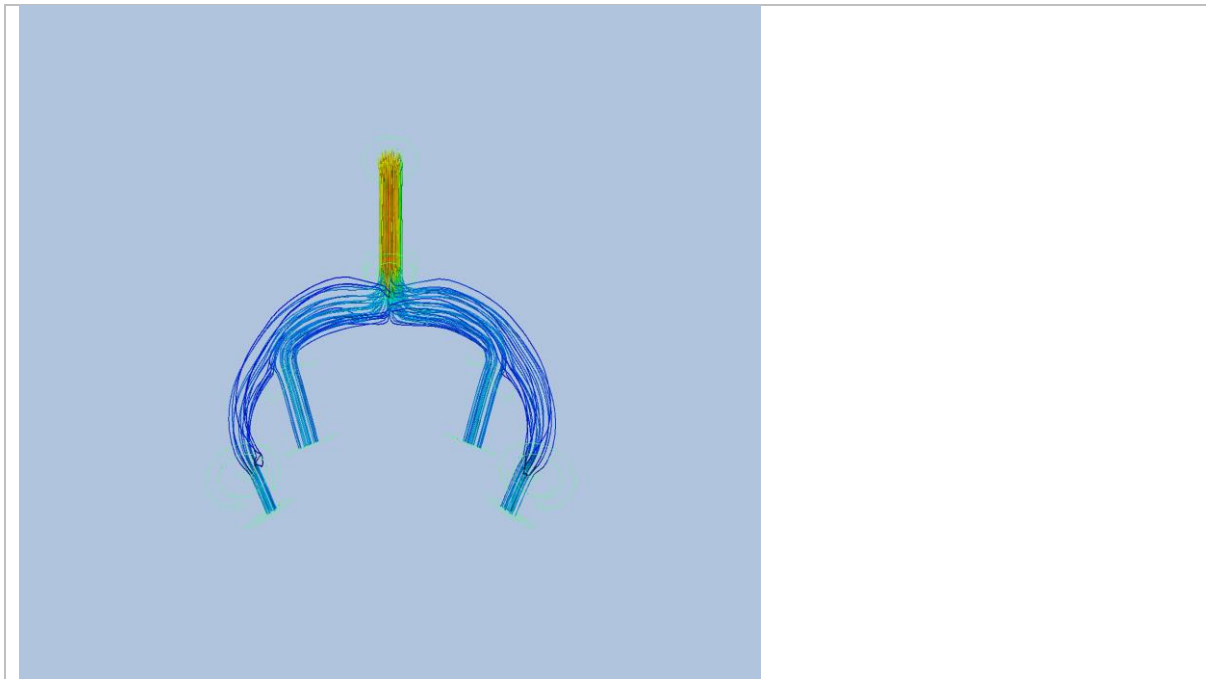
In	Out
----	-----

# Simulation within Odour Distributor Model

XXXVIII

Mass flow	0.166367 g/s	-0.1654305 g/s
Volume flow	0.166667 cm <sup>3</sup> /s	-0.1657288 cm <sup>3</sup> /s

## Results of the Simulation within Odour Distributor Model



### Inlets and Outlets

inlet 1	inlet bulk pressure	65.3129
	inlet bulk	0.0 C
	inlet mach number	9.614e-10
	mass flow in	0.166367 g/s
	minimum x,y,z of	0.0
	node near minimum	38.0
	reynolds number	83.2737
	surface id	1.0

# Simulation within Odour Distributor Model

XXXIX

	total mass flow in	0.166367 g/s
	total vol. flow in	0.166667 cm <sup>3</sup> /s
	volume flow in	0.166667 cm <sup>3</sup> /s
outlet 1	mass flow out	-0.038156 g/s
	minimum x,y,z of	0.0
	node near minimum	59.0
	outlet bulk pressure	-0.0 dyne/cm <sup>2</sup>
	outlet bulk	-0.0 C
	outlet mach number	1.79717e-10
	reynolds number	19.0987
	surface id	3.0
	volume flow out	-0.0382248 cm <sup>3</sup> /s
outlet 2	mass flow out	-0.0445649 g/s
	minimum x,y,z of	0.0
	node near minimum	643.0
	outlet bulk pressure	-0.0 dyne/cm <sup>2</sup>
	outlet bulk	-0.0 C
	outlet mach number	2.20734e-10
	reynolds number	22.3066
	surface id	5.0
	volume flow out	-0.0446453 cm <sup>3</sup> /s
outlet 3	mass flow out	-0.0444862 g/s
	minimum x,y,z of	0.0
	node near minimum	506.0
	outlet bulk pressure	-0.0 dyne/cm <sup>2</sup>
	outlet bulk	-0.0 C
	outlet mach number	2.21496e-10
	reynolds number	22.2672
	surface id	2.0
	volume flow out	-0.0445664 cm <sup>3</sup> /s
outlet 4	mass flow out	-0.0382234 g/s
	minimum x,y,z of	0.0
	node near minimum	599.0
	outlet bulk pressure	-0.0 dyne/cm <sup>2</sup>
	outlet bulk	-0.0 C
	outlet mach number	1.87764e-10
	reynolds number	19.1324
	surface id	4.0
	total mass flow out	-0.16543 g/s
	total vol. flow out	-0.165729 cm <sup>3</sup> /s
	volume flow out	-0.0382923 cm <sup>3</sup> /s

## Field Variable Results

Variable	Max	Min
cond	2.04 W/cm-K	0.006 W/cm-K
dens	2.707 g/cm <sup>3</sup>	0.9982 g/cm <sup>3</sup>

# Simulation within Odour Distributor Model

XL

econd	0.389394 W/cm-K	0.0 W/cm-K
emiss	1.0	0.0
evisc	0.0434994 g/cm-s	0.0 g/cm-s
gent	1240.0 1/s	0.0316228 1/s
press	72.4002 dyne/cm <sup>2</sup>	0.0 dyne/cm <sup>2</sup>
ptotl	82.317 dyne/cm <sup>2</sup>	0.0 dyne/cm <sup>2</sup>
scal1	0.0	0.0
seebeck	0.0 V/K	0.0 V/K
shgc	0.0	0.0
spech	4.182 J/g-K	0.896 J/g-K
temp	0.0 C	0.0 C
transmiss	0.0	0.0
turbd	2106.39 cm <sup>2</sup> /s <sup>3</sup>	0.00065076 cm <sup>2</sup> /s <sup>3</sup>
turbk	10.4608 cm <sup>2</sup> /s <sup>2</sup>	1.003e-05 cm <sup>2</sup> /s <sup>2</sup>
ufactor	0.0	0.0
visc	0.01003 g/cm-s	0.0 g/cm-s
vx vel	1.59888 cm/s	-1.65583 cm/s
vy vel	0.552461 cm/s	-1.57374 cm/s
vz vel	0.442745 cm/s	-6.92926 cm/s
wrough	0.0 cm	0.0 cm

## Fluid Forces on Walls

pressx	0.00097912 dynes
pressy	0.71265 dynes
pressz	-0.051041 dynes
shearx	-0.0003918 dynes
sheary	-0.23507 dynes
shearz	-2.4392 dynes

Decision Centre

Summary images

Image 01

Design 1::

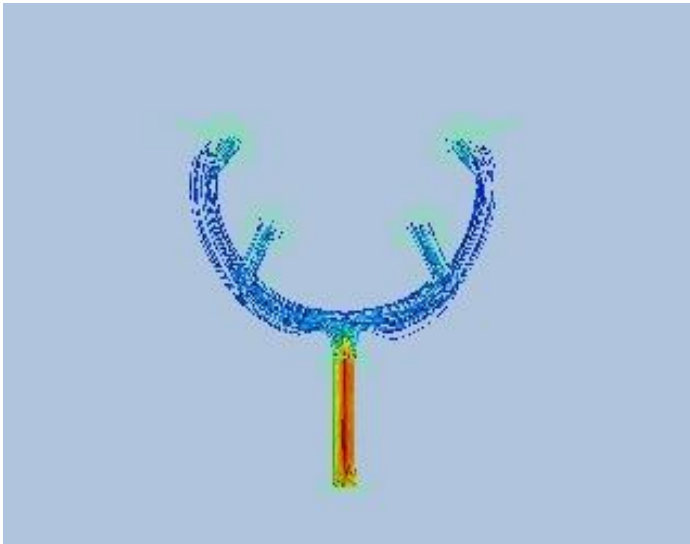
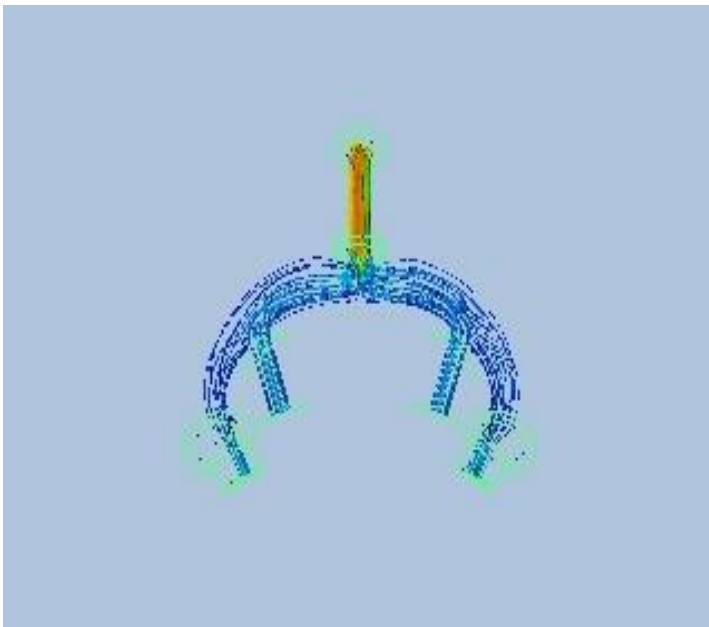


Image 02

Design 1



## C. Odour Simulation within the optical chamber 10 cm<sup>3</sup>/min flow rate

Prepared by: Eckard Schumann

Requested by: Dr. Jürgen Rybak

Date: Thursday, November 29, 2018

### Summary

### Description

Equally important is the behaviour of the odour within the chamber. Therefore simulations of the odour distribution were carried utilizing the special designed prototype while maintaining a constant volume flow rate of 10 cm<sup>3</sup>/min at the inlet A of the odour distributor. Then the flow is directed to the 4 outlets. The odour outlets are positioned in a symmetrically way to guarantee that the same amount of odour travels to both sides

### Software information

Simulation CFD version	18.0
Simulation CFD build code	20170328

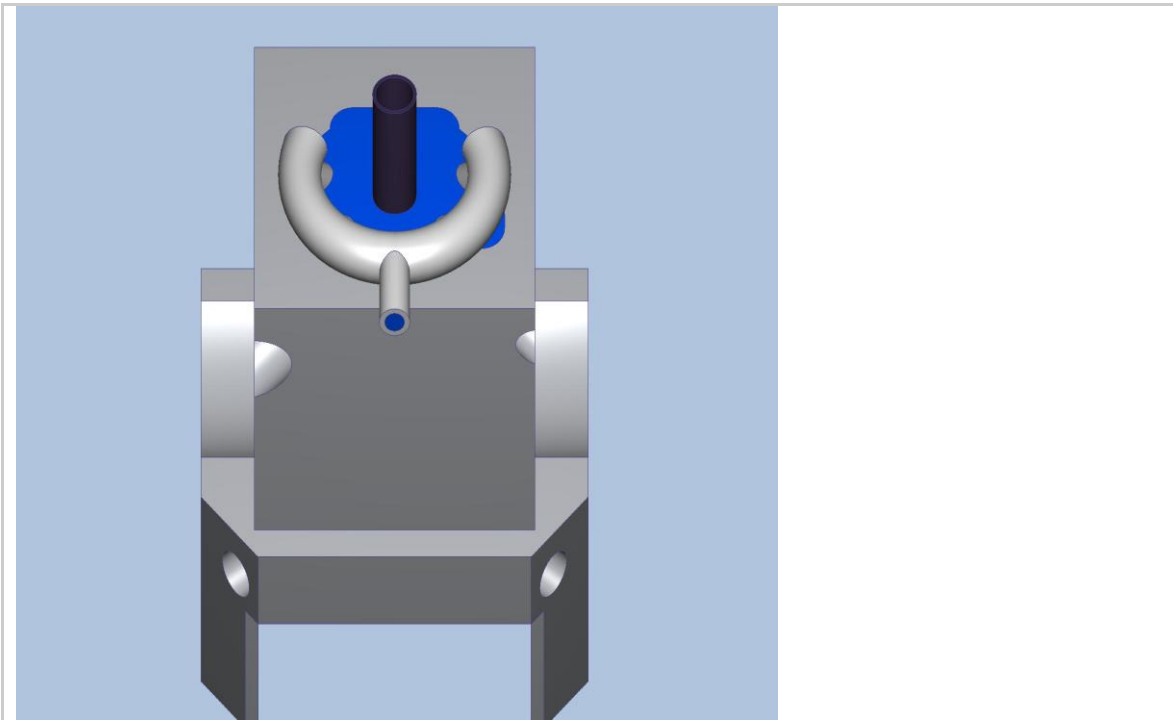
### Design 1

Length units	cm
Coordinate system	Cartesian 3D



## Scenario odour inlet with the outlets 1 and 2

### Materials



Name	ASSIGNED TO	PROPERTIES
Titanium	Chamber:1@Duftverteiler_ASME\Chamber_1:1 Chamber:1@Duftverteiler_ASME\Chamber_1:1 Volumen:1@Duftverteiler_ASME\Chamber_1:1 Chamber:1@Duftverteiler_ASME\Chamber_1:1	X-Direction 21.9 W/m-K Y-Direction Same as X-dir. Z-Direction Same as X-dir. Density 4500.0 kg/m3 Specific heat 522.0 J/kg-K Emissivity 0.5 Transmissivity 0.0 Electrical 4.2e-07 ohm-m Wall 0.0 meter
Stainless Steel (316)	Duftverteiler_ASME Volumen:1@Duftverteiler_ASME\Chamber_1:1_U_Duftverteiler_ASME Volumen:1@Duftverteiler_ASME\Chamber_1:1_U_Duftverteiler_ASME Duftverteiler_ASME_U_Chamber:1@Duftverteiler_ASME\Chamber_1:1 Duftverteiler_ASME_U_Chamber:1@Duftverteiler_ASME\Chamber_1:1 Volumen:1@Duftverteiler_ASME\Chamber_1:1_U_Duftverteiler_ASME Volumen:1@Duftverteiler_ASME\Chamber_1:1_U_Duftverteiler_ASME	X- 16.3 Y- Same as Z- Same as Density 8.0 Specific 0.5 J/g-K Emissivity 0.35 Transmiss 0.0 Electrical 7.4e-05 Wall 0.0

# Odour Simulation within the optical chamber

XLIV

Water	Volumen:1@Duftverteiler_ASME\Chamber_1:1 Volumen_ odour:1@Duftverteiler_ASME Volumen_ odour:1@Duftverteiler_ASME_U Volumen:1@Duftverteiler_ASME\Chamber_1:1 Volumen_ odour:1@Duftverteiler_ASME_U Volumen:1@Duftverteiler_ASME\Chamber_1:1 Volumen_ odour:1@Duftverteiler_ASME_U Volumen:1@Duftverteiler_ASME\Chamber_1:1 Volumen_ odour:1@Duftverteiler_ASME_U Volumen:1@Duftverteiler_ASME\Chamber_1:1	Density Viscosity Conducti Specific Compres Emissivit Wall Phase	Piecowis 0.001003 0.6 W/m- 4182.0 2185650 1.0 0.0 Linked
Glass	Chamber_1:1@Duftverteiler_ASME Volumen:1@Duftverteiler_ASME\Chamber_1:1 Volumen:1@Duftverteiler_ASME\Chamber_1:1_U Chamber_1:1@Duftverteiler_ASME	X-Direction Y-Direction Z-Direction Density Specific heat Emissivity Transmissivit Electrical Wall	0.78 W/m-K Same as X- Same as X- 2700.0 840.0 J/kg-K 0.92 0.0 50000000.0 0.0 meter

## Boundary conditions

Type	ASSIGNED TO
Pressure(0 dyne/cm <sup>2</sup> Gage)	Surface:32 Surface:33
Volume Flow Rate(10 cm <sup>3</sup> /min)	Surface:147

## Mesh

### Automatic Meshing Settings

Surface refinement	0
Gap refinement	0
Resolution factor	1.0
Edge growth rate	1.1
Minimum points on edge	2
Points on longest edge	10
Surface limiting aspect ratio	20

### Mesh Enhancement Settings

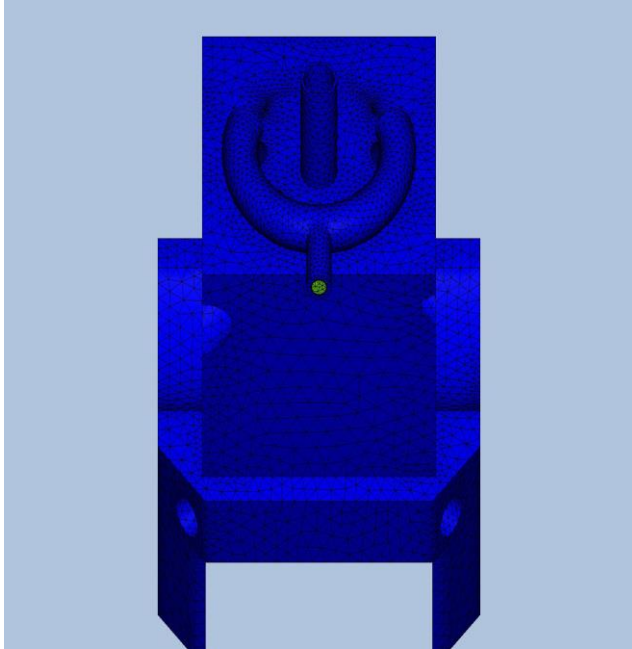
Mesh enhancement	1
Enhancement blending	0
Number of layers	3

# Odour Simulation within the optical chamber

XLV

Layer factor	0.45
Layer gradation	1.05

## Meshed Model



Number of Nodes	110214
Number of Elements	464037

## Physics

Flow	On
Compressibility	Incompressible
Heat Transfer	Off
Auto Forced Convection	Off
Gravity Components	0.0, 0.0, 0.0
Radiation	Off
Scalar	No scalar
Turbulence	On

## Solver Settings

Solution mode	Steady State
Solver computer	MyComputer
Intelligent solution control	On
Advection scheme	ADV 5
Turbulence model	k-epsilon

## Convergence

Iterations run	100
Solve time	220 seconds

# Odour Simulation within the optical chamber

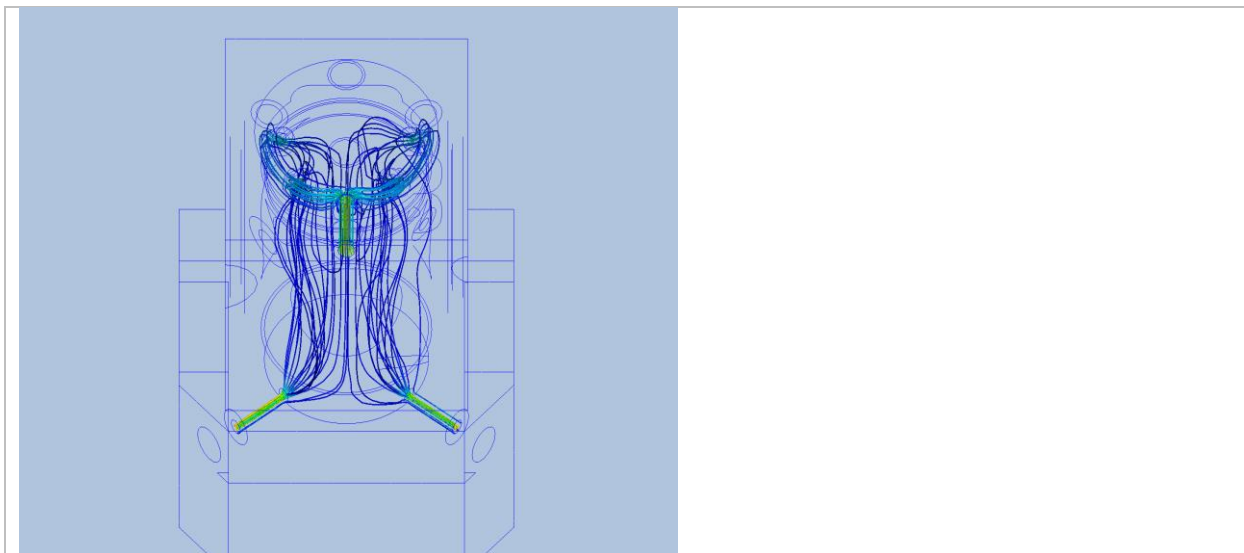
XLVI

Solver version	18.0.20170328
----------------	---------------

## Mass Balance

	In	Out
Mass flow	0.166367 g/s	-0.1637818 g/s
Volume flow	0.166667 cm <sup>3</sup> /s	-0.1640772 cm <sup>3</sup> /s

## Results of the Scenario odour inlet with the outlets 1 and 2



### Inlets and Outlets

inlet 1		
inlet bulk pressure	75.1763	dyne/cm <sup>2</sup>
inlet bulk	0.0	C
inlet mach number	7.29808e-10	
mass flow in	0.166367	g/s
minimum x,y,z of	0.0	
node near minimum	428.0	

# Odour Simulation within the optical chamber

XLVII

	reynolds number 73.6652 surface id 147.0 total mass flow in 0.166367 g/s total vol. flow in 0.166667 cm <sup>3</sup> /s volume flow in 0.166667 cm <sup>3</sup> /s
outlet 1	mass flow out -0.0800671 g/s minimum x,y,z of 0.0 node near minimum 8548.0 outlet bulk pressure -0.0 dyne/cm <sup>2</sup> outlet bulk -0.0 C outlet mach number 2.13602e-10 reynolds number 41.8986 surface id 33.0 volume flow out -0.0802115 cm <sup>3</sup> /s
outlet 2	mass flow out -0.0837147 g/s minimum x,y,z of 0.0 node near minimum 798.0 outlet bulk pressure -0.0 dyne/cm <sup>2</sup> outlet bulk -0.0 C outlet mach number 2.23478e-10 reynolds number 43.8074 surface id 32.0 total mass flow out -0.163782 g/s total vol. flow out -0.164077 cm <sup>3</sup> /s volume flow out -0.0838657 cm <sup>3</sup> /s

## Field Variable Results

Variable	Max	Min
cond	0.219 W/cm-K	0.006 W/cm-K
dens	8.0 g/cm <sup>3</sup>	0.9982 g/cm <sup>3</sup>
econd	59.7662 W/cm-K	0.0 W/cm-K
emiss	1.0	0.0
evisc	13.8565 g/cm-s	0.0 g/cm-s
gent	16523.4 1/s	2.83113e-11 1/s
press	81.6081 dyne/cm <sup>2</sup>	0.0 dyne/cm <sup>2</sup>
ptotl	87.2756 dyne/cm <sup>2</sup>	0.0 dyne/cm <sup>2</sup>
scal1	0.0	0.0
seebeck	0.0 V/K	0.0 V/K
shgc	0.0	0.0
spech	4.182 J/g-K	0.5 J/g-K
temp	0.0 C	0.0 C
transmiss	0.0	0.0
turbd	67315.6 cm <sup>2</sup> /s <sup>3</sup>	9.01419e-14 cm <sup>2</sup> /s <sup>3</sup>
turbk	19.7034 cm <sup>2</sup> /s <sup>2</sup>	1.01757e-06 cm <sup>2</sup> /s <sup>2</sup>
ufactor	0.0	0.0
visc	0.01003 g/cm-s	0.0 g/cm-s
vx vel	3.53265 cm/s	-3.81959 cm/s
vy vel	0.38715 cm/s	-1.70589 cm/s
vz vel	3.20452 cm/s	-5.91216 cm/s
wrough	0.0 cm	0.0 cm

# Odour Simulation within the optical chamber

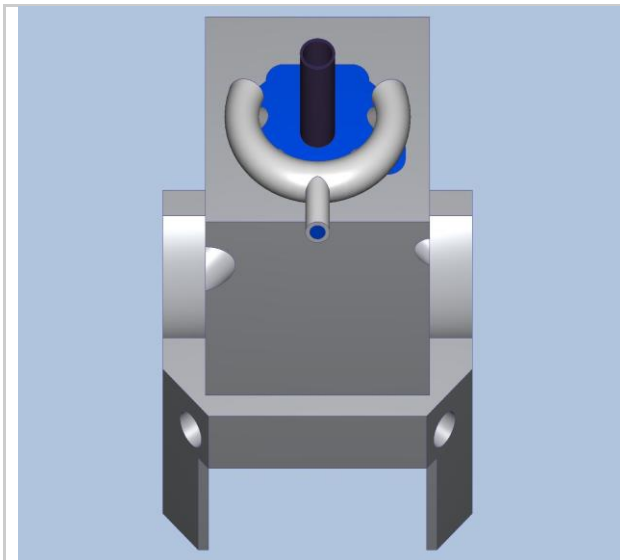
XLVIII

## Fluid Forces on Walls

pressx	0.018681 dynes
pressy	0.60286 dynes
pressz	-3.1185 dynes
shearx	-0.016486 dynes
sheary	-0.43829 dynes
shearz	-1.3376 dynes

## Scenario odour inlet with the outlets 1 and 3

### Materials



Name	ASSIGNED TO	PROPERTIES	
Titanium	Chamber:1@Duftverteiler_ASME\Chamber_1:1 Chamber:1@Duftverteiler_ASME\Chamber_1:1 Volumen:1@Duftverteiler_ASME\Chamber_1:1 Chamber:1@Duftverteiler_ASME\Chamber_1:1	X-Direction	21.9 W/m-K
		Y-Direction	Same as X-dir.
		Z-Direction	Same as X-dir.
		Density	4500.0 kg/m3
		Specific heat	522.0 J/kg-K
		Emissivity	0.5
		Transmissivity	0.0
		Electrical	4.2e-07 ohm-m
		Wall	0.0 meter

# Odour Simulation within the optical chamber

XLIX

Stainless Steel (316)	Duftverteiler_ASME Volumen:1@Duftverteiler_ASME\Chamber_1:1_U_Duftverteiler_ASME Volumen:1@Duftverteiler_ASME\Chamber_1:1_U_Duftverteiler_ASME Duftverteiler_ASME_U_Chamber:1@Duftverteiler_ASME\Chamber_1:1 Duftverteiler_ASME_U_Chamber:1@Duftverteiler_ASME\Chamber_1:1 Volumen:1@Duftverteiler_ASME\Chamber_1:1_U_Duftverteiler_ASME Volumen:1@Duftverteiler_ASME\Chamber_1:1_U_Duftverteiler_ASME	X- 16.3 Y- Same as Z- Same as Density 8.0 Specific 0.5 J/g-K Emissivit 0.35 Transmis 0.0 Electrical 7.4e-05 Wall 0.0
Water	Volumen:1@Duftverteiler_ASME\Chamber_1:1 Volumen_odour:1@Duftverteiler_ASME Volumen_odour:1@Duftverteiler_ASME_U_Volumen:1@Duftverteiler_ASME\Chamber_1:1 Volumen_odour:1@Duftverteiler_ASME_U_Volumen:1@Duftverteiler_ASME\Chamber_1:1 Volumen_odour:1@Duftverteiler_ASME_U_Volumen:1@Duftverteiler_ASME\Chamber_1:1 Volumen_odour:1@Duftverteiler_ASME_U_Volumen:1@Duftverteiler_ASME\Chamber_1:1	Density Piecewis Viscosity 0.001003 Conducti 0.6 W/m- Specific 4182.0 Compres 2185650 Emissivit 1.0 Wall 0.0 Phase Linked
Glass	Chamber_1:1@Duftverteiler_ASME Volumen:1@Duftverteiler_ASME\Chamber_1:1 Volumen:1@Duftverteiler_ASME\Chamber_1:1_U_Chamber_1:1@Duftverteiler_ASME	X-Direction 0.78 W/m-K Y-Direction Same as X- Z-Direction Same as X- Density 2700.0 Specific heat 840.0 J/kg-K Emissivity 0.92 Transmissivit 0.0 Electrical 50000000.0 Wall 0.0 meter

## Boundary conditions

Type	ASSIGNED TO
Pressure(0 dyne/cm2 Gage)	Surface:32 Surface:34
Volume Flow Rate(10 cm3/min)	Surface:147

## Mesh

# Odour Simulation within the optical chamber

L

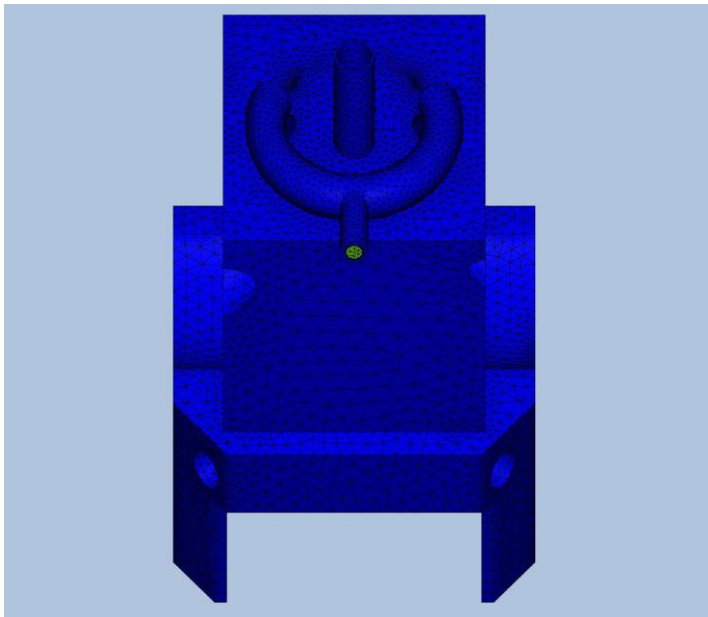
## Automatic Meshing Settings

Surface refinement	0
Gap refinement	0
Resolution factor	1.0
Edge growth rate	1.1
Minimum points on edge	2
Points on longest edge	10
Surface limiting aspect ratio	20

## Mesh Enhancement Settings

Mesh enhancement	1
Enhancement blending	0
Number of layers	3
Layer factor	0.45
Layer gradation	1.05

## Meshed Model



Number of Nodes	110189
Number of Elements	463978

## Physics

Flow	On
Compressibility	Incompressible
Heat Transfer	Off
Auto Forced Convection	Off
Gravity Components	0.0, 0.0, 0.0
Radiation	Off
Scalar	No scalar
Turbulence	On



# Odour Simulation within the optical chamber

LI

## Solver Settings

Solution mode	Steady State
Solver computer	MyComputer
Intelligent solution control	On
Advection scheme	ADV 5
Turbulence model	k-epsilon

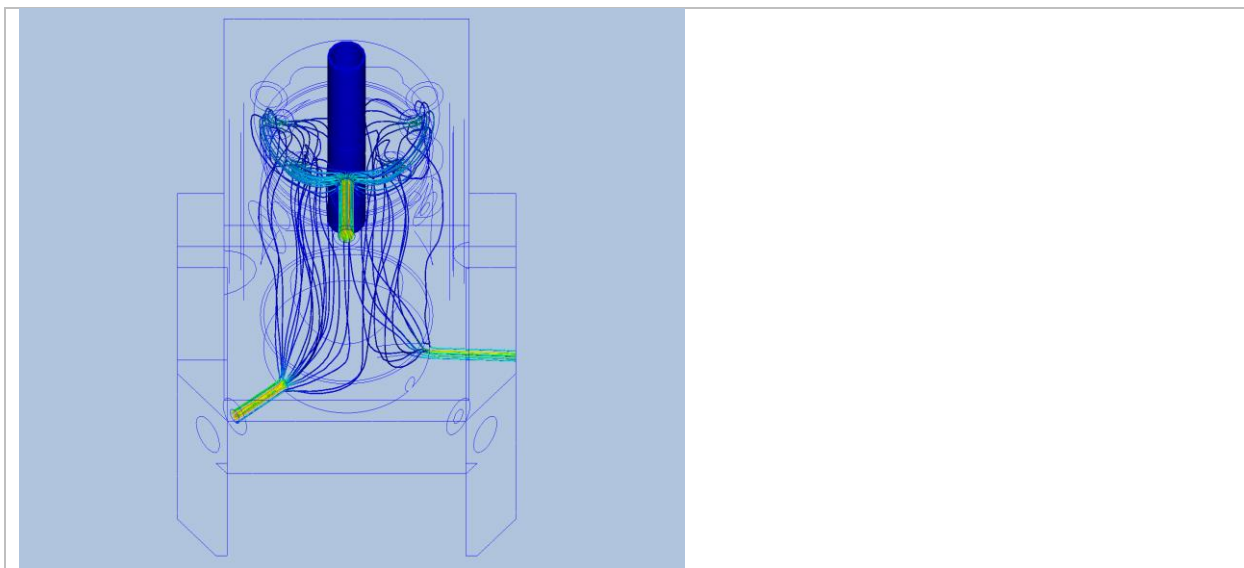
## Convergence

Iterations run	100
Solve time	221 seconds
Solver version	18.0.20170328

## Mass Balance

	In	Out
Mass flow	0.166367 g/s	-0.1637664 g/s
Volume flow	0.166667 cm <sup>3</sup> /s	-0.1640617 cm <sup>3</sup> /s

## Results of the Scenario odour inlet with the outlets 1 and 3



## Inlets and Outlets

inlet 1		
inlet bulk pressure		79.6885 dyne/cm <sup>2</sup>
inlet bulk		0.0 C
inlet mach number		7.29808e-10
mass flow in		0.166367 g/s
minimum x,y,z of		0.0
node near minimum		428.0
reynolds number		73.6652

# Odour Simulation within the optical chamber

LII

	surface id	147.0
	total mass flow in	0.166367 g/s
	total vol. flow in	0.166667 cm <sup>3</sup> /s
	volume flow in	0.166667 cm <sup>3</sup> /s
outlet 1	mass flow out	-0.0925246 g/s
	minimum x,y,z of	0.0
	node near minimum	798.0
	outlet bulk pressure	-0.0 dyne/cm <sup>2</sup>
	outlet bulk	-0.0 C
	outlet mach number	2.47912e-10
	reynolds number	48.4176
	surface id	32.0
	volume flow out	-0.0926914 cm <sup>3</sup> /s
outlet 2	mass flow out	-0.0712418 g/s
	minimum x,y,z of	0.0
	node near minimum	819.0
	outlet bulk pressure	-0.0 dyne/cm <sup>2</sup>
	outlet bulk	-0.0 C
	outlet mach number	1.99658e-10
	reynolds number	37.2066
	surface id	34.0
	total mass flow out	-0.163766 g/s
	total vol. flow out	-0.164062 cm <sup>3</sup> /s
	volume flow out	-0.0713703 cm <sup>3</sup> /s

## Field Variable Results

Variable	Max	Min
cond	0.219 W/cm-K	0.006 W/cm-K
dens	8.0 g/cm <sup>3</sup>	0.9982 g/cm <sup>3</sup>
econd	49.6504 W/cm-K	0.0 W/cm-K
emiss	1.0	0.0
evisc	11.8488 g/cm-s	0.0 g/cm-s
gent	18907.9 1/s	3.77218e-11 1/s
press	86.1218 dyne/cm <sup>2</sup>	0.0 dyne/cm <sup>2</sup>
ptotl	91.7893 dyne/cm <sup>2</sup>	0.0 dyne/cm <sup>2</sup>
scal1	0.0	0.0
seebeck	0.0 V/K	0.0 V/K
shgc	0.0	0.0
spech	4.182 J/g-K	0.5 J/g-K
temp	0.0 C	0.0 C
transmiss	0.0	0.0
turbd	88749.6 cm <sup>2</sup> /s <sup>3</sup>	1.08746e-13 cm <sup>2</sup> /s <sup>3</sup>
turbk	25.4863 cm <sup>2</sup> /s <sup>2</sup>	1.01663e-06 cm <sup>2</sup> /s <sup>2</sup>
ufactor	0.0	0.0
visc	0.01003 g/cm-s	0.0 g/cm-s
vx vel	4.08793 cm/s	-4.21832 cm/s
vy vel	0.387189 cm/s	-2.06759 cm/s
vz vel	3.53749 cm/s	-5.91218 cm/s
wrough	0.0 cm	0.0 cm

## Fluid Forces on Walls

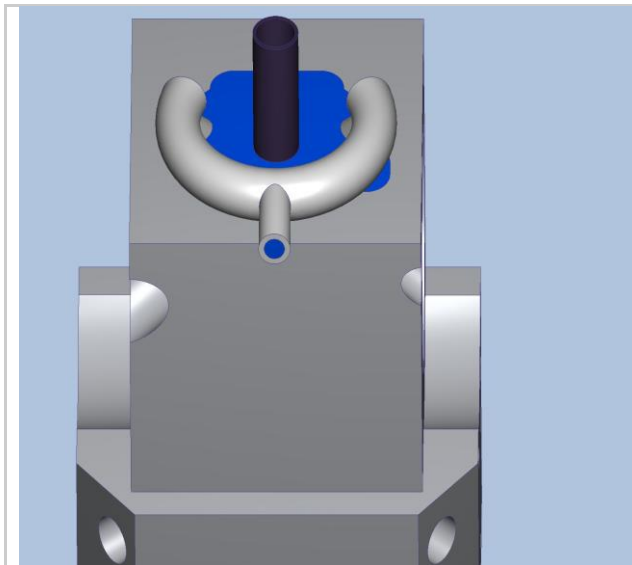
# Odour Simulation within the optical chamber

LIII

pressx	-0.24696 dynes
pressy	0.58546 dynes
pressz	-2.789 dynes
shearx	0.86125 dynes
sheary	-0.46166 dynes
shearz	-1.6734 dynes

## Scenario odour inlet with the outlets 1, 2 and 3

### Materials



Name	ASSIGNED TO	PROPERTIES	
Titanium	Chamber:1@Duftverteiler_ASME\Chamber_1:1 Chamber:1@Duftverteiler_ASME\Chamber_1:1 Volumen:1@Duftverteiler_ASME\Chamber_1:1 Chamber:1@Duftverteiler_ASME\Chamber_1:1	X-Direction	21.9 W/m-K
		Y-Direction	Same as X-dir.
		Z-Direction	Same as X-dir.
		Density	4500.0 kg/m3
		Specific heat	522.0 J/kg-K
		Emissivity	0.5
		Transmissivity	0.0
		Electrical Wall	4.2e-07 ohm-m 0.0 meter
Stainless Steel (316)	Duftverteiler_ASME Volumen:1@Duftverteiler_ASME\Chamber_1:1_U_Duftverteiler_ASME Volumen:1@Duftverteiler_ASME\Chamber_1:1_U_Duftverteiler_ASME Duftverteiler_ASME_U_Chamber:1@Duftverteiler_ASME\Chamber_1:1 Duftverteiler_ASME_U_Chamber:1@Duftverteiler_ASME\Chamber_1:1 Volumen:1@Duftverteiler_ASME\Chamber_1:1_U_Duftverteiler_ASME Volumen:1@Duftverteiler_ASME\Chamber_1:1_U_Duftverteiler_ASME	X-	16.3
		Y-	Same as
		Z-	Same as
		Density	8.0
		Specific	0.5 J/g-K
		Emissivit	0.35
		Transmis	0.0
		Electrical Wall	7.4e-05 0.0

# Odour Simulation within the optical chamber

LIV

Water	Volumen:1@Duftverteiler_ASME\Chamber_1:1 Volumen_odour:1@Duftverteiler_ASME Volumen_odour:1@Duftverteiler_ASME_U_Volumen:1@Duftverteiler_ASME\Chamber_1:1 Volumen_odour:1@Duftverteiler_ASME_U_Volumen:1@Duftverteiler_ASME\Chamber_1:1 Volumen_odour:1@Duftverteiler_ASME_U_Volumen:1@Duftverteiler_ASME\Chamber_1:1 Volumen_odour:1@Duftverteiler_ASME_U_Volumen:1@Duftverteiler_ASME\Chamber_1:1 Volumen_odour:1@Duftverteiler_ASME_U_Volumen:1@Duftverteiler_ASME\Chamber_1:1	Density Viscosity Conducti Specific Compres Emissivit Wall Phase	Piecowis 0.001003 0.6 W/m- 4182.0 2185650 1.0 0.0 Linked
Glass	Chamber_1:1@Duftverteiler_ASME_Volumen:1@Duftverteiler_ASME\Chamber_1:1 Volumen:1@Duftverteiler_ASME\Chamber_1:1_U_Chamber_1:1@Duftverteiler_ASME	X-Direction Y-Direction Z-Direction Density Specific heat Emissivity Transmissivit Electrical Wall	0.78 W/m-K Same as X- Same as X- 2700.0 840.0 J/kg-K 0.92 0.0 50000000.0 0.0 meter

## Boundary conditions

Type	ASSIGNED TO
Pressure(0 dyne/cm <sup>2</sup> Gage)	Surface:32 Surface:33 Surface:34
Volume Flow Rate(10 cm <sup>3</sup> /min)	Surface:147

## Mesh

### Automatic Meshing Settings

Surface refinement	0
Gap refinement	0
Resolution factor	1.0
Edge growth rate	1.1
Minimum points on edge	2
Points on longest edge	10
Surface limiting aspect ratio	20

### Mesh Enhancement Settings

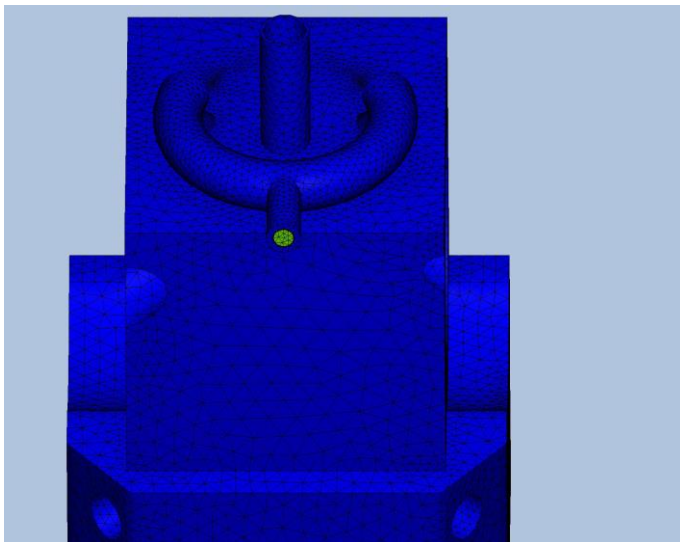
Mesh enhancement	1
------------------	---

# Odour Simulation within the optical chamber

LV

Enhancement blending	0
Number of layers	3
Layer factor	0.45
Layer gradation	1.05

## Meshed Model



Number of Nodes	110139
Number of Elements	463820

## Physics

Flow	On
Compressibility	Incompressible
Heat Transfer	Off
Auto Forced Convection	Off
Gravity Components	0.0, 0.0, 0.0
Radiation	Off
Scalar	No scalar
Turbulence	On

## Solver Settings

Solution mode	Steady State
Solver computer	MyComputer
Intelligent solution control	On
Advection scheme	ADV 5
Turbulence model	k-epsilon

## Convergence

Iterations run	100
Solve time	225 seconds
Solver version	18.0.20170328

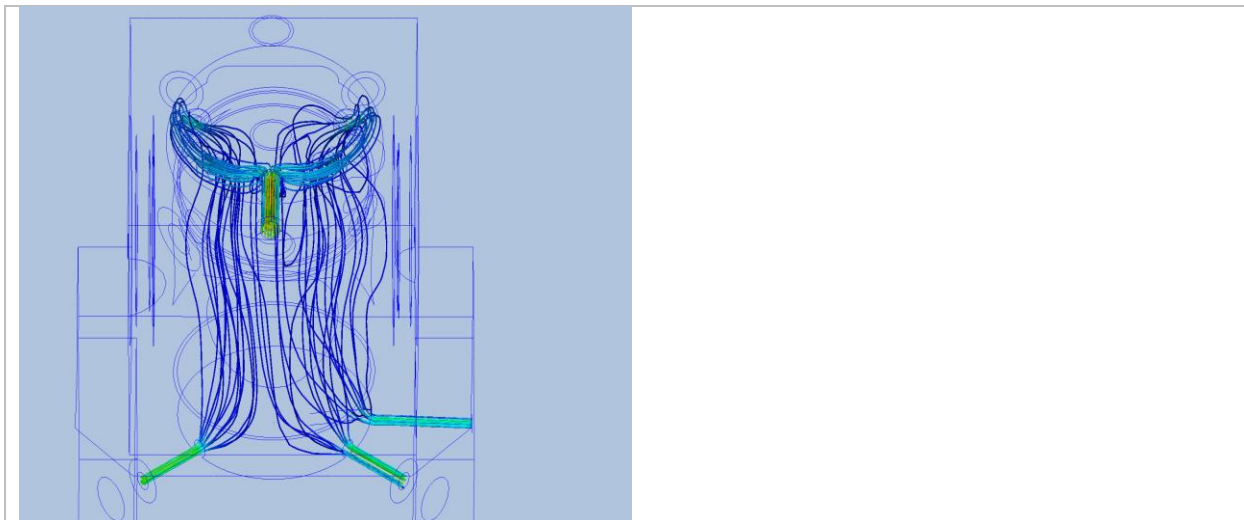
# Odour Simulation within the optical chamber

LVI

## Mass Balance

	In	Out
Mass flow	0.166367 g/s	-0.163819 g/s
Volume flow	0.166667 cm <sup>3</sup> /s	-0.1641143 cm <sup>3</sup> /s

## Results Scenario odour inlet with the outlets 1, 2 and 3



## Inlets and Outlets

inlet 1	inlet bulk pressure	63.818 dyne/cm <sup>2</sup>
	inlet bulk	0.0 C
	inlet mach number	7.29808e-10
	mass flow in	0.166367 g/s
	minimum x,y,z of	0.0
	node near minimum	428.0
	reynolds number	73.6652
	surface id	147.0
	total mass flow in	0.166367 g/s
	total vol. flow in	0.166667 cm <sup>3</sup> /s
volume flow in	0.166667 cm <sup>3</sup> /s	
outlet 1	mass flow out	-0.0580479 g/s
	minimum x,y,z of	0.0

# Odour Simulation within the optical chamber

LVII

	node near minimum	8548.0
	outlet bulk pressure	-0.0 dyne/cm <sup>2</sup>
	outlet bulk	-0.0 C
	outlet mach number	1.54347e-10
	reynolds number	30.3761
	surface id	33.0
	volume flow out	-0.0581525 cm <sup>3</sup> /s
outlet 2	mass flow out	-0.0603581 g/s
	minimum x,y,z of	0.0
	node near minimum	798.0
	outlet bulk pressure	-0.0 dyne/cm <sup>2</sup>
	outlet bulk	-0.0 C
	outlet mach number	1.60485e-10
	reynolds number	31.585
	surface id	32.0
	volume flow out	-0.0604669 cm <sup>3</sup> /s
outlet 3	mass flow out	-0.045413 g/s
	minimum x,y,z of	0.0
	node near minimum	819.0
	outlet bulk pressure	-0.0 dyne/cm <sup>2</sup>
	outlet bulk	-0.0 C
	outlet mach number	1.26913e-10
	reynolds number	23.7173
	surface id	34.0
	total mass flow out	-0.163819 g/s
	total vol. flow out	-0.164114 cm <sup>3</sup> /s
	volume flow out	-0.0454949 cm <sup>3</sup> /s

## Field Variable Results

Variable	Max	Min
cond	0.219 W/cm-K	0.006 W/cm-K
dens	8.0 g/cm <sup>3</sup>	0.9982 g/cm <sup>3</sup>
econd	0.229076 W/cm-K	0.0 W/cm-K
emiss	1.0	0.0
evisc	0.0509065 g/cm-s	0.0 g/cm-s
gent	13829.1 1/s	0.000116093 1/s
press	70.2491 dyne/cm <sup>2</sup>	0.0 dyne/cm <sup>2</sup>
ptotl	75.9166 dyne/cm <sup>2</sup>	0.0 dyne/cm <sup>2</sup>
scal1	0.0	0.0
seebeck	0.0 V/K	0.0 V/K
shgc	0.0	0.0
spech	4.182 J/g-K	0.5 J/g-K
temp	0.0 C	0.0 C
transmiss	0.0	0.0
turbd	37663.2 cm <sup>2</sup> /s <sup>3</sup>	3.4483e-07 cm <sup>2</sup> /s <sup>3</sup>
turbk	13.6942 cm <sup>2</sup> /s <sup>2</sup>	1.14075e-06 cm <sup>2</sup> /s <sup>2</sup>
ufactor	0.0	0.0
visc	0.01003 g/cm-s	0.0 g/cm-s
vx vel	2.61539 cm/s	-2.76435 cm/s
vy vel	0.387132 cm/s	-1.70596 cm/s

# Odour Simulation within the optical chamber

LVIII

vz vel	2.31843 cm/s	-5.91223 cm/s
wrough	0.0 cm	0.0 cm

## Fluid Forces on Walls

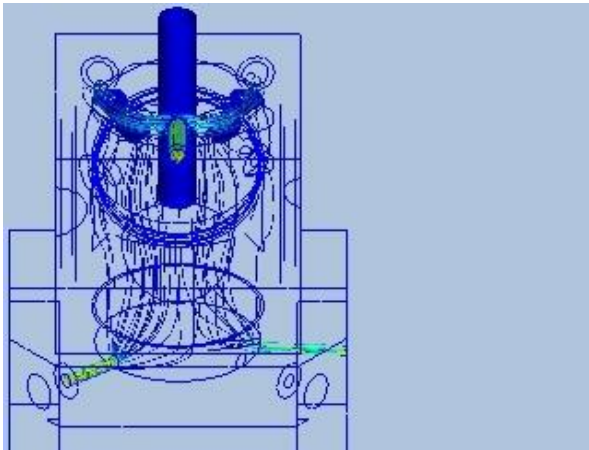
pressx	-0.66807 dynes
pressy	0.58367 dynes
pressz	-2.0264 dynes
shearx	0.97488 dynes
sheary	-0.44715 dynes
shearz	-1.5863 dynes

## Decision Centre

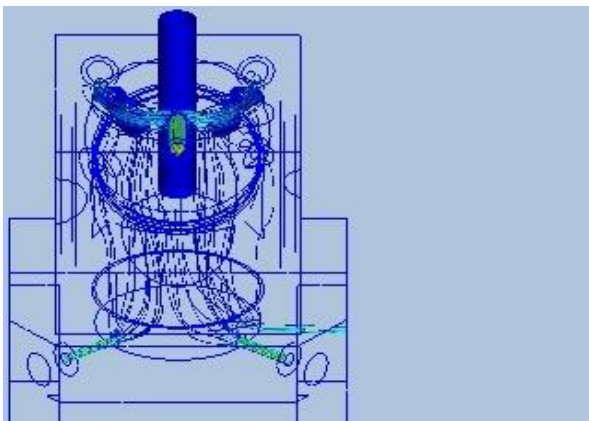
### Summary images

#### Image 01

Design 1::10Scenario odour inlet 10cm3 1&3 outlet



Design 1::11Scenario odour inlet 10cm3 1&2&3 outlets



Design 1::8Scenario odour inlet 10cm3 1&2 outlets



# Odour Simulation within the optical chamber

LIX

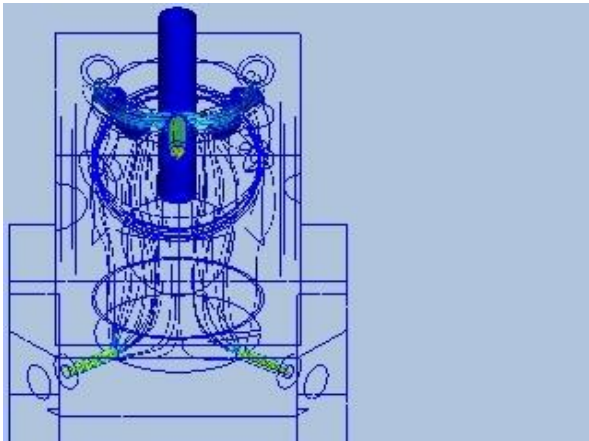
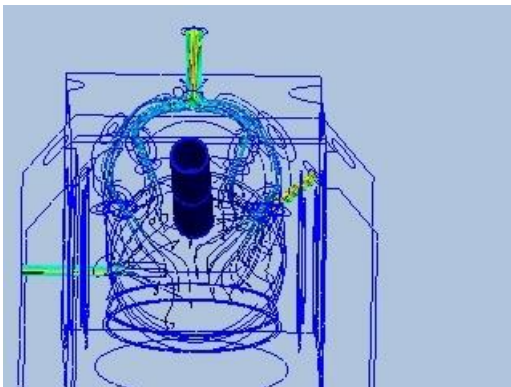
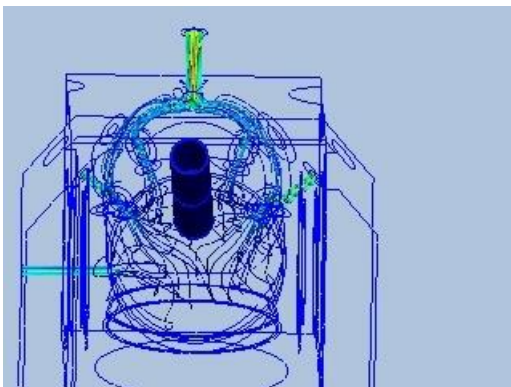


Image 02

Design 1::Scenario odour inlet 10cm3 1&3 outlet



Design 1::Scenario odour inlet outlets1 and 2 and 3



Design 1::Scenario odour inlet and outlets 1 and 2

# Odour Simulation within the optical chamber

LX

